This article was published in: Comprehensive Organometallic Chemistry IV. Editors-in-Chief: Gerard Parkin, Karsten Meyer, Dermot O'Hare. Elsevier, 2022; Vol. 14, Applications III. Materials Science, Nanoscience, Polymer Science and Surface Chemistry, Chapter 14.09, pp 285–338. https://doi.org/10.1016/B978-0-12-820206-7.00119-0 .

Comprehensive Organometallic Chemistry IV

This template guides you through the elements that you should include in your chapter. Over-type the grey highlighted text to be sure to include everything that you need. You will find further details in the ***Instructions to Authors***.

Chapter title: Organometallic Mesogens
Manuscript code: 80020
Section Editor: Dr. Derek Gates
Applications III. Materials science, nanoscience, polymer science and surface chemistry.

Author and Co-author Contact Information
List all authors with their first names first, and then the middle initials and last names. Provide correct and current affiliations with full postal details (including e-mails of all). Indicate the corresponding author.

Dr. Manuel Bardají
IU CINQUIMA/Química Inorgánica
Facultad de Ciencias
Paseo de Belen 7
Universidad de Valladolid
47011-VALLADOLID (SPAIN)
E-mail: mbardaji@uva.es
Telephone: +34983184519

Dr. Silverio Coco
IU CINQUIMA/Química Inorgánica
Facultad de Ciencias
Paseo de Belen 7
Universidad de Valladolid
47011-VALLADOLID (SPAIN)
E-mail: silverio.coco@uva.es
Telephone: +34983184624

Please provide up to a 50-100 word abstract of the chapter, which will be used to summarise the work when presented online.

Abstract
This chapter discusses organometallic complexes that behave like liquid crystals. The most common syntheses, types of compounds and ligands for these derivatives are described. It is reviewed how these organometallic mesogens self-organize within the phases, what are the mesophases obtained and their transition temperatures. The relevant physical properties of these compounds are also reviewed, especially the optical and electro–optical properties. The reader is provided with an introduction to the topic, an overview of the state of the art at this time, and many references are collected to delve into it.

Please provide up to 10-15 keywords, which will be used for indexing purposes only.

Keywords

organometallic, mesogen, liquid crystal, metallomesogen, luminescence, phosphorescence, mesophase, ferrocene, gold, iridium, palladium, platinum, silver, ortho-metalate, isocyanide.

Main text

Divided into appropriate sections, covering the contents as agreed with the Editors.

Index

1 Preamble

This chapter can be considered as an update of the chapter entitled Metallomesogens In Comprehensive Organometallic Chemistry III,[1] therefore it deals with metallomesogens described from 2007 to 2020. This chapter focuses primarily on small molecules or ions of an organometallic nature, which self-organize as liquid crystals. Therefore, as in the previous reference, the objective of this chapter is to provide a specific review to the area of organometallic mesogens. It does not cover liquid crystals in polymeric systems[2,3] or combined with nanoparticles,[4,5,6] which have been recently reviewed.

The chapter begins by introducing a basic terminology, the types of mesophases and their characterization, as well as their physical properties and main applications. The subject matter in this review is organized according to groups from the periodic table and then by ligand or compound type.

There has been a series of previous reviews about metallomesogens or metal-containing liquid crystals, although not specifically about organometallics, the latest and most extensive are collected here.[7–10]

2 General Introduction

2.1 Terminology in Liquid Crystals

We must start by remembering some concepts in this subject. The terminology relating to low molar mass liquid crystals follows the recommendations made by the IUPAC and the International Liquid Crystal Society in 2001.[11]

The liquid crystal state (LC) is a phase of matter which is intermediate between the crystalline solid and the isotropic liquid states, where a combination of properties is shown: mobility and fluidity as a liquid, some positional and/or orientational order, self-assembly and anisotropism as a solid crystal. Mesogen or mesomorphic compound is a compound which behaves as a liquid crystal and displays mesophases (liquid crystal phases). The liquid crystal state depends on the intermolecular forces, such as dipole–dipole, van der Waals interactions, π–π stacking; if they are too strong or too weak the mesophase is lost.

The self-assembly associated with liquid crystals may be generated through the use of temperature (thermotropic LC), a solvent (lyotropic LC) or both (amphitropic LC). Therefore, the mesophases exist in a range of temperature or solvent concentration. In these materials, it can be distinguished: a) the melting point, the temperature at which a thermotropic mesogen goes from the solid to a fluid mesophase; b) the transition temperatures, to pass between different mesophases; c) the clearing or isotropization point: the temperature at which the mesophase transforms into an isotropic liquid.

Two types of thermotropic mesophases can be distinguished. On the one hand, enantiotropic mesophases, which are thermodynamically stable over a definite temperature, and are observed both upon heating and on cooling. On the other hand, monotropic mesophases, which are metastable in nature and only appear in the cooling process.
Thermotropic mesogens can be classified into four principal types, by taking into account structural factors of the units (molecules) forming the mesophase (Figure 1): calamitic (formed by rod-like molecules), discotic (formed by disk-like molecules), polycatenar mesogens (based on molecules with a rather extended calamitic central core containing several long substituents), and banana-shaped liquid crystals (formed by bent-core molecules). These types of structures determine the molecular self-assembly process and, consequently, the structure of the mesophase.

<Figure 1 near here>

Figure 1. Schematic representation of a) calamitic (rod), b) discotic (disk), c) polycatenar, and d) banana liquid crystals.

The mesophases of calamitic mesogens are classified in two groups: *nematic* and *smectic* . The nematic mesophase (N) is characterized by an orientational order of the molecules that are aligned along a preferred direction (defined by a *director* **n**) (Figure 2). The molecules can slide and move in the nematic mesophase (while roughly keeping their molecular orientation) and rotate around their main axis. This is the less ordered mesophase and usually it is very fluid.
In the smectic mesophases the molecules are oriented, as in a nematic mesophase, with their principal axis roughly parallel to the director, but they are also defining layers. These layers can be perpendicular to the director, as in the *smetic A* mesophase (SmA), or tilted, as in the *smectic C* (SmC). The SmA and SmC mesophases are the less ordered and more common smectic mesophases. Other less common types of smectic mesophases are known, which differ in the degree or kind of molecular ordering within and between the layers. A more precise description of the smectic phase structure can be found in the following references.[12,13]

<Figure 2 near here>

Figure 2. Schematic representation of N, SmA and SmC calamitic mesophases with the corresponding director vector.

The discotic mesophases are classified in two types: *columnar*, and *nematic discotic*. The structure of the nematic discotic mesophase (N_D, Figure 3, left) is similar to that of rod-like molecules, but constituted by disk-like units. In columnar mesophases, the molecules are staking in a columnar disposition and depending on the type of columnar arrangement several columnar mesophases are known. Some common lattices of the columnar phases are columnar nematic (N_{Col}), columnar hexagonal (Col_h), columnar rectangular (Col_r), and columnar oblique (Col_{ob}) mesophases.

<Figure 3 near here>

Figure 3. Schematic representation of N, Col_h and Col_r discotic mesophases.

Polycatenar mesogens display mesomorphism characteristic of rod-like or disk-like mesogens depending on the number, length and arrangement of the chains. Detailed descriptions of these materials may be found elsewhere.[14,15]

In the case of banana liquid crystals, the bent-shaped molecules can adopt a compact packing arrangement that restricts rotational freedom, thus allowing the molecules to organize into novel types of liquid crystalline phases. These new mesophases are denoted by the letter B, which refers to the characteristic banana or bent molecular shape. For example, B_1, B_2, B_3, *etc.* have been used to designate different phases, chronologically as they have been discovered.[16]

When the mesomorphic compounds are chiral (or when chiral molecules are added as dopants) chiral mesophases can be produced, characterized by helical ordering of the constituent molecules in the mesophase. The simplest and most common is the chiral nematic phase (N*), which is also called *cholesteric*, taken from its first observation in a cholesteryl derivative. These chiral structures have reduced symmetry, which can lead to a variety of interesting physical properties such as thermochromism, ferroelectricity, etc.

Finally, there are lyotropic mesophases, which are typically formed by surfactant molecules in water. These molecules consist of a polar hydrophilic head and one or several hydrophobic aliphatic chains, which aggregates to form micelles in water. Depending on temperature, concentration and solvent different mesophases are found by aggregation of such micelles. Three representative types of micelles are presented in Figure 4.

<Figure 4 near here>

Figure 4. Schematic representation of micelle shapes: spherical, cylindrical and plate.

A book containing the essentials of liquid crystal science from the perspectives of chemistry and physics has recently been published, updating earlier versions by one of the authors.[17–19]

From a historical point of view, liquid crystals started with Reinitzer's pioneering work in the late 19th century. He found that cholesteryl benzoate displays two different melting points.[20] It is generally accepted that the first report on metal-containing liquid crystals was made by Vorländer in 1923, who reported on a series of mesomorphic mercury complexes: actually, organometallic compounds (Figure 5).[21] Heintz in 1855 had reported carboxylate magnesium soaps.[22] The term metallomesogens was proposed by Giroud-Godquin and Maitlis to refer to liquid crystalline materials containing metals.[23] They combine the variety of coordination chemistry with the exceptional properties of liquid crystals to form metal complexes organized in fluid phases. The incorporation of metallic fragments into mesophases enhances useful characteristics such as polarizability and birefringence, modifies other physical properties, such as color, electrical conductivity, luminescence and magnetism, which broadens the preparation of new materials with new applications.

<Figure 5 near here>

Figure 5. First organometallic mesogens.

2.2 Liquid Crystals Characterization

Mesophase characterization of liquid crystalline materials can be achieved by a combination of different techniques. The three basic procedures are briefly described.

Liquid crystals are characterized by Polarized Optical Microscopy (POM), an optical microscope equipped with a heating stage and two polarizing filters. Mesogens possess birefringence due their anisotropic refractive index and each mesophase appears to have a characteristic texture resulting from the different domains, which can often be used to assign the type of mesophase. In contrast, an isotropic liquid is dark under crossed polarizers. This technique allows the determination of transition temperatures and temperature ranges.

Liquid crystals are always characterized by Differential Scanning Calorimetry (DSC), which is complementary to POM. It is a technique that measures changes in heat capacity as a function of temperature, and it is used to detect phase transitions. Obviously, transition temperatures, energy involved and thermal stability (reproducibility of the heating–cooling cycles) can be determined more accurately with DSC. A review with data for 3000 organic liquid crystals was published.[24]

Finally, small-angle X-ray diffraction can determine the structure of a liquid crystal phase. It is important to note that X-ray diffraction experiments on the mesophase offer much less information than single crystal experiments. The number of observed reflections is low because of the disordered nature of the phases, and sample alignment is strongly recommended. The technique provides data such as the interplanar distance, the relative orientation of different sets of planes, the thickness of the layer, or the number of columns. In addition, the wide-angle X-ray region displays a broad peak corresponding to short range correlations between the molten hydrocarbon chains.

2.3 Physical Properties and Applications

As stated above, liquid crystals are anisotropic fluids, which implies that their physical properties are also anisotropic and this is the basis for the widespread application of the materials. For instance, the anisotropic refractive indices lead to birefringence and it is the primary way to characterize a mesophase. Other physical properties such as linear polarizability, dielectric permittivity, and diamagnetism can show anisotropy. Furthermore, these properties in thermotropic liquid crystals will depend on the temperature.

The physical properties will determine the applications. The first application reported for mesogens was as temperature sensors, based on the thermochromic behavior of the chiral nematic liquid crystals. This technology is still in use.

The development of very stable room temperature liquid crystals such as cyanobiphenyls[25] and the formulation of mixtures with temperature ranges sufficiently broad to be used in display applications (around −20 to 70 ^{o}C) led to the main application of this material: Liquid Crystal Displays (LCD) for flat panel displays. First, twisted nematic phase mode LCDs were common, then, TFT–LCDs (thin film transistor) enabled a large number of segments (for example 640 x 1024) and improve image qualities such as addressability and contrast. LCDs exhibit advantages as low weight, low space requirement, low power consumption, emits almost no undesirable electromagnetic radiation and can be made in almost any size or shape (up to 82-inch diagonal). That is why they are used in notebooks, desktop computers, television monitors, mobile phones, handheld devices, video game systems, navigation systems, and car dashboards. The display size and performance have been

dramatically improved, by the introduction of fast switching, better viewing angle dependency, good color quality, high brightness and contrast, to such an extent that LCD screens have ousted the traditional cathode ray tube (CRT) monitors. It is important to note that LCDs use the light-modulating properties of liquid crystals combined with polarizers, and need a backlight as source of illumination, lately light-emitting diodes (LEDs) have been used for this purpose. Despite the dominance of LCDs, other flat panel display technologies continue to be developed to address their shortcomings. The main competitor is OLED (organic light-emitting diode) displays: an OLED, organic LED, or organic electroluminescent diode, consists of a film of organic compound that emits light in response to an electrical current. This technology is already in the market and is competing strongly with LCD technology. A book has been written about liquid crystal devices, from fundamentals to the last advancements within LCD technology. [26]

Liquid crystals have become a major, multidisciplinary field of research, for LCD applications and beyond. For instance a theme issue beyond display applications,[27] reviews on applications for discotic liquid crystals,[28,29] ionic liquid crystals,[30] light responsive liquid crystals,[31] functional films for display applications, [32] liquid crystals in industry,[33,34] have been published. A book has appeared that deals specifically with semiconductor liquid crystals.[35]

Many common fluids are in fact liquid crystals, as for instance soap, which forms a variety of lyotropic liquid crystal phases depending on its concentration in water. There are also biological liquid crystals, which show typical lyotropic liquid crystalline phases (e.g., peptides, protein assemblies, cell membranes, and so on).[36]

Metallomesogens continue to be compounds of great interest in materials science due to their optical, mechanical, electrical and magnetic properties, obtained by combining the properties of metallic fragments with the fluidity and self-organization of liquid crystals. Therefore, in recent years many efforts have been carried out to add physical properties to mesogens in order to synthesize polyfunctional materials. These properties can be tuned with temperature by taking advantage of phase changes related to the liquid crystal behavior.

To date, a considerable number of luminescent, especially phosphorescent, metallomesogens have been produced mainly based on lanthanides, platinum, iridium, palladium, and gold. The most effective strategy for designing them has been the modification of known chromophores in order to introduce the anisotropy necessary to be mesomorphic. Luminescence has been obtained not only in solution or in the solid state but in the mesophase and can be tuned by temperature and the aggregation state (e.g., aggregation–induced phosphorescence leads to on–off systems). Metallomesogen-based emitting materials have been proposed for applications in LEDs (Light Emitting Diodes), information storage, sensors and optoelectronic devices.

Many studies have been conducted on spin crossover metallomesogens, which contain d-metal fragments with different magnetic and electronic properties due to their accessible high and low spin states. Some relationships between transition temperatures and these magnetic and electronic properties have been reported. Electrical and magnetic properties of metallomesogens containing d- or f-metal fragments as well as changes with temperature and phase state have also been studied in detail.

The more relevant results for these physical properties on metallomesogens are collected in various reviews and many will be explained later in this chapter.[9, 37–43] There are many lanthanide liquid crystals and a specific name to refer to them has been proposed: lanthanidomesogens. They have been recently reviewed but unfortunately no organometallic compounds have been reported.[44–46]

In summary, liquid crystal research is an ever-expanding field that especially attracts synthetic chemists and physicists with new materials and new phases for new or improved applications.

3 Organometallic Liquid Crystals of the Main Group Elements

Organometallic liquid crystals of the Main Group Elements remain scarce. The examples known are practically limited to some boron compounds, a number of silicon derivatives and a series of alkylgermanes.

Most of the mesomorphic boron compounds are based on clusters such as those shown as **1**, which display mainly smectic A mesophases.[47,48] Discotic borolane[49] (**2**) and boroxine derivatives (**3**)[50] showing columnar hexagonal mesophases have also been reported. It is worth noting that the mesophases of the borolane derivatives show good charge carrier mobilities (up to 8 x 10^{-2} cm^2 $V^{-1}s^{-1}$, Time-of-flight method).

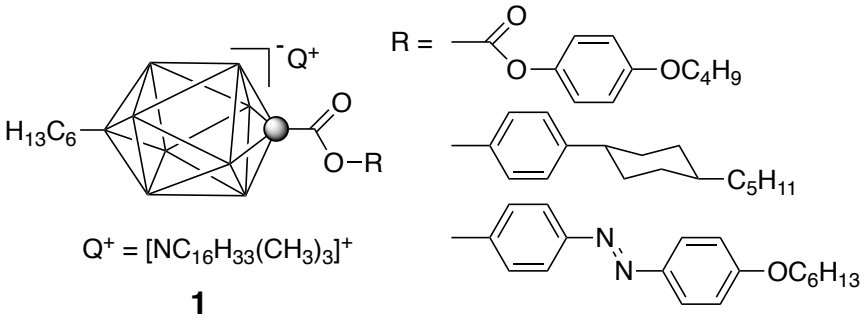

1

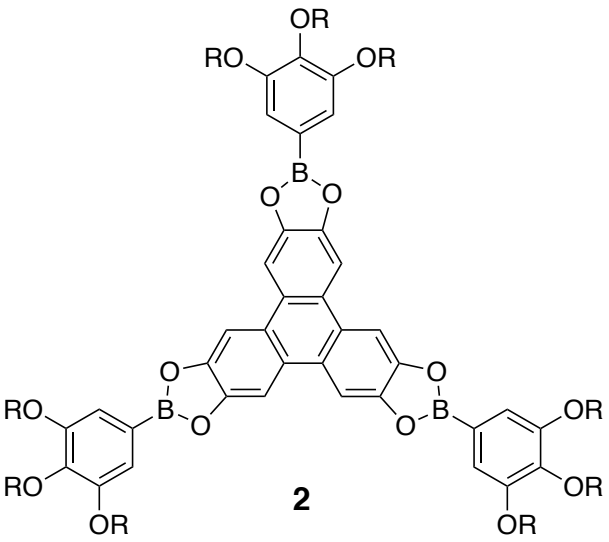

2

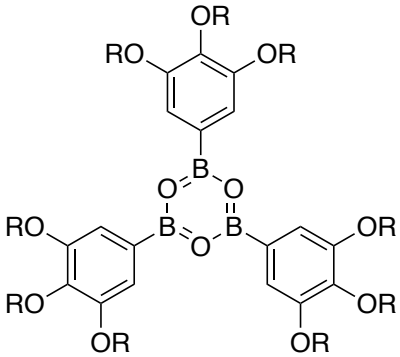

3

N-methyliminodiacetic acid (MIDA) boronates with different degree of substitution on the phenyl ring have also been studied (**4**). Their mesophase type is determined by the number and length of alkoxy chains.[51] Compounds bearing one or two short tails (n = 6, 8) display smectic A phases while the dialkoxy derivatives with longer substituents, and the trialkoxy series led to hexagonal columnar mesophases.

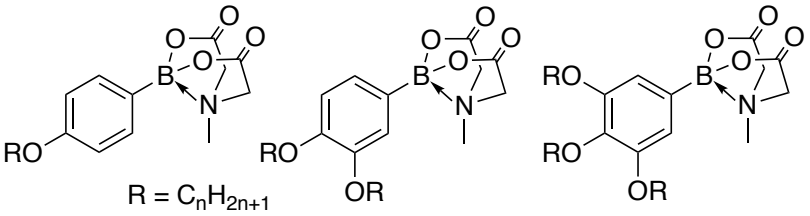

4

Recently, a few examples of N-heterocyclic carbene boranes (**5**) displaying smectic mesophases have also been prepared.[52] Some of them show polymesomorphism, but a complete characterization of the mesophases has not been done.

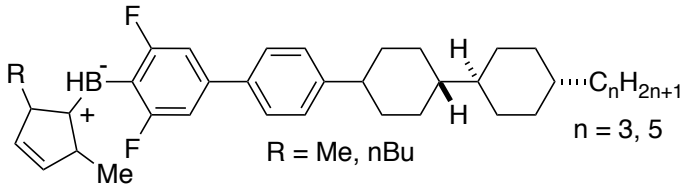

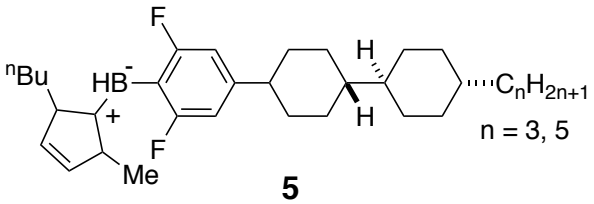

5

The organometallic liquid crystals of silicon are mainly based on oligomeric silsesquioxane molecules, in which a number of conventional mesogens are linked to the inorganic silsesquioxane cube through flexible spacers (**6**). Their mesomorphic properties can be modulated trough the shape of the mesogens, the spacer length, as well as the number of substituted corner chains.[53,54]

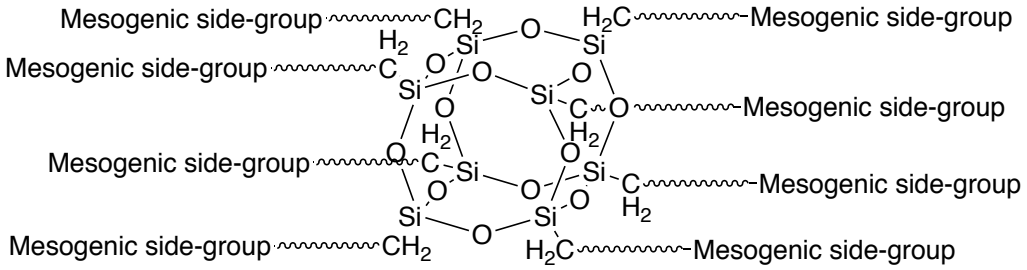

6

A variety of mesomorphic systems displaying different mesophases have been reported. For instance, 4'-ω-alkyl-4-cyanobiphenyls derivatives **7** displaying SmA mesophases,[55] derivatives bearing perfluorinated tails (**8**) showing lamellar mesophases,[56] or triphenylene compounds **9** and **10** that display columnar[57] or lamellar[58] phases respectively.

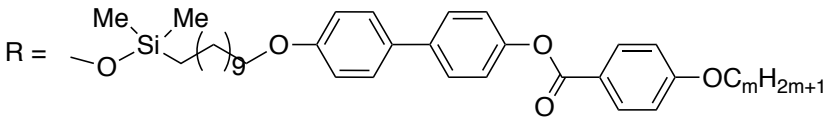

7

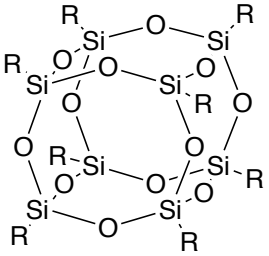

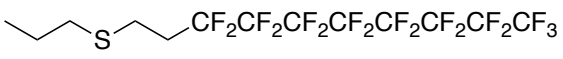

8

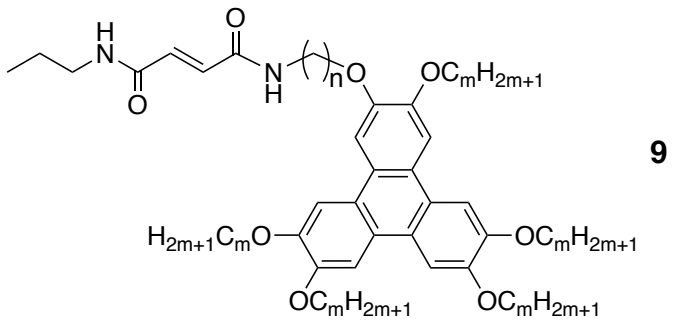

9

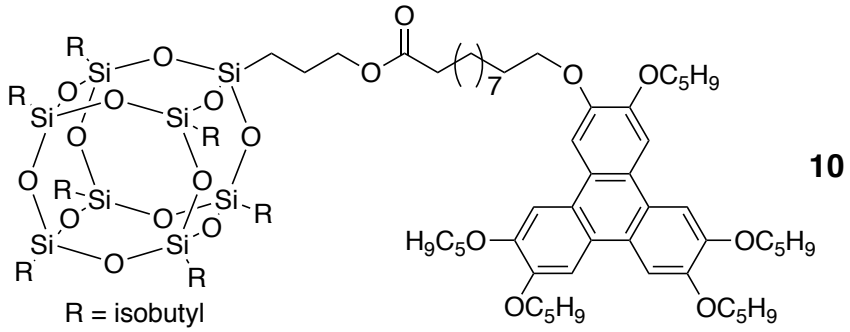

10

Concerning organometallic germanium liquid crystals, the examples reported are trialkylgermanes of the type **11**, in which the mesomorphic behavior is tuned by the number, nature and distribution of both the aromatic rings, and the tails.[59] Most of these complexes exhibit smectic and nematic mesophases. Ferroelectric behavior has also been found in complexes with chiral chains (SmC*).

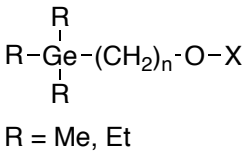

11

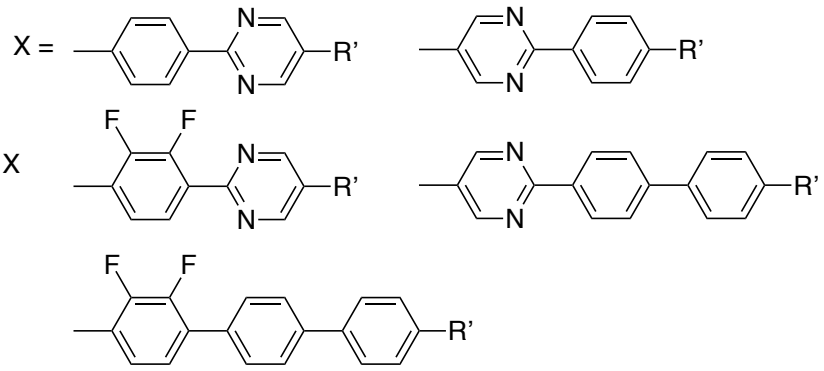

4 Organometallic Liquid Crystals of the Group 6 Elements

Previously, several liquid crystals of formula $M(CO)_3$(arene) were reported, but none during the period of time covered in this review.[1] However, some mesogens have been described by using the fragments $M(CO)_{4–5}$. For instance, the Mo(0) surfactants **12** (n =2, 6, 10) contain a hydrophobic metal

carbonyl fragment and are easily prepared from surfactant phosphine ligands. The supramolecular arrangement of these surfactants leads to molybdenum vesicles in water.[60]

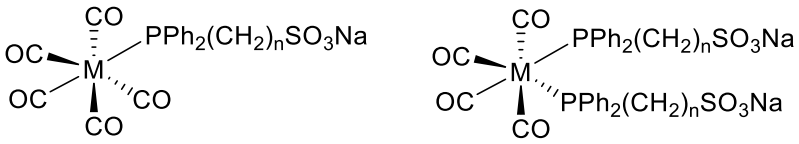

12

H-bonds are not quite strong, but are thermally stable at low to moderate temperatures and have been widely used to prepare liquid crystals, as can be seen in Section 9.1.5. This approach was carried out using 2,4,6-triarylamino-1,3,5-triazines equipped by 9 peripheral alkoxy chains, which behave as discotic liquid crystals at room temperature. These compounds are combined with *para*-isocyanobenzoic metal complexes, namely $[M(CNC_6H_4CO_2H)(CO)_5]$ (M = Cr, Mo, W) to give H-bonded aggregates **13**, and room temperature hexagonal columnar mesophases.[61] The clearing temperatures are in the range 77–84 °C, higher than for the free triazine (57 °C) and following the order: Cr>Mo>W. The supramolecular aggregates display high thermal stability, even in the isotropic state as confirmed by the infrared spectra (CN and CO vibrations). All the metal complexes (molecular or supramolecular) show a broad emission band at about 375 nm in solution at room temperature. Only the Mo and W complexes (molecular or supramolecular) display an intense yellow-green phosphorescence (maximum around 533 nm), assigned to a metal-to-ligand charge-transfer (MLCT), and with a lifetime of 53.9 µs. The corresponding gold(I) isocyanobenzoic acid complexes does not produce such adducts, likely due to the weak H-bonds with the triazine and the high insolubility of the gold acids.

An extension of this work was carried out by synthesizing gold(I) (see Section 9.1.5) and chromium(0) $[Cr(CO)_5(z\text{-}PPh_2C_6H_4COOH)]$ (z = 2 or 4) *ortho* and *para* phosphino metallo-acids.[62] X-Ray diffraction shows dimeric structures with the expected double carboxylic H-bonds in $[Cr(CO)_5(2\text{-}PPh_2C_6H_4COOH)]$. Reactions with the triazine mesogen lead to hydrogen-bonded chromium(0) supramolecular adducts, although only the 4-diphenylphosphinobenzoic adduct **14** shows a columnar hexagonal mesophase at room temperature with a clearing temperature of 38 °C (lower than 57 °C found for the free triazine). Therefore, the triazine bearing nine lateral alkoxy chains leads to mesomorphic adducts even for bulky metal–organic fragments, although the lability of the H-bonds limits the thermal stability.

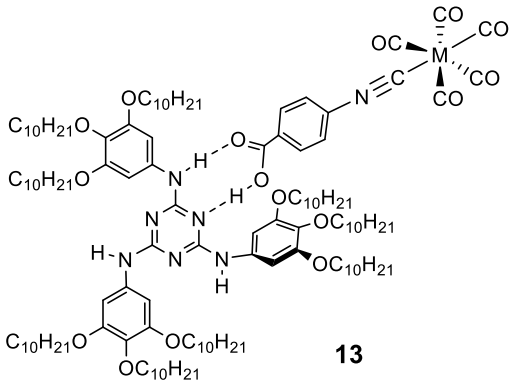

13

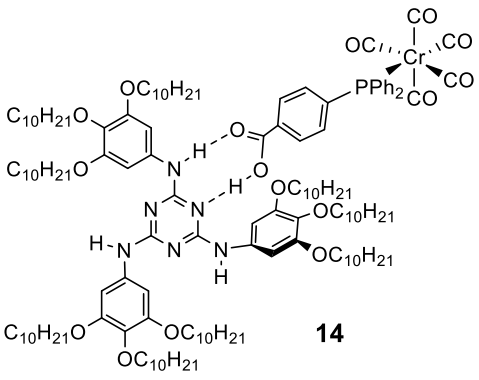

14

For this group, only a series of Re(I) compounds **15** (n = 12, 18) have been synthesized with dialkyl 2,2'-bipyridine-4,4'-dicarboxylate ligands.[63] The ligands and **15** (n = 12) are not mesomorphic, whereas **15** (n = 18) shows a short range existence unidentified mesophase (only 5°C; clearing at 117 °C). The corresponding coordination compounds with the fragment $CdCl_2$ are not mesomorphic, while with the $PtCl_2$ (n = 16) unit shows a smectic phase from 22 to 129 °C.

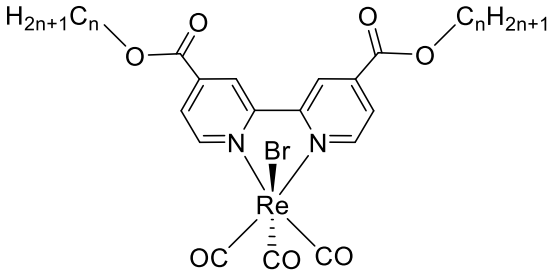

15

Bipyridine and phenanthroline ligands have also been used, but carbonyl rhenium (I) compounds were always non-mesomorphic, although the ligand or other coordinating compounds behave like liquid crystals. This has been related to steric effects due to the large volume of this octahedral fragment.[64–66]

6 Organometallic Liquid Crystals of the Group 8 Elements

6.1 Complexes of Iron without Cp

Many efforts have been carried out in order to prepare iron liquid crystals and also to relate the spin transition with the transition temperatures. In some cases there is an apparent synergy between spin-crossover and liquid crystalline transition and this coupling allows dielectric and magnetic properties induced by light, temperature, and pressure. The designed compounds are not properly organometallics and have been reviewed previously.[9,10,38,46]

During the time covered in this review, only a family of Fe(II) organometallic compounds without cyclopentadienyl have been described: a series of imines containing bis(tricarbollide)Fe(II) **16** (R = C_nH_{2n+1}; n = 4, 6, 8, 10, 12, 18), where each vertex of the icosahedron is a BH.[67] Each anionic carborane cluster (imine-$C_3B_8H_{10}^-$) is isolobal with the cyclopentadienyl anion and allows to prepare the analog ferrocene derivatives. These compounds exhibit nematic and smectic phases with clearing temperatures above 200 °C.

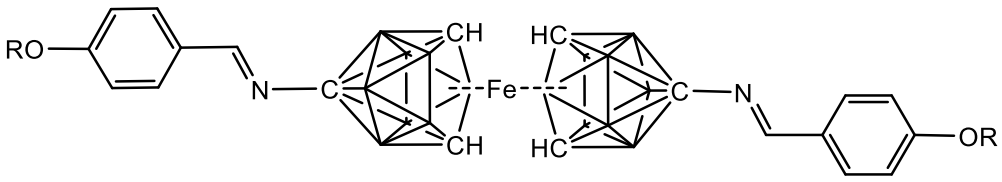

16

Furthermore, some Fe(0) carbonyl mesogens have been reported. An alkoxy phenyl isocyanide containing a partially fluorinated hydrocarbon chain has been used to prepare the corresponding

Fe(0) complex **17**, as part of a study containing this ligand and several metallic fragments.[68] The compound melts at 92 °C and is not mesomorphic, although most of the close complexes (metal groups 10–11) display SmA phases.

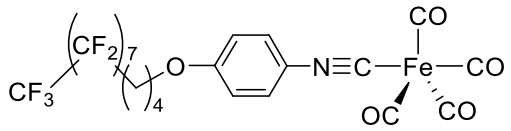

17

As described in Section 4 above for group 6 metals, the H-bond adduct **18** obtained by reaction of the *para*-isocyanobenzoic Fe(0) complex $[Fe(CNC_6H_4CO_2H)(CO)_4]$ with 2,4,6-triarylamino-1,3,5-triazine lead to room temperature hexagonal columnar mesophases.[61] This phase exists in the range 8–86 °C, with an isotropization temperature higher than for the free triazine and slightly higher than for the analogous Cr, Mo and W complexes. In solution at room temperature the complex and the aggregate display an emission band around 375 nm.

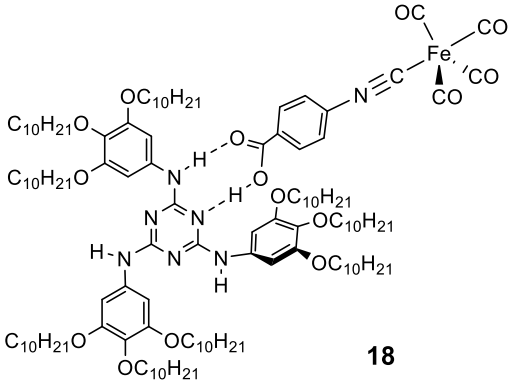

18

6.2 Ruthenium Organometallic Liquid Crystals.

Dinuclear ruthenium(I) dendritic complexes **19**, namely $Ru_2(CO)_4(O_2CR^1)_2L_2$ (generation 1 and 2; L = PPh_3, pyridine, 4-picoline; generation 3, L = PPh_3) have been prepared for dendrons of generation 1, 2 and 3.[69] They consist of a Ru–Ru bonded $Ru_2(CO)_4$ sawhorse unit bridged by two dendritic carboxylate ligands containing cyanobiphenyl moieties. All of them behave as quite stable enantiotropic liquid crystals, giving rise to smectic A (glass transition in the range 38–45 °C to isotropic from 150 to 204 °C) or smectic A (glass transition in the range 55–62 °C to nematic from 143 to 170 °C) and nematic (only for a short range of 3–12 °C before clearing) mesophases.

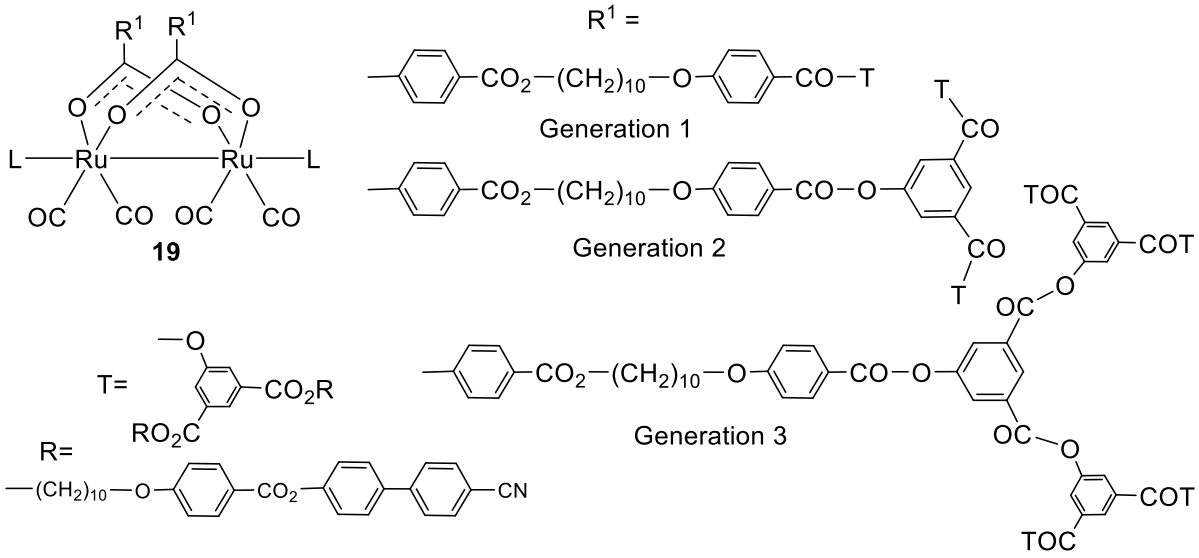

As commented above, the use of carbonyl carboxylato ruthenium is a typical way of producing liquid crystals. Another typical strategy is by means of arene ruthenium fragments. Reactions of the arene ruthenium metallacycle $[Ru_4(p\text{-cymene})_4(bpe)_2(donq)_2][DDS]_4$ (bpe = 1,2-bis(4-pyridyl)-ethylene, donq = 5,8-dioxydo-1,4-naphtoquinonato, DDS = dodecyl sulfate) with mesomorphic dendrimers containing pyrenyl-functionalized poly(arylester) and cyanobiphenyl, lead to host–guest supramolecular liquid crystals **20** (for generation 2 and 3).[70] The pyrenyl fragment is located in the central cavity of the tetranuclear ruthenium complex. The mesophases display a multilayered structure due to the tendency of each component to separate in different organized zones by chemical nature (microsegregation). The pyrenyl dendrimer ligands display a multilayered smectic A-like phase, with a glass transition at 33 and 66 ^{o}C, and an isotropization temperature of 165 and 219 ^{o}C, respectively, for generations 2 and 3. On the other hand, the adducts exhibit a multicontinuous thermotropic cubic phase as deduced by SAXS, which decompose above 100 °C due to the weak host–guest interaction. It is a spectacular example of liquid-crystalline behavior observed for such a large complex.

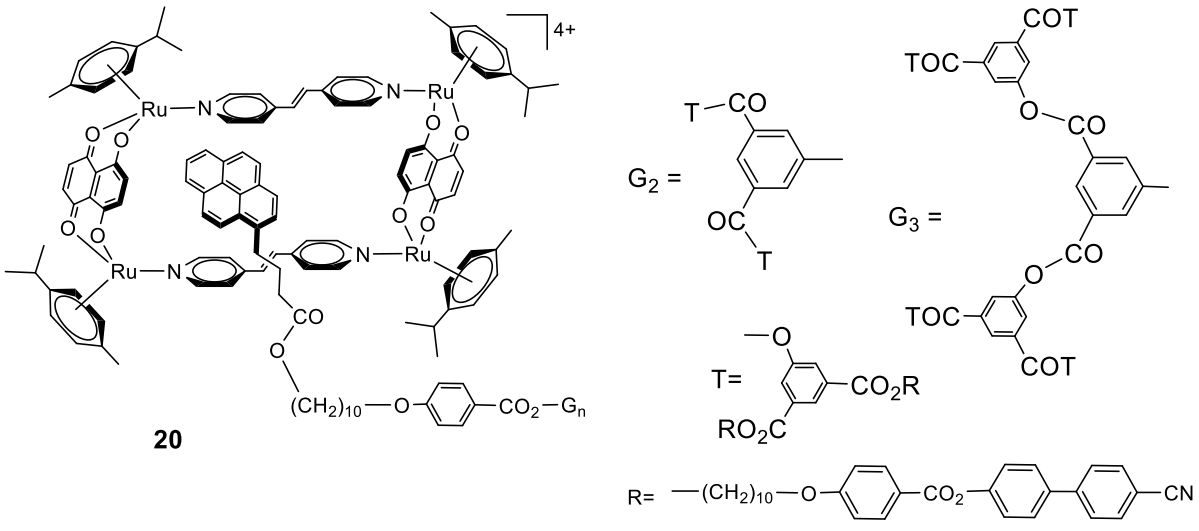

An extension of the previous work reported **21** $[Ru_4(p\text{-cymene})_4(L)_2(donq)_2][DDS]_4$ (donq = 5,8-dioxydo-1,4-naphtoquinonato, DDS = dodecyl sulfate), being L the bidentate N-donor ligand 1,4-di(4-

pyridinyl)-benzene with poly(arylester) dendrimers.[71] L and Ru_4-L_2 exhibit smectic phases (multilayered) above 50 °C, with an isotropization temperature of 180 °C for L, while Ru_4-L_2 decomposes at 160 °C.

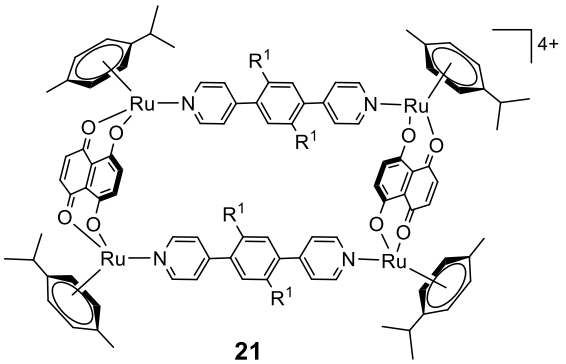

21

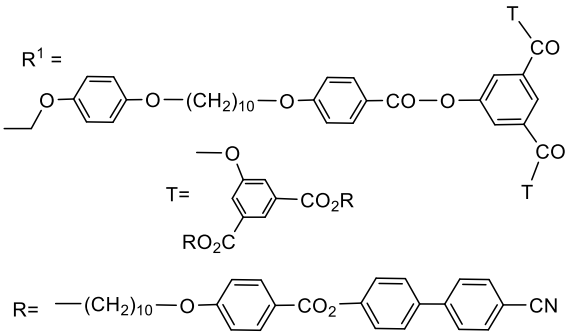

6.3 Ferrocene-Containing Liquid Crystals

6.3.1 Introduction

Ferrocene compounds have attracted much attention due to their well-developed synthetic chemistry, good solubility and high chemical stability.[72] Besides, its unique electrochemical properties have been exploited for the synthesis of sensors, biosensors and redox active supramolecular switches. Furthermore, its high thermal stability has allowed the synthesis of a great variety of liquid-crystalline materials.[9,10,73,74] Therefore, systems with ferrocene are one of the most common in organometallic liquid crystals. This chapter will show the main results obtained for ferrocene-containing liquid crystals, including mono- and disubstituted ferrocenes, systems based on ferrocenophane, heteronuclear complexes with ferrocene-containing ligands and ferrocene decorated fullerenes. Note that ferrocene-containing liquid-crystalline polymers will not be presented here, as stated in the general introduction, although some specific references are given.[75–79]

6.3.2 Monosubstituted ferrocenes

Monosubstituted ferrocenes are the most common ferrocenes with liquid crystal behavior. Moreover, monosubstituted ferrocenophanes are included in this section.

Aryl monosubstituted ferrocenes **22** (R = $C_{18}H_{37}$, C(O)-$C_{17}H_{35}$) and **23** (R = $C_{18}H_{37}$, C(O)-$C_{17}H_{35}$) containing a Schiff base and at least three phenyl rings are mesomorphic (with only two rings are non-mesomorphic).[80] Compounds display an unidentified phase in the range 133–144 °C (**22**, alkoxy), 126–154 °C (**22**, ester), 114–145 °C (**23**, alkoxy) and 129–155 °C (**23**, ester).

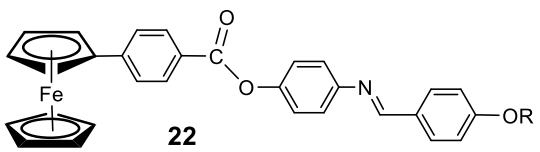

22

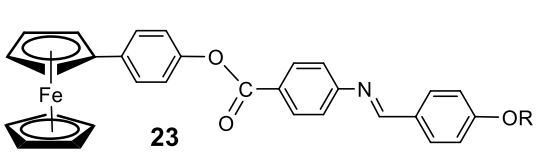

23

Close aryl monosubstituted ferrocenes **24** and **25** (R = $C_{18}H_{37}$, C(O)-$C_{17}H_{35}$) containing not only imine but azo functional groups have been prepared.[81] All the compounds exhibit enantiotropic nematic phases with melting points from 130 to 166 °C and clearing points in the range 154–247 °C, being the largest mesophase range of 81 °C (on heating) and 93 °C (on cooling) for compound **25** (R = $C_{18}H_{37}$).

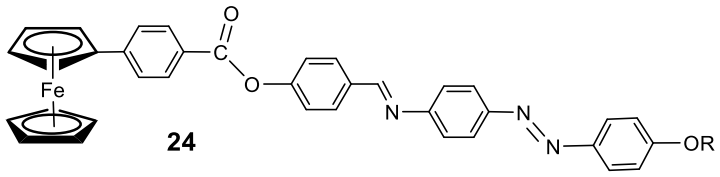

24

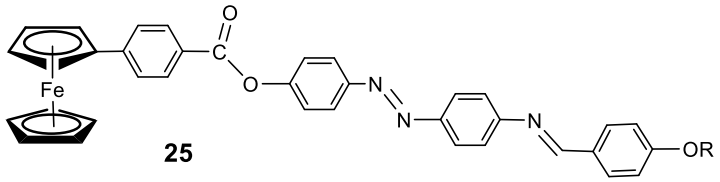

25

Aryl monosubstituted ferrocene mesogens **26** (n = 6–9) have been prepared by using ester connections and different chain length for the flexible spacer, but now with a terminal biphenyl group.[82] Derivative with n = 6 displays an enantiotropic nematic phase in a short range of temperatures, from 148 to 155°C. The others show only monotropic nematic phases from 113–142 °C to 40–76 °C. As expected the substitution of phenyl by biphenyl lead to higher phase transitions points as well as wider mesophase ranges.

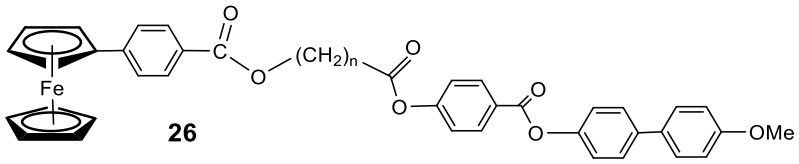

26

Rotationally fixed [3]ferrocenophane leads to a higher variety of molecular geometries in comparison with ferrocenes. Monosubstituted ferrocenophanes **27** (X = H, R = $OC_{12}H_{25}$; X = OH, R = $OC_{12}H_{25}$; X = H, OH, R = OOC-C_6H_4-$OC_{12}H_{25}$), **28** (R = $OC_{12}H_{25}$, OOC-C_6H_4-$OC_{12}H_{25}$), and the [3]ferrocenophane monosubstituted with a β-enaminoketone **29**, have been prepared. Compounds **27** with three phenyl rings display enantiotropic nematic phases as the corresponding ferrocenes. However **27** with only two phenyl rings and **28** derivatives are not mesomorphic or show monotropic nematic phases. Moreover, compound **29** display nematic and SmC phases on cooling. Thus, the introduction of the propylidene bridge at the β-position to the substituent on the cyclopentadienyl ring enhances mesomorphism. In contrast, the presence of the propylidene group in the α-position drastically reduces liquid crystal behavior compared to the corresponding monosusbstituted ferrocenes.

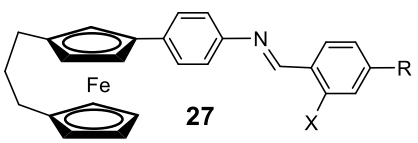

27

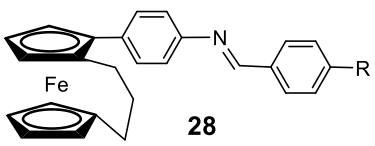

28

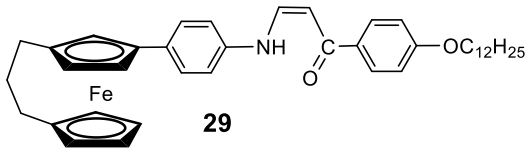

29

Ferrocene-carboxylates **30** (n = 2–12) have also been synthesized.[84] Only derivatives with longer spacer (n = 9–12) show monotropic nematic and smectic phases at room temperature, with temperature ranges of 25–37 °C. The liquid crystal behavior is much more limited that for the corresponding 1, 1'-disubstituted compounds.[85]

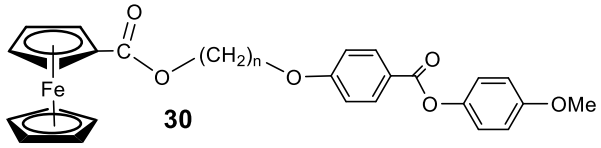

30

With the objective of achieving chiral phases, alkyl monosubstituted ferrocene **31** (n = 6, 11) and **32** (n = 6 , X = N, Y = C, $R^1 = R^2 = H$; n = 11 , X = C, Y = N, $R^1 = R^2 = H$; n = 6 , X = C, Y = N, R^1 = OH, R^2 = H; ; n = 6 , X = C, Y = N, $R^1 = NO_2$, R^2 = H) containing a cholesteryl have been synthesized.[86] Compound **31** (n = 6) exhibits a chiral nematic phase at 113 °C (clearing at 158 °C), while for n = 11 display a SmA phase at 110 °C, followed by short range twist grain boundary (TGB) and N* phases (clearing at 155 °C). All the compounds **32** show only a chiral nematic phase over a wide temperature range (from 90 to 240 °C), except for n = 11 where a SmA phase is observed before the N*.

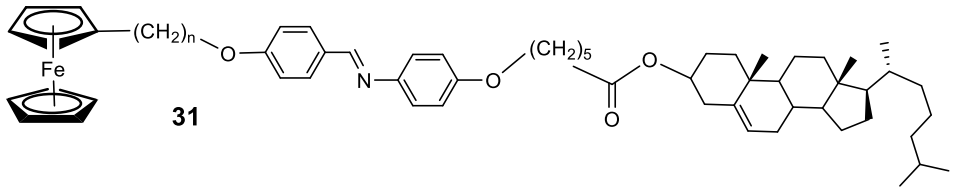

31

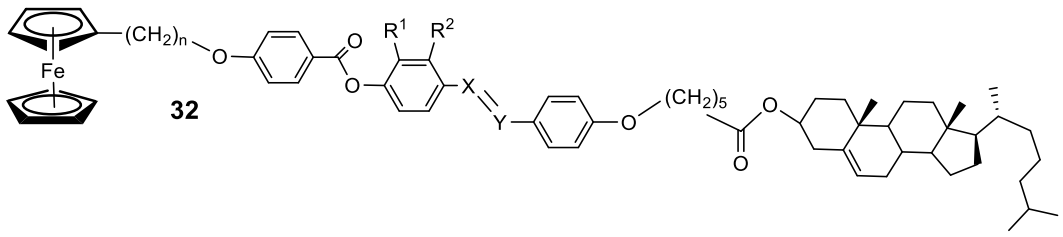

32

A series of ferrocene compounds **33** (n = 6, 11; R = H, OH; $R^1 = C_{12}H_{25}$, $C_{14}H_{29}$) has been synthesized in which the oxadiazole unit is in a terminal position connected to the ferrocene moiety through three phenyl with ester, ether or imine connections.[87] All of them exhibit a smectic phase starting at 101–149 °C, which converts into a nematic phase in the range of 170–195 °C (except the derivative with n = 11, R = OH, $R^1 = C_{14}H_{29}$, that isotropizes directly at 194 °C), and finally the clearing point from 177 to 203 °C.

Similarly, **34** compounds (n = 6, 11; R = H, OH; m = 5, 10) were prepared taking advantage of the same complex skeleton, where a cholesteryl group was placed at the end through an ester linkage.[88] All of them exhibit a TGBC* twist grain boundary phase having SmC* slabs, with melting points from 137 to 186 °C, which evolves to a N* phase from 155 to 225 °C. Finally, the clearing points go from 202 to 250 °C. A blue phase I and blue phase II is observed in a short range of 3 °C. It is remarkable

the presence of a TGBC* phase in a wide thermal range in the heating and cooling cycles for these chiral unsymmetrical metallomesogens.

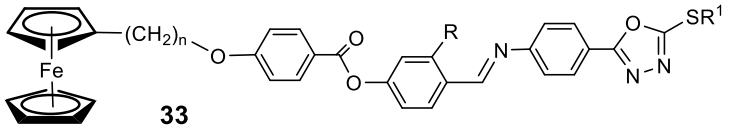

33

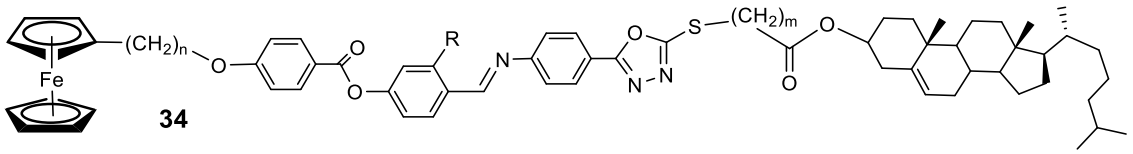

34

A series of ferrocene compounds **35** (n = 6, 11; m = 14, 16, 18) equipped with a 2-phenylbenzoxazole and variable length alkyl spacer and terminal alkoxy chains have been synthesised.[89] All of them exhibit enantiotropic smectic C phases with melting temperatures from 111 to 127 °C, and isotropization temperatures around 200 °C. Remarkably, the phases are stable over a wide temperature range due to the presence not only of long spacer and terminal chains, but also intramolecular hydrogen bonds.

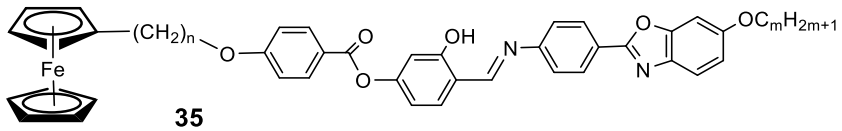

35

Ferrocene liquid crystals **36** and **37** containing 1,4-substituted-1,2,3-triazole and 5-halogen-1,4-substituted-1,2,3-triazole have been synthesized in order to stabilize the nematic phase, diminish the transition temperatures and to get larger mesomorphic ranges.[90] Compounds with X = H exhibit the typical nematic phase at high temperatures (around 200 °C) and short ranges. Halogen substituted derivatives display a wider mesomorphic temperature range (about 100 °C on cooling) but worse thermal stability; the transition temperatures are still higher than 100 °C except on cooling. The absorption spectra exhibit a peak at 480 nm for all of them, while the fluorescence emission spectra in solution display the maxima around 400 nm.

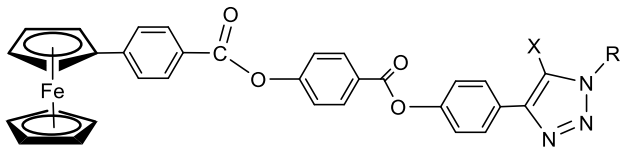

37 R = n-$C_{12}H_{25}$, X = H, Br, I

36 R =

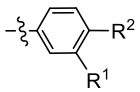

X = H, Br; R^1 = H, R^2 = $OC_{10}H_{21}$, $OC_{12}H_{25}$

R^1 = R^2 = OC_6H_{13},

Monosubstituted ferrocene compounds **38** (n = 8, 14, 16) have been prepared, which contain a heterocyclic unit as 1,2,3-triazole directly attached to the ferrocene moiety.[91] They show unidentified mesophases with melting points from 74 to 83 °C, and clearing points in the range 143–145 °C. Energies involved in isotropization transitions are quite high and the textures are unclear.

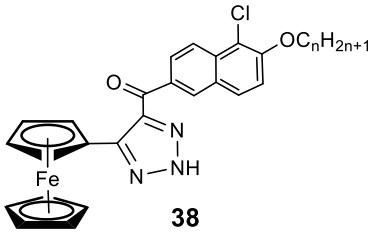

38

Most ferrocene mesogens show high transitions phase temperatures and typical ways of decreasing these temperatures is by lowering symmetry of the substituents and by adding cyclohexane fragments. A series of cyclohexane-containing aryl monosubstituted ferrocene **39** (Z = nothing, -N=CH-; n = 5, 10), **40** (without fluor) and [3]ferrocenophane **41** (Z = nothing, -N=CH-; n = 5, 10) have been synthesized.[92] Compound **39** biphenyl (Z = nothing) is not liquid crystal but the same **39** with imine display enantiotropic nematic phases in the ranges 119–135 °C (n = 5) and 110–117 °C (n = 10) for the first heating. Ferrocene-imine **40** and ferrocenophane **41** show monotropic nematic phases on cooling from 134 to 127 °C (**40**), 86–83 °C (**41**, biphenyl, n = 5), 82–61 °C (**41**, biphenyl, n = 10), from 143°C (**41**, imine, n = 5) and 117–61 °C (**41**, imine, n = 10). In general, lateral fluoro-substituents and [3]ferrocenophane play a positive effect over the nematic state. Complex thermal behavior is observed after several heating–cooling cycles.

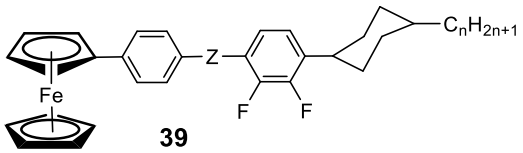

39

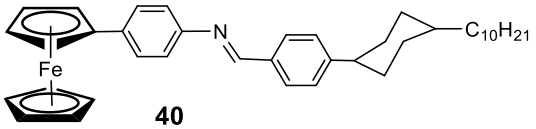

40

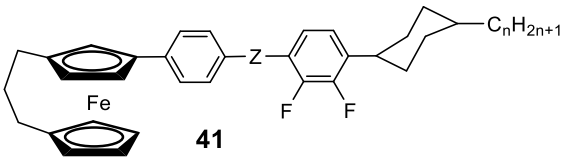

41

Combination of ferrocene and naphthalene moieties has also been carried out in order to get low temperature mesomorphism (below 100 °C), which can be of interest for many applications in devices. The resulting compounds **42** (n = 8, 10, 12, 14, 16) exhibit monotropic nematic phases in a short range (14–17 °C) and isotropization temperatures in the range 69–88 °C.[93]

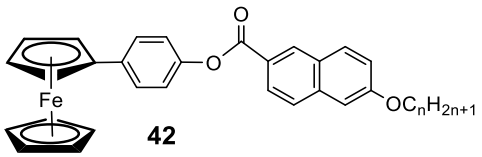

42

During the last years, various interesting possibilities for ferrocene compounds have been reported, we can highlight lyotropic phases and chiral dopants. The surfactant with ferrocenyl group **43** has been synthesized.[94] Surfactants are functional molecules containing a hydrophilic head (as ammonium) and a hydrophobic tail (as alkylferrocene). An ordered lamellar lyotropic liquid crystal is observed when the concentration of ionic derivative **43** in water solution is over 40 wt %. Moreover, this lyotropic liquid-crystalline organization can be controlled by redox reaction (ferrocene/ferrocenium redox couple) and photopolymerization. Ferrocene maybe useful as redox–

responsive chiral dopant, as reported for compound **44**, capable of reversibly modulating color (from blue to green) in a cholesteric liquid crystal such as 4'-pentyloxy-4-cyanobiphenyl.[95]

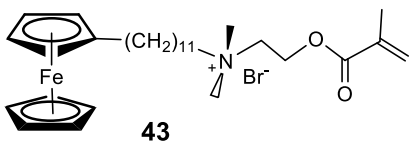

43

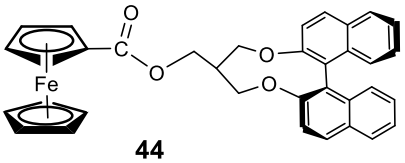

44

6.3.3 Disubstituted ferrocenes

Disubstituted ferrocene liquid-crystalline compounds can be classified into two types as a function of the position of the substituents: heteroannularly disubstituted 1, 1'-, and homoannularly 1, 3-. The former type gives place to "S" or "U" shapes, while the latter type leads to a "T" shape, all of them enhance mesomorphism compared to the corresponding monosubstituted compounds. Other possibilities as for instance 1, 2- substitutions are detrimental for this property due to the hairpin shape.

Rotationally fixed disubstituted [3]ferrocenophanes **45** (R = $OC_{12}H_{25}$, OOC-C_6H_4-$OC_{12}H_{25}$) and **46** (R = $OC_{12}H_{25}$, OOC-C_6H_4-$OC_{12}H_{25}$) are prepared, but the geometries are detrimental for mesomorphism: **45** derivatives with the two substituents in the same Cp are not mesomorphic, while **46** derivatives (1, 1'-substitution) show monotropic unstable N or Sm phases.[83] The liquid crystal properties are worse than those found for the corresponding monosubstituted compounds (reported in the same article but commented in the previous section).

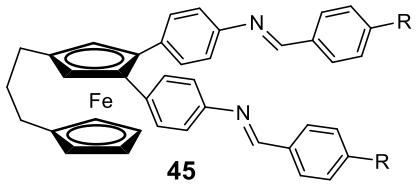

45

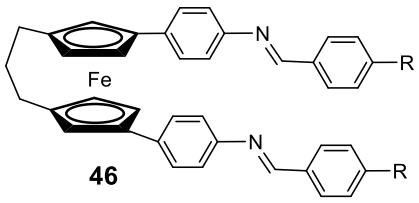

46

Some relevant results were reported by preparing unsymmetrically 1,1'-bis-substituted ferrocene **47**, which contains an extended ferrocene core due to a standard phenylimine and a difluorobiphenyl group.[96] Besides, a flexible *p*-decylciclohexane moiety is bonded to the biphenyl. Non-conventional tetrahedratic smectic C (SmC_T*) and tetrahedratic nematic (N_T*) mesophases have been observed, in the short range 203–216 °C and from 216 to 275 °C, respectively. A reasonable explanation for the macroscopic chiral domains and helical superstructures can be drawn from the tetrahedral liquid crystal order. An extension of this work led to a series of symmetrically and asymmetrically 1,1'-disubstituted ferrocene compounds **48–50**, with related ligands and able to display again non-conventional lamellar (SmA_T* and SmC_T*), nematic (N_T*) and even columnar (Col_{mix}) phases.[97] The main features of these mesophases include spontaneously developed macroscopic homochiral domains, helical and myelinic supramolecular formations, and some optical biaxiality. Free rotation of the cyclopentadienyl rings in the ferrocene lead to bent conformations and the conformational enantiomers stabilize by assembly into tetrahedral molecular units. The columnar mesophase is formed by a mixture of bent and nonbent conformers. The compounds melt around 200 °C (except for **48** with n = 10, Col_{mix} at 163 °C), and isotropizations temperatures go from 206 to 287 °C.

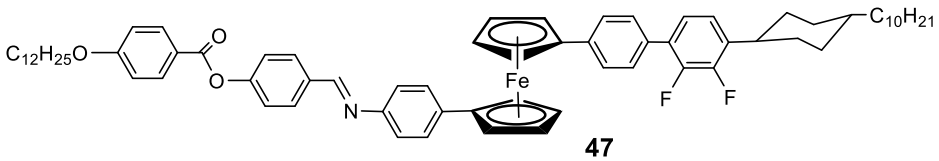

47

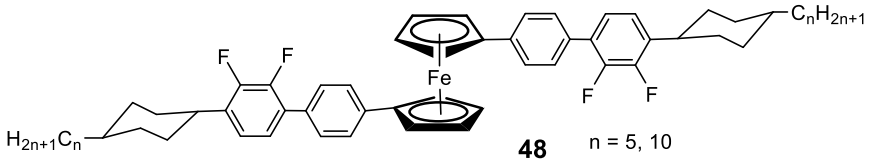

48 n = 5, 10

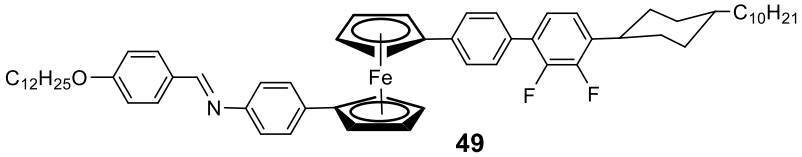

49

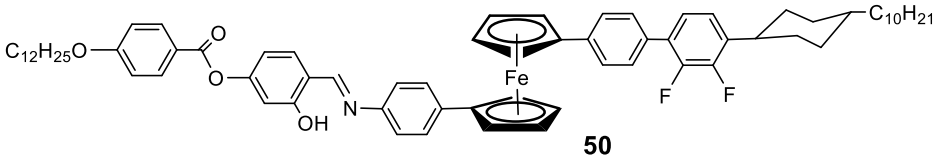

50

Some efforts have been carried out to solve X-ray single crystal structures of mesogens in order to establish crystal structure/mesophase relationships. For instance the single crystal structure of 1,1'-bis[3-[4-(4-methoxyphenoxycarbonyl)phenoxy]propyloxycarbonyl]ferrocene **51** show that the two substituents lie in the same direction (U shape), and not one on each side, which is related to the observed nematic phase.[98]

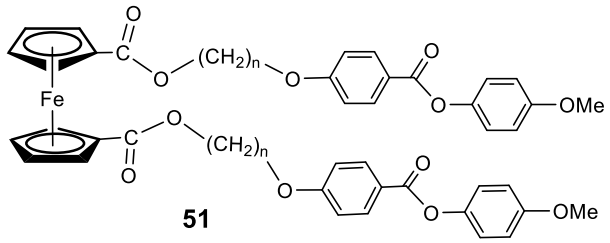

51

1,3-disubstituted ferrocene derivatives **52** (n from 2 to 10) were also prepared.[99] They display monotropic nematic mesophases (except for n = 2 and 4) in short ranges of temperature. The results are rationalized by noting that: when n is odd the molecule is more linear but more banana if n is even.

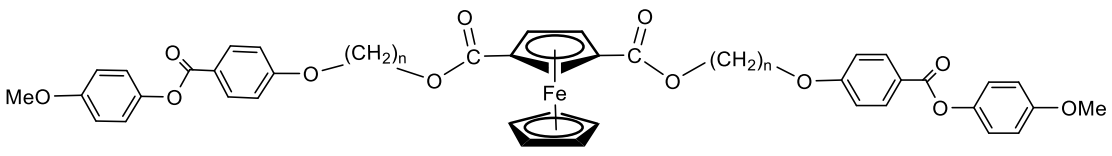

52

Recently, the disubstituted ferrocene compound, 1-triisopropylsilylethynyl-1'-trimethylammoniummethylferrocene **53** has been synthesized.[100] It is a surfactant that forms micelles and vesicles by aggregation at a very low concentration as well as lyotropic liquid crystals, not only with water, but also with a variety of organic solvents. Furthermore, the alkyne group can be deprotected and used as ligand to coordinate to metallic fragments.

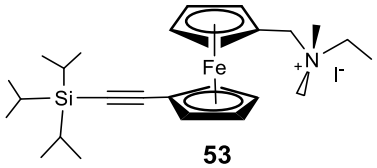

53

6.3.4 Heteronuclear complexes with ferrocene as ligand

Ferrocene or ferrocenophane compounds have been extensively used as ligands to prepare heteronuclear complexes of various metals, which can combine the optical, magnetic or electric properties of both metallic fragments. Note that these complexes are only described here, but not in the corresponding second metal section.

In such a way monosubstituted ferrocenophane equipped with a base Schiff, yield *ortho*-palladated compounds **54**–**57**.[101] **54** are non-mesomorphic, whereas **55** display SmA mesophases in the range 198–260 °C (mixed with some decomposition at the isotropization) and **56**–**57** nematic mesophases phases over a broad temperature range from 71 to 205 °C.

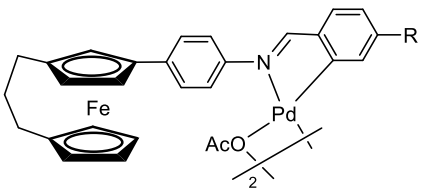

54

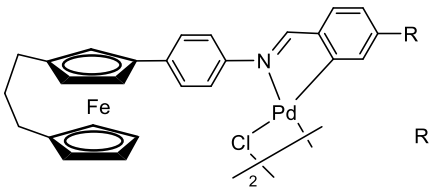

55

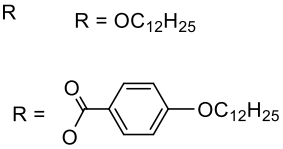

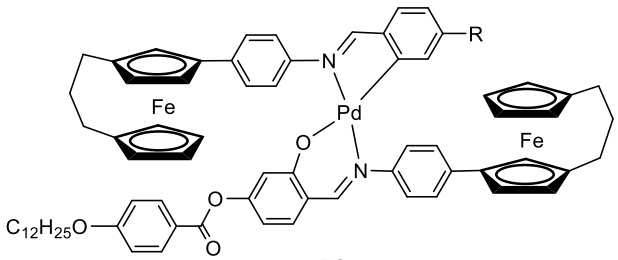

56

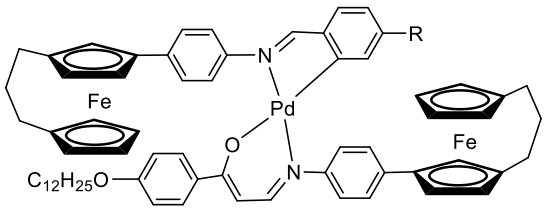

57

An extension of this work has been carried out by functionalization of the ferrocenophane group with salycilidene and additional chelation to copper(II), nickel(II), palladium(II) and oxovanadium(IV), to give complexes **58**. Similarly, copper(II) and palladium(II) compounds **59** have also been prepared after functionalization with aminovinylketone.[102] The heteropolynuclear complexes **58** exhibit high temperature enantiotropic nematic phases for copper (199 to 230 °C), palladium (257 to 277 °C) and oxovanadium (217 to 242 °C), while complexes **59** display monotropic nematic phases for copper (at 131 °C) and palladium (at 188 °C), in the last case followed by a SmC phase at 173 °C.

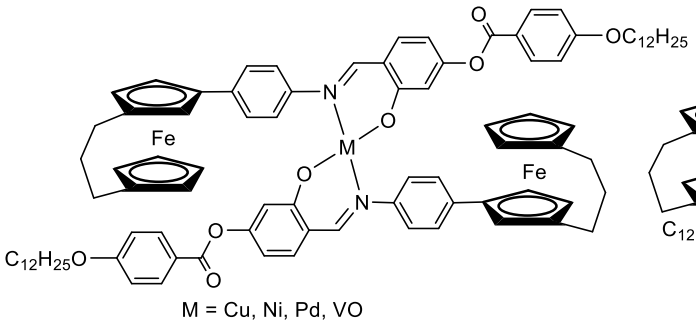

58

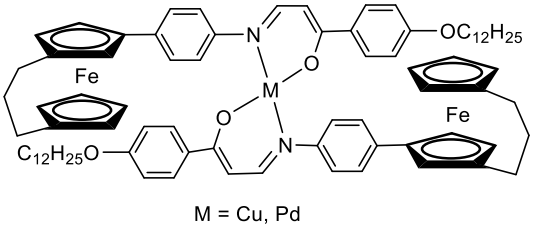

59

The analog monosubstituted ferrocene ligands containing an enaminoketone have been synthesized and then chelated to Cu(II) and Pd(II) ions in a 2:1 molar ratio (**60**).[103] Cu(II) complexes show disordered soft crystal phases (on cooling at 107 or 120 °C for n = 12 or 16, respectively) while Pd(II) complexes display monotropic smectic C phases (on cooling at 136 or 140 °C for n =12 or 16, respectively).

Monosubstituted ferrocene ligands equipped with a diketonato were prepared, as well as the corresponding chelated copper(II) and zinc(II) complexes **61** (n = 8, 9, 10, 12, 14, 16).[104] The copper compounds display melting points in the range 76–106 °C and clearing points from 106 to 163 °C. On the other hand, the zinc compounds show lower melting (from 23 to 49 °C) and clearing points (from 97 to 139 °C), as well as a wider mesophase range compared with the copper derivative.

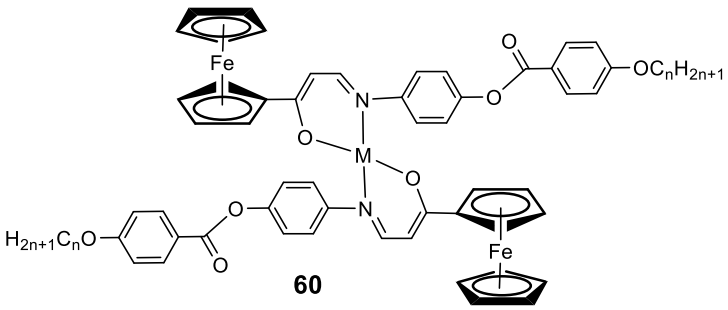

60

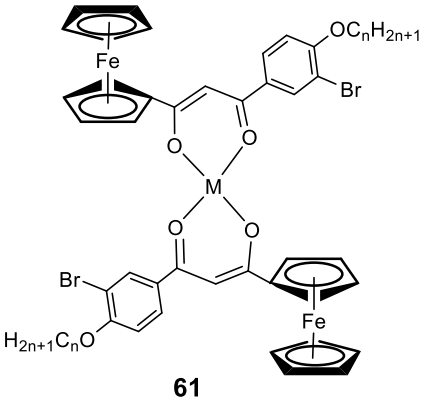

61

6.3.5 Ferrocene-containing fullerenes

Liquid-crystalline materials equipped with fullerenes have attracted much interest for the development of supramolecular switches and in solar cells.[105]

Monosubstituted nonamethylferrocene compound **62** and the model compound **63** (without a large mesogenic fragment) are prepared by attachment to a fulleropyrrolidine.[106] Only the dyad **62** exhibits an enantiotropic smectic A phase in the range 57–155 °C.

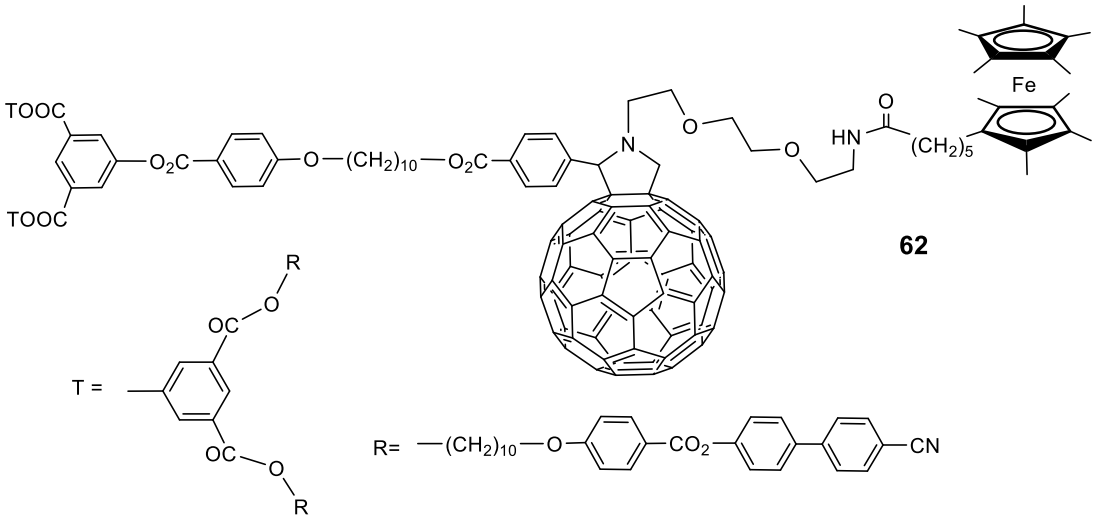

62

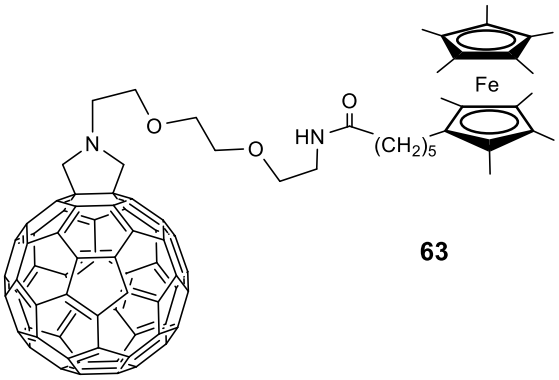

63

Monosubstituted nonamethylferrocene compound **64** and the corresponding ferrocenium compound **65** (not drawn: as **64** but monocationic, anion is 4-methylbenzenesulfonate), which contain C_{60} in the middle and ferrocene and a mesogenic unit as terminal ends, are enantiotropic liquid crystals.[107] Both exhibit sequentially SmA and SmB phases with melting points around 80–90 °C, mesophase transition around 125 °C and clearing point about 130 °C. These compounds were studied by ^{13}C NMR in isotropic, liquid crystal and crystalline phases to find out that the fullerene–ferrocene dyads rotate fast to form highly dynamic liquid-crystalline phases.

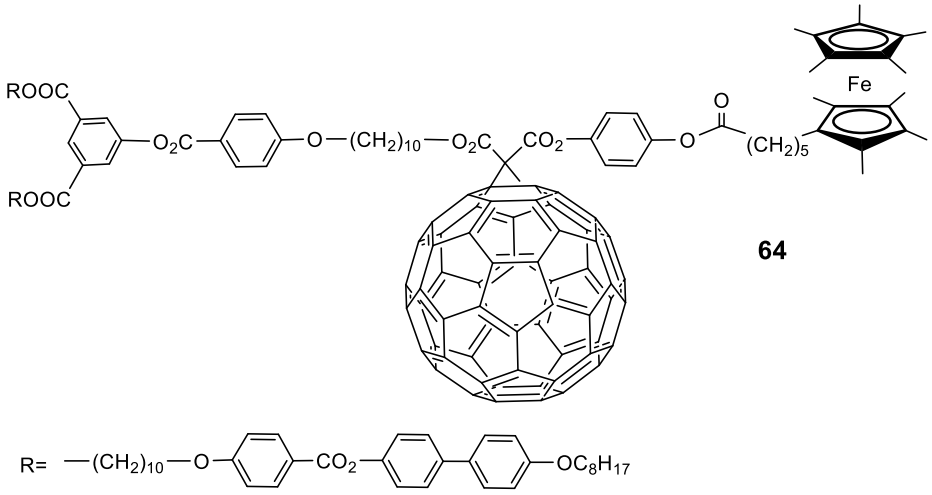

64

Compound **66** (R = n-$C_{12}H_{25}$, n-$C_{18}H_{37}$) contains a polar iron–ferrocene fragment, a conical shape, and long alkyl chains, which allow the formation of liquid crystalline phases in a large range of temperatures, from 55 to 230 °C for C_{12}, and from room temperature to 186 °C for C_{18}.[108] The molecules exhibit microphase separation to form a crystalline and a thermotropic liquid crystalline phase. Moreover, the compounds are redox active (C_{60}-ferrocene) and emissive (central cyclophenacene emits at 480–700 nm).

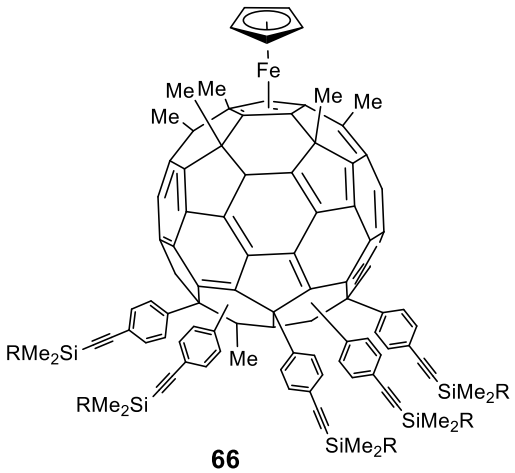

66

6.3.6 Conclusions

Ferrocene is still one of the most used systems to prepare organometallic mesogens. A great variety of compounds have been described because of the versatile synthetic chemistry that can be carried out and its high thermal stability. Shape–structure–property relationships have been stablished in order to understand the properties obtained. New carefully designed materials, can add the components properties to the final material.

7 Organometallic Liquid Crystals of the Group 9 Elements

7.1 Rhodium carbonyl complexes

A series of *cis*-[RhCl(CO)$_2$(Ln)] complexes derived from polycatenar pyrazole ligands (Ln) have been described (**67**).[109] However, only the complex containing six decyloxy substituents (R_1, R_2, R_3 = $OC_{10}H_{21}$; R_4 = H) is liquid crystal. It shows an enantiotropic columnar mesophase in the range 31–47 °C. Although these molecules are not discotic when considered individually, stacked in an alternating antiparallel arrangement, they are able to generate columns with an almost circular cross section. The diameter of the column is less than twice the molecular radius, indicating that there is slight interdigitation between neighboring antiparallel molecules.

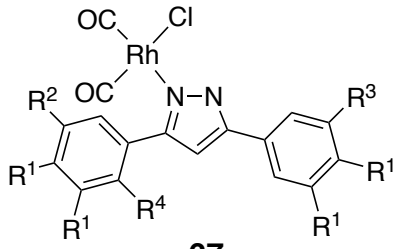

67

$R_1 = OC_{10}H_{21}$; R_2, R_3, $R_4 = H$
R_1, $R_2 = OC_{10}H_{21}$; R_3, $R_4 = H$
R_1, $R_2 = OC_{10}H_{21}$; R_3, $R_4 = H$
R_1, R_3, $R_4 = OC_{14}H_{29}$; $R_2 = H$
R_1, R_2, $R_3 = OC_{10}H_{21}$; $R_4 = H$

7.2 Cyclometalated Iridium complexes

Octahedral cyclometalated Ir(III) complexes are interesting systems of high importance as phosphorescent emitters. Their photophysical properties can be fine-modulated by selective functionalization on both the cyclometalated and the ancillary ligands, extending their potentiality beyond usual light emitting application. Perhaps, that versatility to tune their properties together with the fact that cyclometalated Ir (III) complexes constitute a fairly stable system, can explain their great development in recent years.[110]

The first reported example of liquid crystal based on cyclometalated Ir(III) complexes was the bipyridine complex **68**, which displays a monotropic hexagonal columnar phase (Col_h).[111] The compound displays a phosphorescent emission in solution, in the solid state and in the mesophase, corresponding to a mixed ^{3}LLCT/^{3}MLCT transition (LLCT = ligand-to-ligand charge). The emission bands of the liquid-crystalline and crystalline phases were both blue shifted, with significantly higher quantum yield, compared to those observed in dichloromethane. The dodecyloxy derivative has also been prepared, displaying an enantiotropic columnar mesophase from room temperature until 115 °C. This chromophore, inside micelles formed by the poly(ethylene oxide)$_{100}$-poly(propyleneoxide)$_{70}$-poly(ethylene oxide)$_{100}$ copolymer in water, leads to luminescent lyotropic phases.[112]

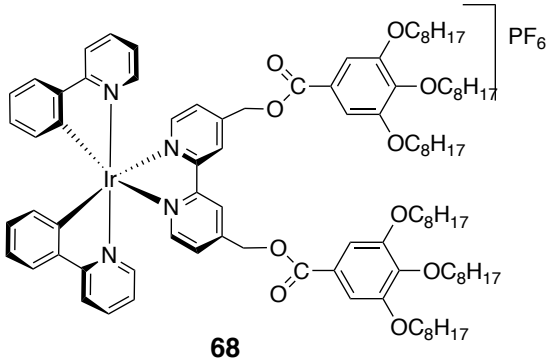

68

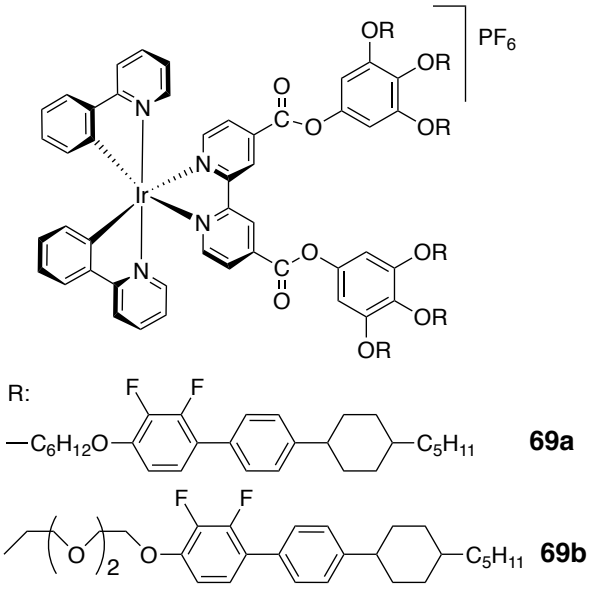

69a

69b

Two similar complexes (**69**), but with a different linker between the bipyridyl moiety and the mesogenic pendent groups, display smectic A mesophases (**69a**: 216–235 °C; **69b**: 156–177 °C).[113]

This system constituted the first example of directly polarized electroluminescence based on phosphorescent iridium complexes.

Cyclometalated Ir(III) complexes bearing anisotropic polycatenar 2,5-diphenylpyridine ligands also lead to liquid-crystalline complexes (**70**–**73**).[114]

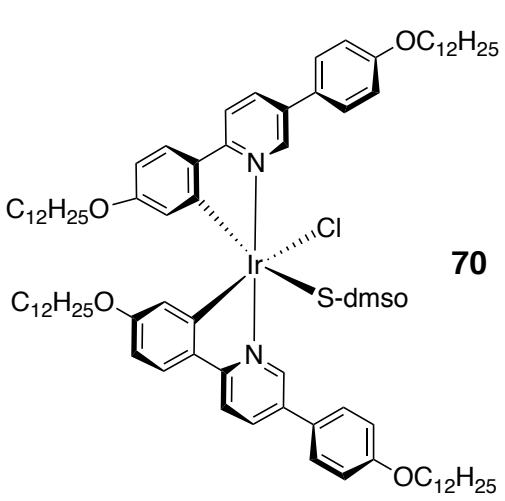

70

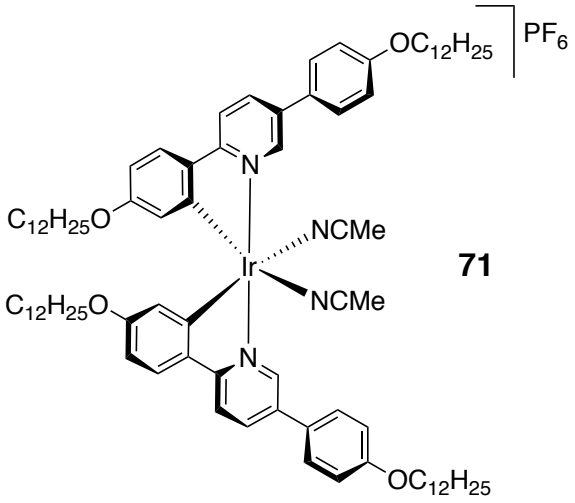

71

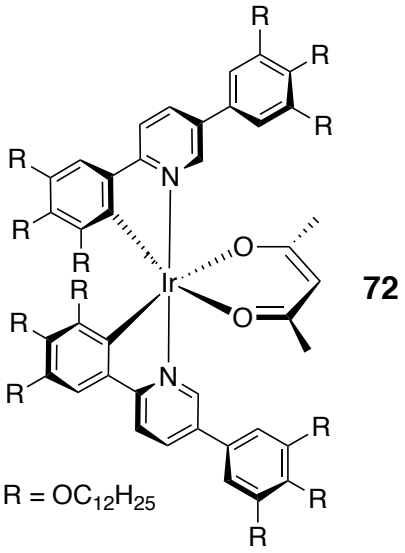

72

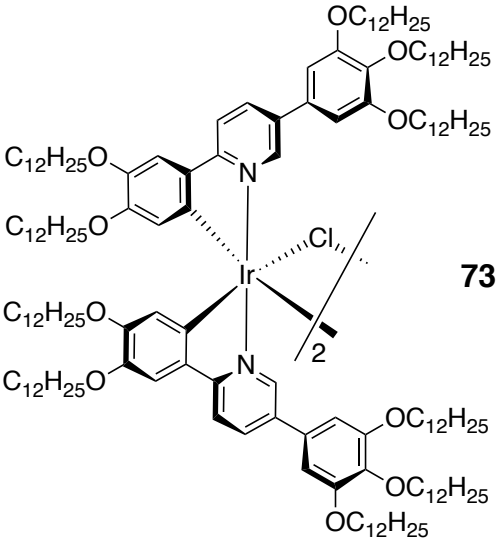

73

The complex **70** was obtained by cleavage of the corresponding di-μ-chlorodiiridium-(III) dimer with dimethyl sulfoxide. This compound is not stable over time, but shows a centered rectangular mesophase (*c*2mm, a = 60.92 Å, b = 43.1 Å), which could be indicative of either a columnar rectangular phase or a ribbon phase. In contrast, the bis-acetonitrile cationic complex **71** displays good stability and shows a columnar mesophase between 145 °C and 163 °C. Both complexes were slightly emissive in CH_2Cl_2 solution. Looking for luminescent iridium-based LCs, attention was then turned to neutral complexes bearing acetylacetonate (acac) as the ancillary ligand. **72** is liquid crystal, exhibiting an emissive columnar hexagonal phase between 31 °C and 66 °C (λ = 582 nm, Φ = 9.1%). Similarly, the di-μ-chlorodiiridium-(III) dimer **73** also exhibit a columnar liquid crystal phase from room temperature to 75 °C, but in this case with a weaker emissive character (λ = 570 nm, Φ = 0.8%).

Using strongly mesogenic groups attached to an acetylacetonate ancillary ligand, mesomorphic iridium complexes have also been prepared (**74**). All of them display a smectic A mesophase, which

in the case of the fluorinated derivatives, is monotropic in nature. These systems show blue- and green- phosphorescence in solution, as well as high hole mobility in solid films.[115]

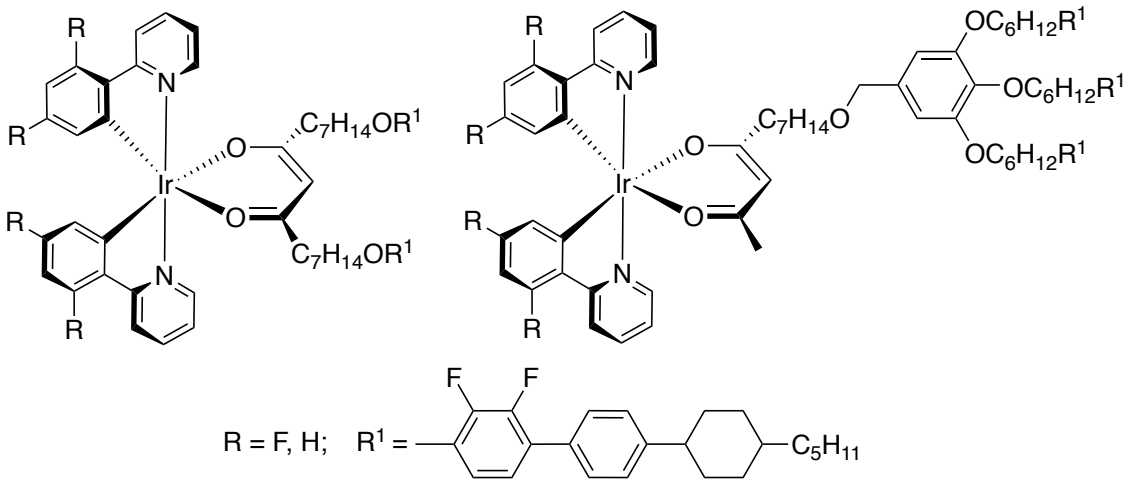

74

Related dinuclear Ir(III) complexes based on polycatenar diphenylpyridine ligands with 1,1,2,2-tetraacetylethane as the bridging ligand **(75)**,[116] exhibit orange luminescence in solution of CH_2Cl_2, and luminescent columnar hexagonal mesophases. As the two iridium centers are asymmetric, two diastereoisomers are possible (meso form with Λ-, Δ-stereochemistry and the racemate form with Δ,Δ- and Λ,Λ- stereochemistry). All the complexes were isolated as a mixture of these two stereoisomers, which, in the case of complex **B**, could be separated by column chromatography. However, it did not prove possible to identify their respective absolute configurations. Despite both isomers exhibiting identical emission properties and columnar hexagonal phases, their mesophase temperature ranges differed from 79–126 °C for one isomer to 63–95 °C for the other.

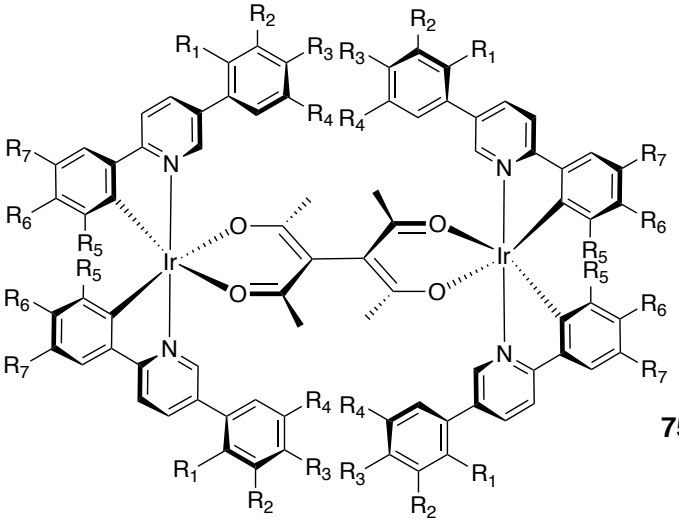

75

R_2, R_3, R_4, R_6, R_7 = $OC_{12}H_{25}$; R_1, R_5 = H (**A**)
R_1, R_2, R_3, R_6, R_7 = $OC_{12}H_{25}$; R_4, R_5 = H (**B**)
R_2, R_3, R_4, R_5, R_6, R_7 = $OC_{12}H_{25}$; R_1 = H (**C**)
R_3, R_5, R_6, R_7 = $OC_{12}H_{25}$; R_1, R_2, R_4 = H (**D**)

More recently, related neutral liquid-crystalline iridium(III) complexes with pyridyltetrazolate ligands have been reported (**76**). They display hexagonal columnar mesophases with an ambipolar carrier mobility behavior along the columns.[117]

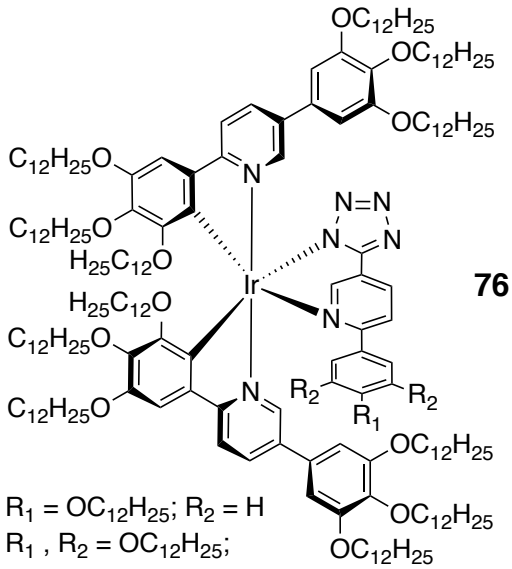

76

8 Organometallic Liquid Crystals of the Group 10 Elements

8.1 Isocyanide complexes

Isocyanides (CNR) are versatile ligands which give stable complexes of many metals, including the group 10 elements. A variety of types of mesomorphic palladium and platinum isocyanide complexes are known. All of them are phenyl isocyanide derivatives bearing different substituents in the *para* position of the aromatic ring.

A series of mesomorphic palladium and platinum complexes, *trans*-[$MI_2(CNC_6H_4O(CH_2)_4(CF_2)_8F)$] (**77**), containing an isocyanide ligand with a semifluorinated alkoxy chain, have been prepared.[68] Complexes of Ag, Au and Cu complexes with this isocyanide have also been studied, and their mesomorphic properties will be described in the corresponding section.

The free ligand melts at 62 °C and displays a SmA mesophase in a narrow range of temperature (2 °C), in contrast to its hydrocarbon analogue that is not liquid crystal. The palladium and platinum complexes display a SmA mesophase too, from 56 to 115 ºC for palladium and in the range 60–92 °C for platinum. It is worth noting that the corresponding hydrocarbon analogues show no mesomorphic behavior.

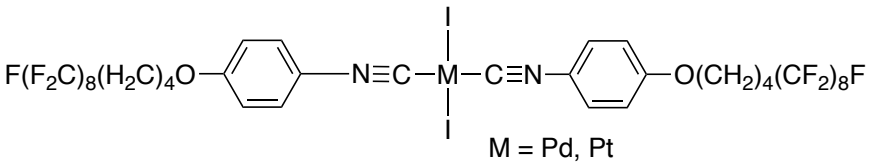

77

Palladium and platinum complexes with the unusual isocyanide ligand 4-isocyanobenzoic acid, *cis*-[$MCl_2(CNC_6H_4COOH)_2$] and *trans*-[$MI_2(CNC_6H_4COOH)_2$] (M = Pd, Pt) have been isolated.[118] The carboxylic acid group of the coordinated isocyanide acts as a hydrogen donor for hydrogen bonding and hydrogen-bonded liquid crystalline metal complexes have been prepared with stilbazoles (**78**). When 4-decyloxystilbazole is used, only the *trans* hydrogen-bonded decyloxystilbazole complexes, which have a rod-like structure, display enantiotropic nematic mesophases.[119] With tris(3,4,5-

decyloxy)stilbazole, all the supramolecular palladium and platinum polycatenar aggregates, which have a *trans*- arrangement of the ligands, display a hexagonal columnar mesophase.[120]

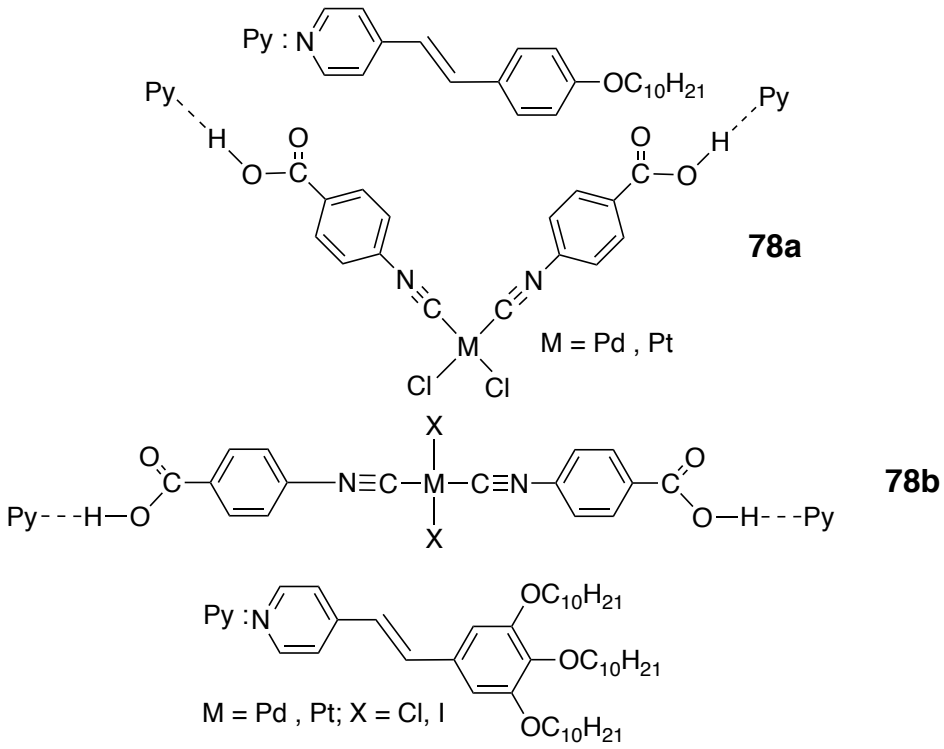

However, these aggregates have low thermal stability, most likely due to the thermal lability of the hydrogen bond. This led to the development of systems with higher stability based on isocyano–triphenylene complexes of palladium and platinum as those shown as **79**, with a *cis* **79a** or *trans* **79b** configuration.[121]

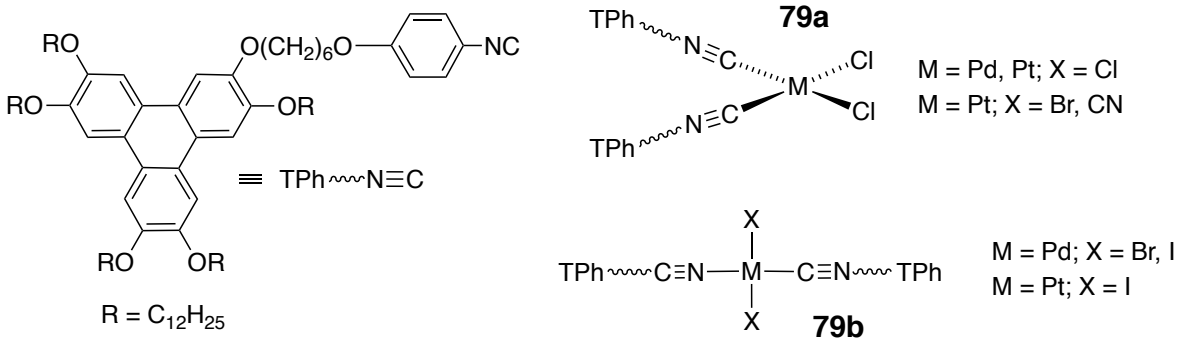

Neither the free isocyanide ligand, nor the *trans*-isocyanide complexes **79b** are mesomorphic, but the *cis*-isocyanide palladium and platinum complexes **79a** display an enantiotropic columnar rectangular mesophase close to room temperature. Concerning the different thermal behavior observed in these systems, it is worth noting that both structures, *cis* and *trans*, can generate columnar stacking, but only the *cis* complexes possess a net dipolar moment associated with the metal fragment, whereas the *trans* isomers are non-polar. Thus, the deeply stabilizing intermolecular antiparallel dipole–dipole interactions seem decisive to support the stacked arrangement after chain melting, resulting in mesophases only for the *cis* complexes.

The structure of the mesophase, determined by X-ray diffraction methods, is uncommon and is formed by the simultaneous π-stacking of the triphenylene discs into one-dimensional columns and the aggregation of the metallic fragments into tortuous threads, running parallel to the triphenylene columns, both segregated from the molten chains merged into an infinite continuum (Figure 6).

<Figure 6 near here>

Figure 6. Proposed packing for the columnar mesophase of **79a**.

Interestingly, these inorganic/organic dual columnar mesophases show high hole mobility (above 1 $cm^2\ V^{-1}\ s^{-1}$) along the columnar stacking. In addition, the dicyanoplatinum complex displays mesophase phosphorescence based on Pt···Pt interactions. Similar results were found for ionic *Ortho*-metalated benzoquinolate (bzq) complexes [Pt(bzq(CN-C_6H_4-O-$(CH_2)_6$-TriPh)$_2$]A (A = NO_3^-, BF_4^-, PF_6^-) with the triphenylene–isocyanide mentioned above (**80**).[121,122] All of them display a similar semiconducting columnar mesophase with high one-dimensional hole mobility. Again, the structure of the mesophase is hybrid organic/inorganic in nature. It is constituted by a central column formed by the stacking of the organometallic benzoquinoline–platinum fragments, surrounded by six columns in hexagonal disposition formed by stacking the triphenylene groups (Figure 7). These materials show aggregation–induced phosphorescence based on inter-disk Pt···Pt interactions.

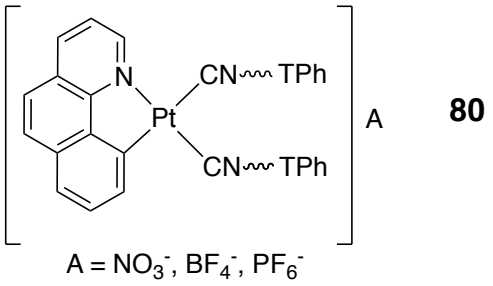

80

<Figure 7 near here>

Figure 7. Proposed schematic representation for the columnar mesophase of **80**. Reproduced from Ref. 122 with permission from The Royal Society of Chemistry.

The structure of the aryl isocyanide ligand has been further modified to introduce more paraffinic chains, and examples of metallodendrimers containing monodendrons with an isocyanide group in the focal point, and its organometallic complexes **81** *trans*-[MI_2(CN-G^n)$_2$] (M = Pd, Pt, n = 1, 2) have been reported.[123]

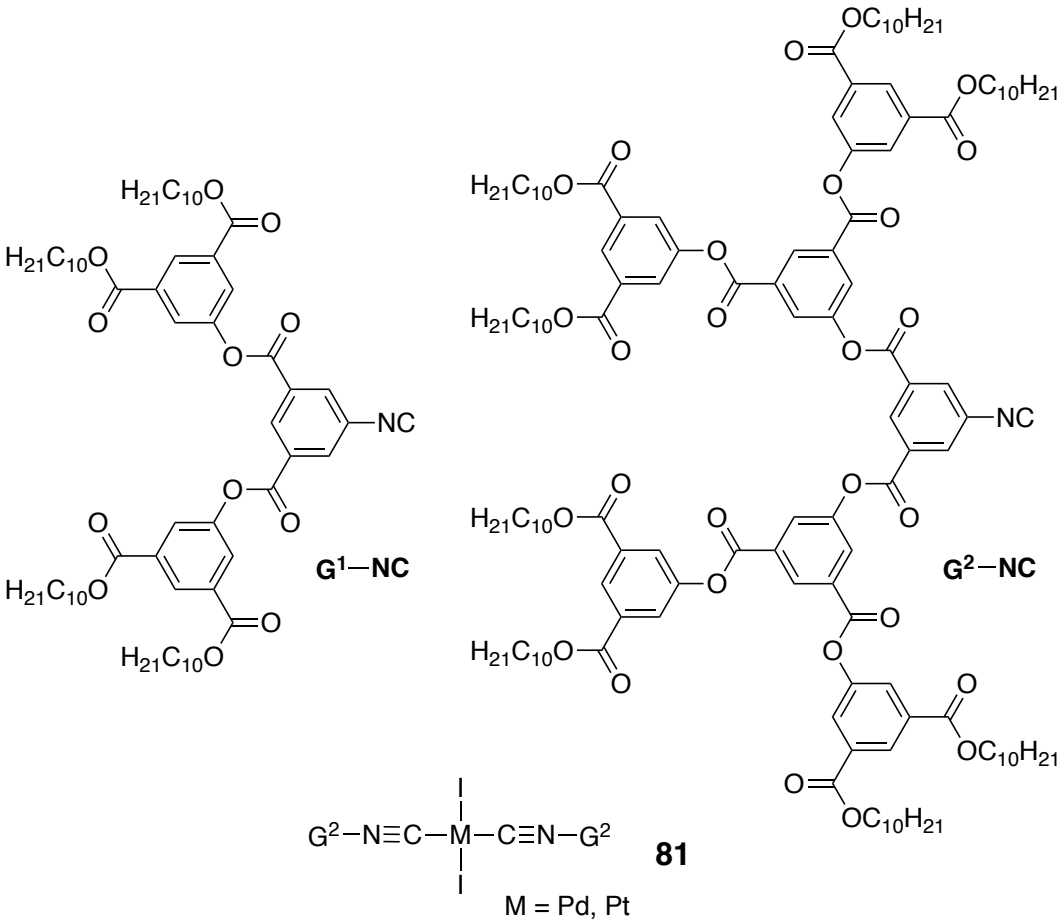

Although the free isocyanide dendrons and firs generation complexes are no mesomorphic, the palladium and platinum compounds for generation 2 display a micellar cubic mesophase $Im\bar{3}m$ over a wide range of temperatures, which is similar to those described for related gold and copper complexes (see Section 9.1.4). Small-angle X-ray diffraction data on the mesophase support that each micelle contains twelve conical monodendrons, which in this case, correspond to six molecules of $[MI_2(CN\text{-}G^2)_2]$ (M = Pd, Pt) (Figure 8).

<Figure 8 near here>

Figure 8. Schematic representation of structure for compound **81**.

8.2 Carbene complexes

Bis(carbene)nickel(II) complexes **82a** have been prepared as potential pre-catalyst systems for olefin dimerization reactions in ionic liquid crystalline media.[124] These complexes are not liquid crystals themselves, but their solutions in the liquid crystalline 1,3-didodecylimidazolium tetrafluoroborate, with concentrations of up to 10% weight Ni complex, retain the smectic mesophase of the imidazolium salt (55–71 °C).

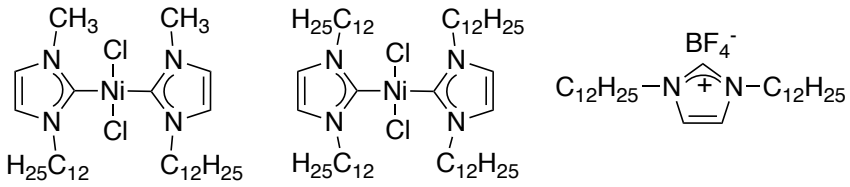

82a

Analogous carbene platinum complexes **82b** containing two or four pentadodecyloxytriphenylene units, have also been prepared.[125] They display rectangular columnar mesophases in the temperature range of 50–76 °C (R = Me, R' = Tph) and from 30 to 57 °C (R = R' = Tph). In the mesophases, the triphenylene cores and the metal fragments segregate into different columnar units, leading to multicolumnar structures. In addition, the compounds display emission spectra related to the triphenylene core in solution, in the mesophase, in the isotropic liquid, and in the solid state. Similar results have been reported for related metal carbene of copper, silver and gold (Section 9.2).

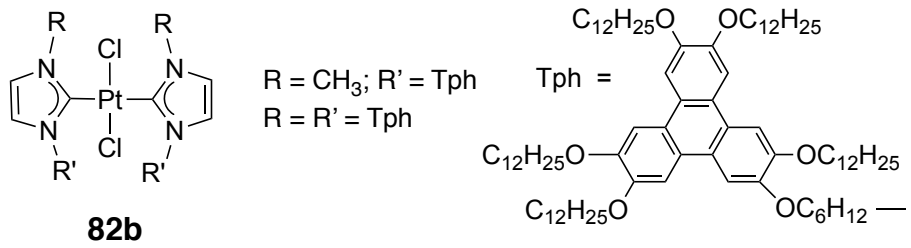

82b

8.3 σ-Acetylide complexes.

The mesomorphic σ-alkynyl platinum(II) terpyridine complex **83** exhibits strong solvatochromism. **83** shows a hexagonal columnar phase (20–200 °C), in which the molecular self-assembly is reinforced by Pt···Pt and Pt···alkyne interactions.[125a] Substitution of the branched chains by linear dodecyl chains, suppresses the mesomorphic behavior. However, the dodecyl complex **83b** is a good dodecane gelator, and forms gels that exhibit a strong near-infrared emission.

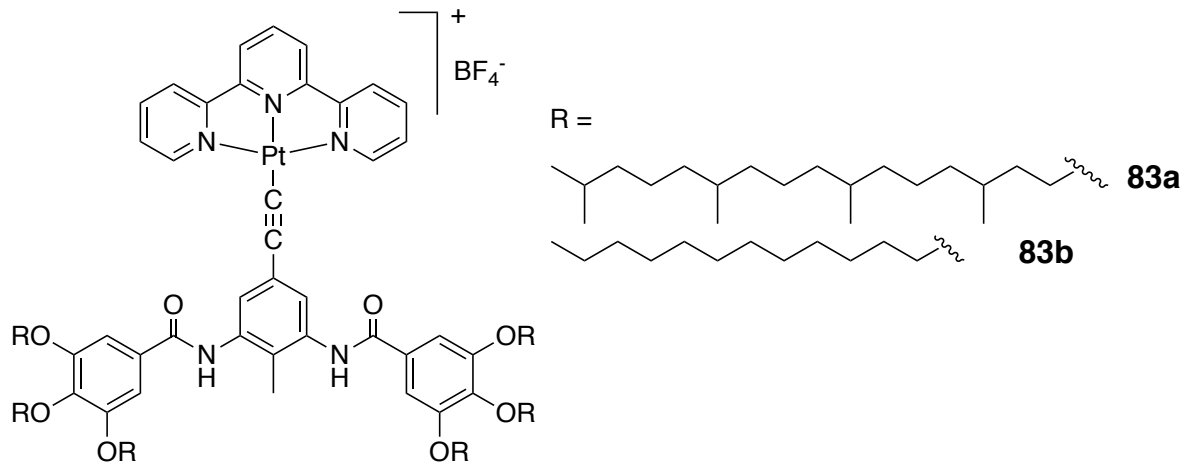

83a

83b

8.4 Allyl and olefin complexes of Palladium

Ionic allyl palladium(II) complexes [Pd(η^3-C_3H_5)(HLR^{py})][PF_6] (**84a**) and [Pd(η^3-C_3H_5)(LR^{pyH})][PF_6] (**84b**) containing β-diketone ligands bearing pyridyl and pyridiniumyl substituents have been reported. Only the palladium complexes with longer alkoxy substituents (n > 16 for **84a** and n > 14 for **84b**) are liquid crystals displaying a enantioptropic smectic C mesophase.[126] Luminescent studies for compound [Pd(η^3-C_3H_5)(LR^{pyH})][PF_6] with n = 14 show that it is fluorescent in solution, in the solid state, in the mesophase and even in the isotropic liquid.[127]

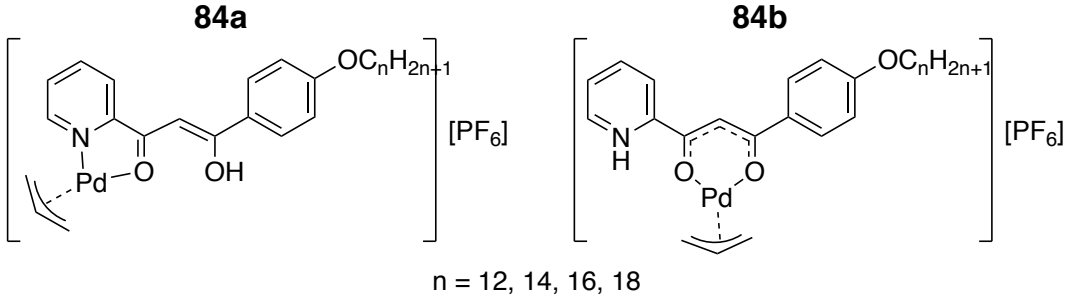

The mesomorphic behavior of a series of triolefinic palladium(0) complexes **85** bearing a different number of alkoxy substituents, has been studied.[128] Curiously, only the palladium complex that contains two dodecyloxy tails on each aromatic ring is liquid crystal, displaying a Col_r mesophase (54–72 °C).

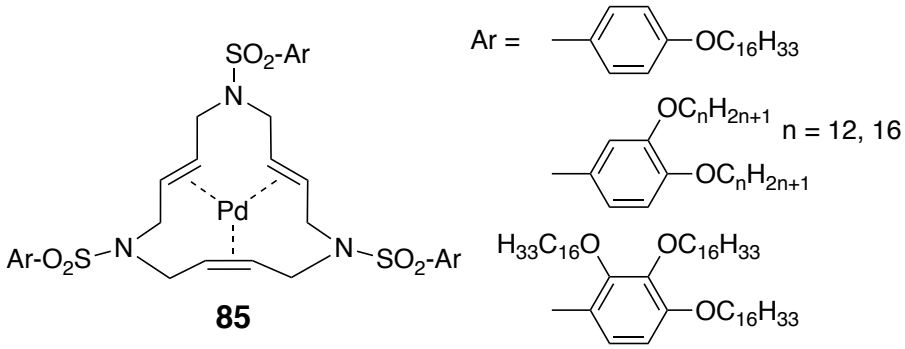

8.5 *Ortho*-Metalated Palladium(II) and Platinum(II) complexes

Ortho-metalated complexes constitute an interesting and broadly studied type of metallomesogens.[129] Particularly square–planar Pt(II) complexes of this type have received great attention in the last years because of their interesting photophysical properties.

8.5.1 *Ortho*-Metalated azo and azoxy complexes

With the objective of preparing chiral metallomesogens featuring the stereogenic center as close to the metal ion as possible, mononuclear cyclopalladated complexes **86** based on azo or azoxybenzene ligands containing the chiral chelating ligand (D-(-)-α-Phenylglycinol (HPhenylgly) have been synthesized.[130] According to their ^{1}H NMR spectra, only one isomer was formed in the case of azoxy complexes, whereas for the azo complexes isomeric mixtures were obtained as a result of a coordination N,N-*trans* or N,N-*cis* of the anionic phenylglycinol ligand in the mononuclear

complexes. Neither the azo compound with R = C_6H_{13}, [(Azo-6)Pd(Phenylgly)], nor the azoxy derivative [(Azoxy)Pd(Phenylgly)] are liquid crystals, but the rest of *ortho*-palladated complexes display a nematic mesophase.

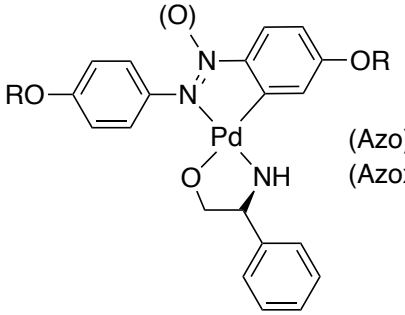

(Azo); R = $-C_6H_{13}$, $-OC-C_6H_4-OC_8H_{17}$
(Azoxy); R = CH_3, $-C_6H_{13}$

86

Complexes formed by a cyclopalladated azobenzene fragment bonded to an ancillary Schiff base ligand (**87**) bearing 11 or 12 peripheral alkyl chains, give rise to photoconducting hexagonal columnar mesophases at room temperature.[131] It is worth noting that complex **87b** shows a normalized photoconductivity of $\sigma/I=1.8 \times 10^{-11}$ S cmW^{-1} at λ=760 nm.

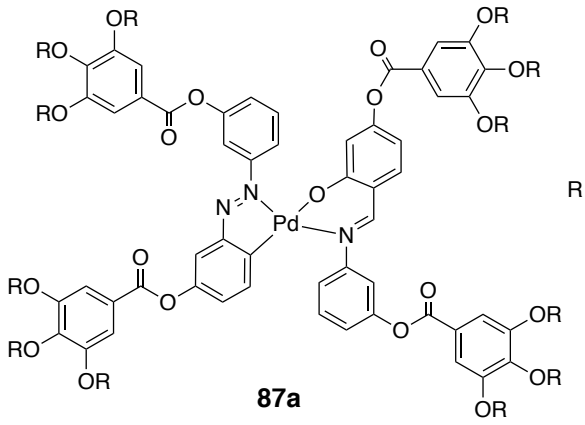

87a

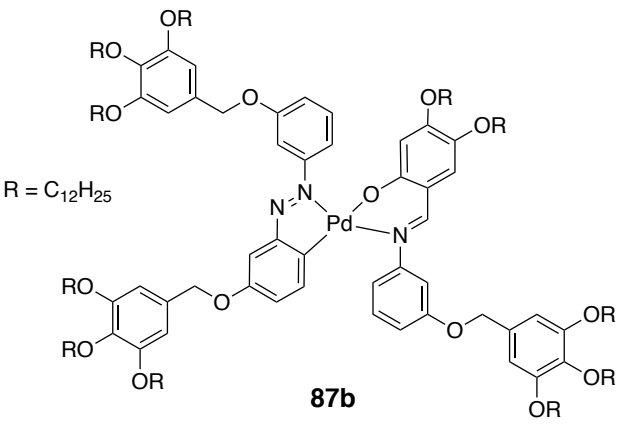

R = $C_{12}H_{25}$

87b

A new series of acetate and chloro-bridged dinuclear *ortho*-palladated complexes **88** derived from azobenzene with different polar groups (Me, Cl, F, NO_2, CN) have also been studied. All chloro-bridged complexes predominantly exhibit SmA mesophases. However the acetato-bridged derivatives due to their typical open book shape do not show mesomorphism, except the cyano and fluoro substituted complexes, which exhibit a monotropic Smectic A mesophase.[132] The melting points decrease in the order NO_2 > CN > CH_3 > Cl > F for the acetate complexes, and F > NO_2 > Cl > CH_3 > CN for the chloro-bridged derivatives.

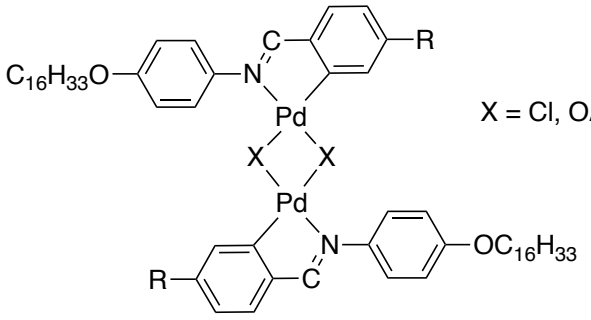

X = Cl, OAc; R = Me, Cl, F, NO_2, CN

88

8.5.2 *Ortho*-Metalated imine complexes

Dinuclear and mononuclear *ortho*-palladated metallomesogens of crown ether derivatized imines **89**, have been reported.[133]

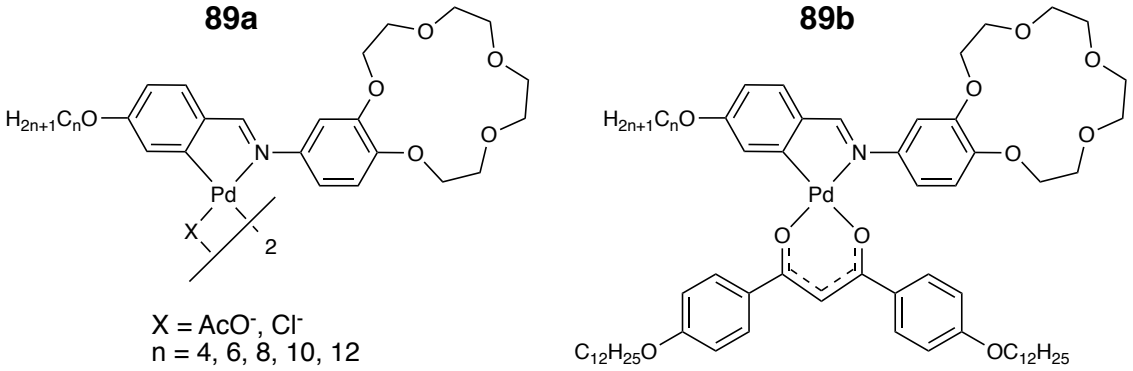

The imine ligands and the acetato bridged complexes are non-mesomorphic while the chloro-bridged and the diketonato complexes display enantiotropic smectic A mesophases. The treatment of these complexes with sodium perchlorate gives rise to the corresponding sodium adducts [(O_2ClO_2)Na-**89a**] and [(O_2ClO_2)Na-**89b**] (n = 4). However, none of the sodium adducts is liquid crystal. The acetato bridged complexes consist of a mixture of *syn* and *anti* isomers and a dramatic increase in the *syn:anti* ratio is produced upon complexation of $NaClO_4$. The crown ether derivatives extract sodium picrate from aqueous solutions and the presence of the palladium centers clearly improves the extraction.

The same research group has also reported mesomorphic dinuclear *ortho*-palladated complexes with substituted dibenzo-18-crown-6-ethers (**90**). In this case, only the *anti* isomer is formed. The free imine ligands are not liquid crystals, but the palladium complexes, including acetato-bridged derivatives, show SmC mesophases. In contrast to the previously mentioned 15-crown-5 ether derivatives, complexation with potassium produces a significant increase in the mesophase range and stability.[134]

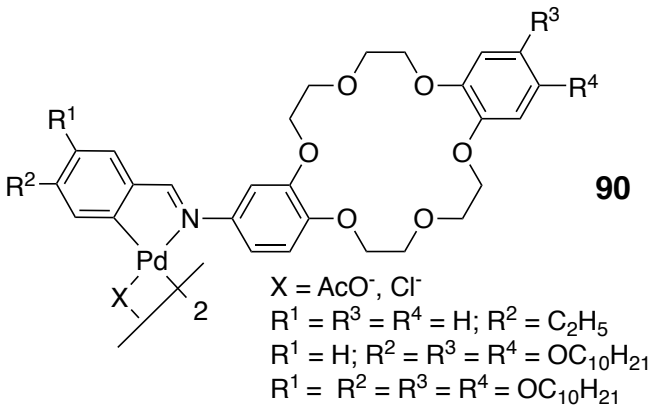

Other mesomorphic dinuclear and mononuclear *ortho*-metalated imine complexes containing semiperfluorinated alkyl chains have been synthesized, where the number of chains and the degree of fluorination has been systematically varied. In the chloro-bridged complexes **91**, the presence of

six semifluorinated chains and two alkyl chains in the system gives rise to hexagonal columnar mesophases with dramatically enhanced mesophase stabilities compared to the homologous hydrocarbon complexes, which show only monotropic discotic nematic mesophases.[135] In contrast, compounds bearing four semifluorinated alkyl chains and two alkyl chains exhibit enantiotropic smectic A, as well as a monotropic smectic C mesophase.[136] Similarly, mononuclear palladium complexes **92** bearing seven chains exhibit hexagonal columnar phases while the mesophases of the analogous compounds with five peripheral chains are smectic and nematic.[137] This change is discontinuous, and the mesophase type is determined by the volume required by the non-polar periphery. Regarding the length of the fluorinated chain, an increase in the number of CF_2 groups leads to a stabilization of the mesophases.

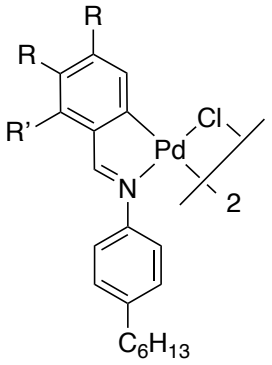

91

R = R' = -O(CH$_2$)$_6$-C$_4$F$_9$
R = R' = -O(CH$_2$)$_4$-C$_6$F$_{13}$
R = -O(CH$_2$)$_6$-C$_4$F$_9$, -O(CH$_2$)$_4$-C$_6$F$_{13}$; R' = H
R = C$_{10}$H$_{21}$; R' = H

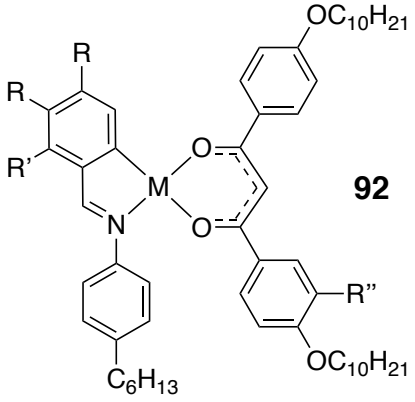

92

Pd; R = R' = -O(CH$_2$)$_6$-C$_4$F$_9$; R" = C$_{10}$H$_{21}$, H
Pd; R = R' = -O(CH$_2$)$_4$-C$_6$F$_{13}$; R" = C$_{10}$H$_{21}$, H
Pd, Pt; R = -O(CH$_2$)$_6$-C$_4$F$_9$; R' = R" = H
Pd; R = -O(CH$_2$)$_4$-C$_6$F$_{13}$; R' = R" = H
Pd; R = -C$_{10}$H$_{21}$; R' = R" = H

Mesomorphic Pd(II) and Pt(II) complexes **93** based on cyclometalated imine ligands and N-benzoylthiourea derivatives as auxiliary ligands, have also been prepared. These complexes display exhibit N or SmA mesophases. The platinum(II) complexes show photoluminescence both in solution and in solid state at room temperature, with the emission band centered around 600 nm.[138] Several studies have been done varying the number of alkoxy groups attached to the imine ligand, alkyl chain length or the use of branched alkoxy terminal groups (**94**). The complexes display SmA and SmC phases, and the introduction of branched alkoxy terminal groups leads to lower transition temperatures and stabilization of SmC mesophases in both the Pd(II) and Pt(II) complexes.[139]

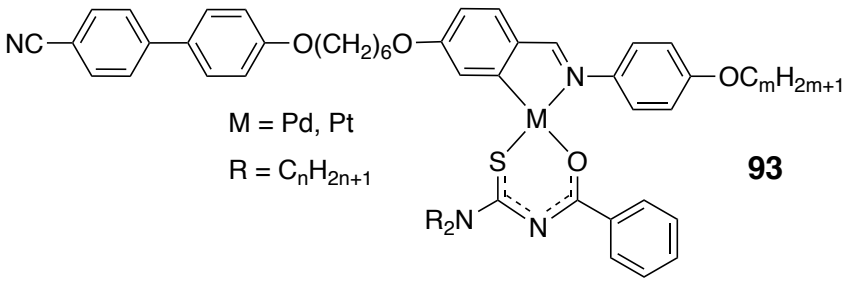

M = Pd, Pt
R = C$_n$H$_{2n+1}$

93

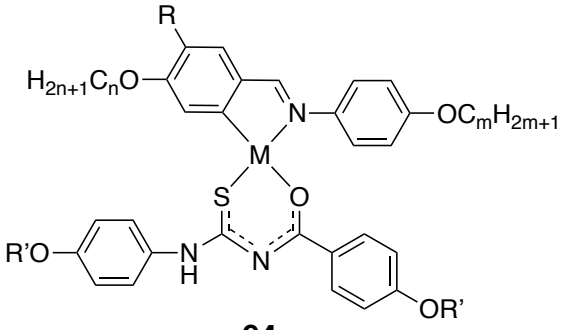

M = Pd; R = H; R' = n-octyl, n = 6, 8
M = Pd; R = n-decyloxy; R' = n-octyl, n = 10
M = Pd; R = H; R' = 2-ethyl-hexyl , n = 6, 8
M = Pd; R = n-decyloxy; R' = 2-ethyl-hexyl , n = 10
M = Pt; R = H; R' = 2-ethyl-hexyl , n = 6, 8
M = Pt; R = n-decyloxy; R' = 2-ethyl-hexyl , n = 10

94

Related *ortho*-palladated imine complexes **95** with di- and tri-alkoxysubstituted N-benzoyl thioureas are also liquid crystals.[140] These complexes are thermally stable on a wide temperature range up to 230 °C, showing SmA and SmC mesophases. In addition, they display a yellow-orange solid–state emission at room temperature with two emission maxima at λ_{max} around 580 and 650 nm. In these complexes, when the number of alkoxy groups on the N-benzoyl thiourea ligand increases, the mesomorphism is lost and only melting in the isotropic liquid state is observed.[141] However, increasing the number of terminal chains produces a transition from lamellar to columnar organization in **96**, which contains the Schiff base α-(4-cyanobiphenyl-4'-yloxy)-ω-(4-n-decyloxyanilinebenzylidene-4'-oxy)hexane.[142] Four alkoxy substituents give rise to a SmA phase, whereas complexes bearing five or six tails show hexagonal columnar mesophases.

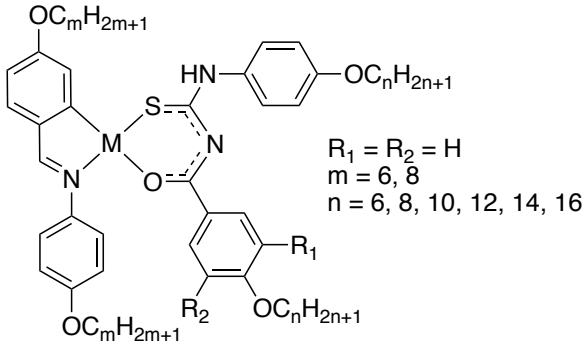

$R_1 = R_2 = H$
m = 6, 8
n = 6, 8, 10, 12, 14, 16

95

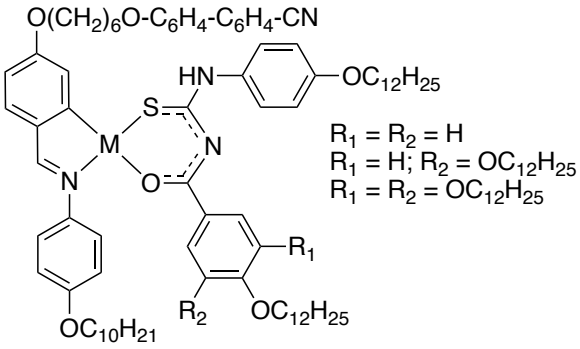

$R_1 = R_2 = H$
$R_1 = H$; $R_2 = OC_{12}H_{25}$
$R_1 = R_2 = OC_{12}H_{25}$

96

With the aim of obtaining photosensitive metallomesogens, palladium complexes derived from an *ortho*-metalated imine, bearing one or two azocarboxylate bridges (**97**), have been synthesized.[143] The mixed thiolate–azocarboxylate bridges complexes display nematic and smectic A mesophases, whereas the biscarboxylate derivatives give rise to "soft" crystal phases. Electronic spectroscopy and ^{1}H NMR show that all of them undergo a *trans–cis* isomerization of the azobenzene moiety at λ = 365 nm, which is faster and more stable when the trisubstituted azocarboxylate is present and the motion of the azo group is not hindered by the *ortho*-metalated imine. The photoresponse has also been observed in the condensed phases, which change from the ordered phase to the isotropic liquid upon irradiation.

97

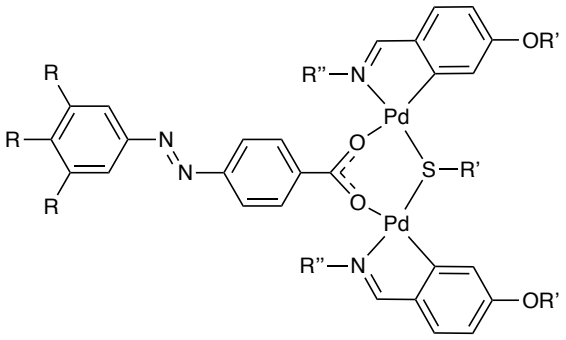

R = H; R' = $C_{10}H_{21}$; R'' = C_6H_4-$OC_{10}H_{21}$-*p*
R = H; R' = $C_{10}H_{21}$; R'' = $C_{14}H_{29}$
R = $OC_{10}H_{21}$; R' = $C_{10}H_{21}$; R'' = C_6H_4-$OC_{10}H_{21}$-*p*

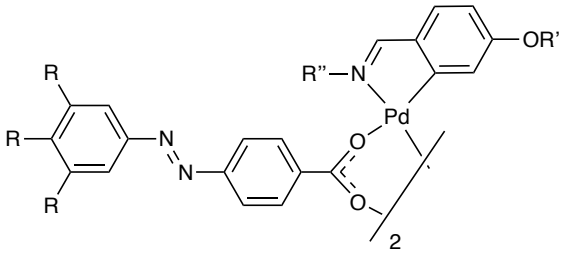

R = H; R' = $C_{10}H_{21}$
R = $OC_{10}H_{21}$; R' = $C_{10}H_{21}$

The substitution of the azo group by a decyloxy tail in the biscarboxylato bridges, together with the incorporation of a second alkoxy substituent in the metalated aromatic ring, **98**, give rise to the appearance mainly of monotropic SmA mesophases.[144] The same behavior has been found for related dinuclear acetate complexes.[145]

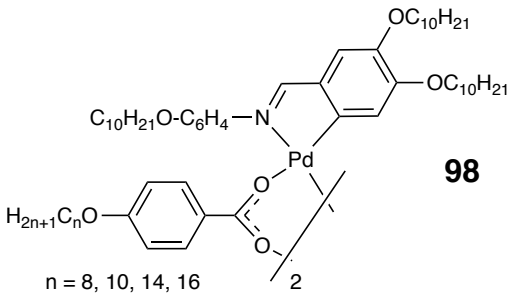

98

n = 8, 10, 14, 16

Mono and dinuclear triphenylene–imine *ortho*-palladated complexes **99** have also been prepared showing unusual columnar mesophases near room temperature.[146]

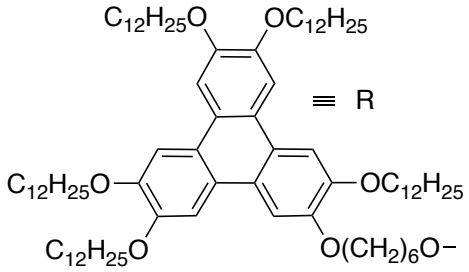

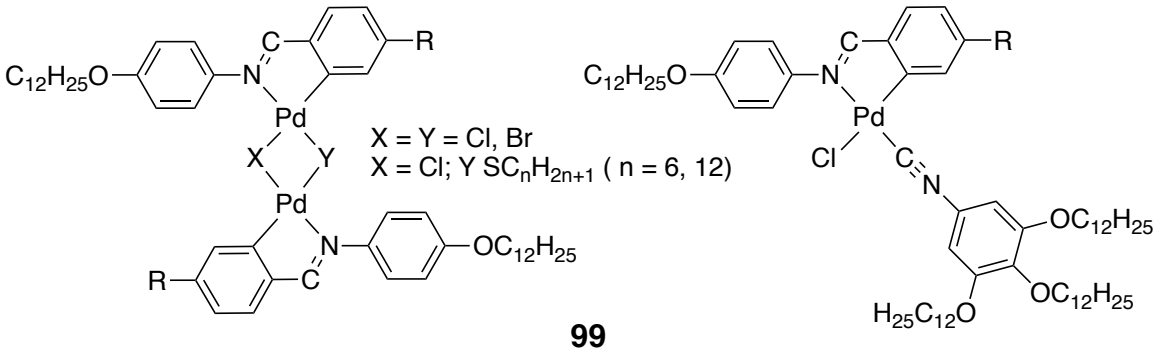

X = Y = Cl, Br
X = Cl; Y SC_nH_{2n+1} (n = 6, 12)

99

Their structures contain columnar packing of triphenylene moieties, so they are organic columns that support an independent stack of metal fragments. Additionally, these palladium complexes exhibit fluorescence at room temperature in dichloromethane solution, associated with the triphenylene core.

8.5.3 *Ortho*-Metalated pyrimidine and pyridine complexes

Ionic *ortho*-palladated phenylpyrimidine complexes **100** have been prepared, showing lamellar mesophases.[147] The key factor to control the mesomorphism in this system (SmA for R = $COC_{22}H_{45}$, and SmC for R = CH_2OH) is the type of substituent on the bipyridine fragment, whereas no significant differences are observed by changing the anion from BF_4^- to ClO_4^-.

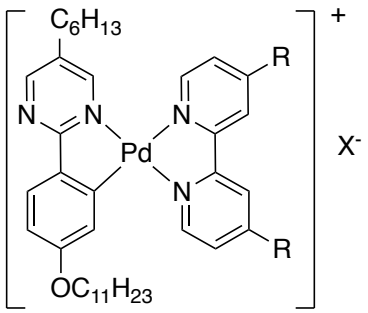

R= $COC_{22}H_{45}$; CH_2OH
X- = BF_4-; ClO_4-

100

Luminescence and photoconductivity of phenylpyrimidine series of ortho-platinated and -palladated metallomesogens previously reported (**101**),[148] have been studied. Only the platinum compounds show luminescence in the solid state and in solution, as well as photoconductivity caused by Pt···Pt closed shell interactions. The substitution pattern conditions and the metallophilic interactions have a significant influence on both properties. After photoexcitation, a competition between radiative deactivation (luminescence) and photo-conductivity was observed. Hence, strong luminescent compounds are non-conductive, whereas comparatively less or non-luminescent materials behave as photoconductors.[149]

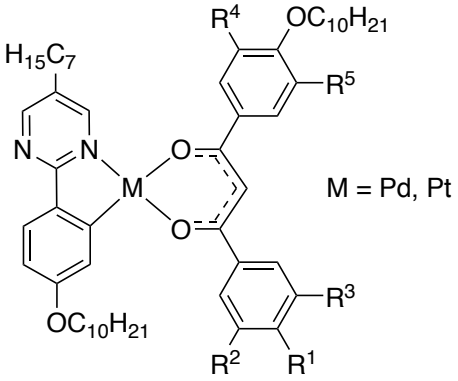

M = Pd, Pt

R1	R2	R3	R4
$OC_{10}H_{21}$	H	H	H
$OC_{10}H_{21}$	$OC_{10}H_{21}$	H	H
$OC_{10}H_{21}$	$OC_{10}H_{21}$	H	$OC_{10}H_{21}$
$OC_{10}H_{21}$	$OC_{10}H_{21}$	$OC_{10}H_{21}$	$OC_{10}H_{21}$
OC_6H_{13}	OC_6H_{13}	OC_6H_{13}	$OC_{10}H_{13}$
$OC_{10}H_{21}$	$OC_{10}H_{21}$	$OC_{10}H_{21}$	$OC_{10}H_{21}$

101

A series of liquid crystals have also been synthesized based upon mononuclear ortho-platinated 2-phenylpyridines and 2-thienylpyridines **102**, and the effect of the number of peripheral chains was studied systematically in several papers. Increasing the number of tails attached to the 1,3-diketonate units produces, as described previously in *ortho*-metalated imine complexes, a transition

from lamellar (SmA) to hexagonal columnar phases (Colh).[150] They all display a luminescence emission in toluene solutions originating from a mixed ligand-centered-MLCT excited state.

102

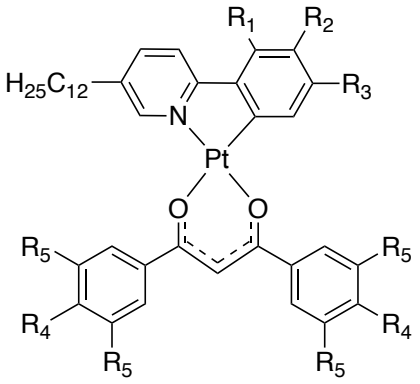

$R_1 = R_2 = R_5 = H$; $R_3 = C_{12}H_{25}$; $R_4 = C_{10}H_{21}$
$R_1 = R_2 = H$; $R_3 = C_{12}H_{25}$; $R_4 = R_5 = OC_{12}H_{25}$
$R_1 = R_2 = H$; $R_3 = OC_{12}H_{25}$; $R_4 = R_5 = OC_{12}H_{25}$
$R_1 = R_2 = OC_{12}H_{25}$; $R_3 = H$; $R_4 = R_5 = OC_{12}H_{25}$
$R_1 = H$; $R_2 = R_3 = R_4 = R_5 = OC_{12}H_{25}$

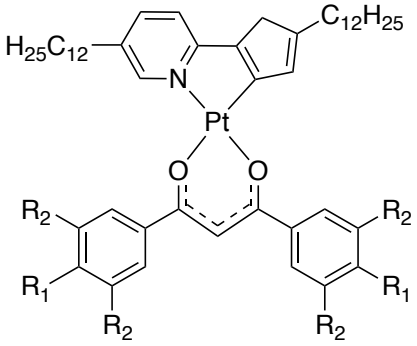

$R_1 = OC_{10}H_{21}$; $R_2 = H$
$R_1 = R_2 = OC_{12}H_{25}$

Another series of cycloplatinated complexes based on 2-(4-alkoxyphenyl)-5-(alkoxymethyl)pyridines, but bearing the less bulky acetylacetonate ancillary ligand, has been synthesized (**103**).[151]

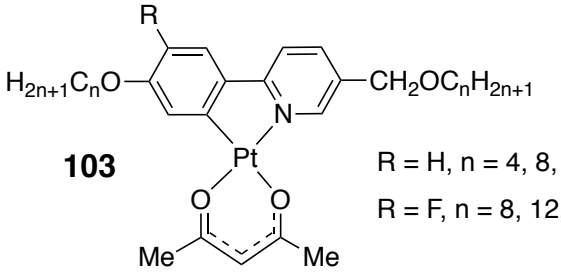

103

R = H, n = 4, 8, 12, 16
R = F, n = 8, 12, 16

Only the complexes with longer substituents (n = 12 and 16) exhibit enantiotropic lamellar mesophases with interdigitation of the molten aliphatic chains. In addition, they show intense polarized luminescence (λ_{max} = 532 nm and a polarization ratio as high as 10.5). More recently, platinum complexes **104** containing β-diketone ligands with biphenyl substituents have been studied, searching for phosphorescent metallomesogens with efficient dichroic ratios and high emission efficiency.[152]

104a **104b**

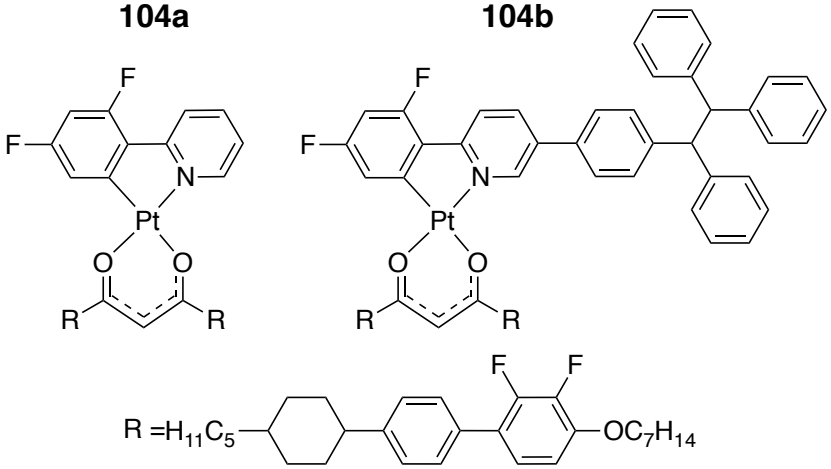

Complex **104a** displays an enantiotropic nematic phase between 118 and 183 °C, and exhibits intense sky-blue emission in solution and in the neat film. Aligned films of a **104a**:polyimide mixture show polarization-dependent photoluminescence with polarized ratio of 5.4. This has allowed the fabrication of polarized organic light-emitting diodes displaying a broad emission spectrum in the range of 450–900 nm with polarized ratio of 1.33 and an external quantum efficiency of 1.1%. The introduction of the tetraphenylethene bulk moiety into the system (**104b**), leads to a monotropic SmA mesophase, but the emission efficiency is drastically decreased.

Using modified 2-phenylpyridine derivatives, in which cyanobiphenyl unit is linked on 4th position of pyridine group, new ortho-platinated metallomesogens **105** have been obtained.[153]

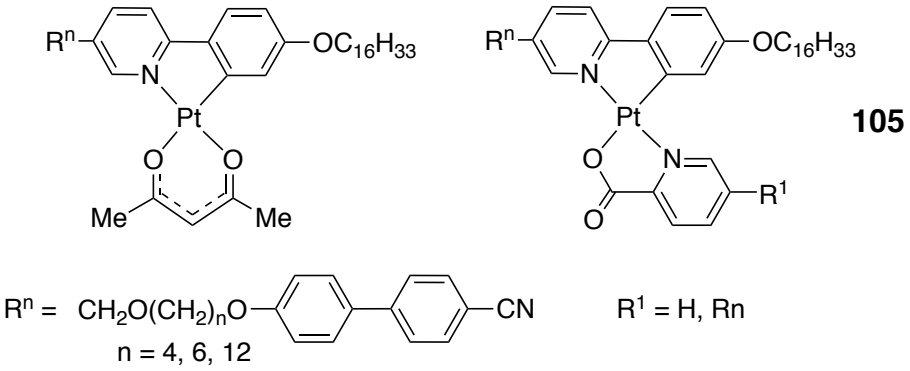

105

Picolinate derivatives with one cyanobiphenyl unit show a SmC mesophase, whereas acetylacetonate complexes and picolinate derivatives with two cyanobiphenyl units exhibit a nematic phase. Moreover, these metallomesogens show strongly polarized photoluminescence in liquid crystalline phases, with a polarized dichroic ratio of up to 24.6 in nematic phase. Interestingly, the introduction of a chiral 2-butanol chain into the picolinate group leads to an chiroptic smectic C phase, in which the molecules form heliconical arrangements and the chirality is transferred from the molecule to the mesophase.[154] The functionalization of the 2-phenylpyridine unit with chiral 2-octanol chain (R and S) has also been studied (**106**).[155] These complexes show chiral smectic (SmA*) and nematic (N*) phases and an intense phosphorescent emission at 504 nm both in solution and in the solid state. Moreover, the neat films annealed at 100 °C (the complexes are in the N* phase), exhibit an intense circularly polarized luminescence (CPL) spectrum with a large g_{lum} value up to 0.02.

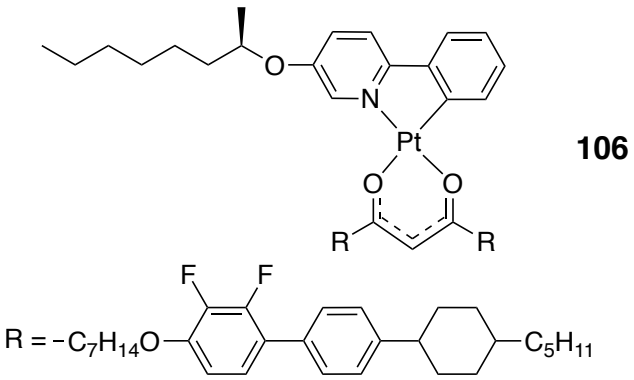

106

Related cycloplatinated complexes with diphenylpyridine groups, [Pt(C^N)Cl(acac)] (**107**, **108)**, also display mesomorphism.[156] Although the parent ligands exhibit a rich smectic polymorphism, the β-diketonate complexes **107** show a SmA mesophase at high temperatures. However, the complexes **108** with the fused cyclopentene ring display monotropic nematic and/or SmA mesophases. It is worth noting that related series of complexes [Pt(C^N)Cl(dmso)], were also mesomorphic with a similar behavior to the acetylacetonate derivatives.

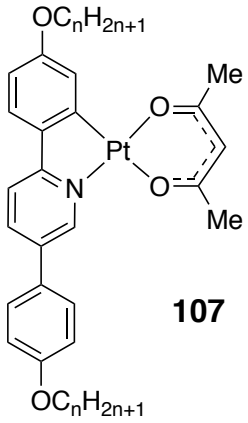

107

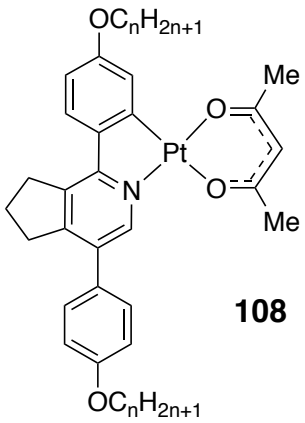

108

All of the β-diketonate complexes are very brightly phosphorescent in dichloromethane solution with emission quantum efficiencies around 0.5. Related derivatives containing hexafluoroacetylacetonate, trifluoroacetylacetonate and 3,5-heptanedionato ligands, have also been synthesized.[157] However, neither mesomorphism nor luminescent properties are improved. In fact, for the hexafluoroacetylacetonate complexes, these properties are even lost.

By combination of the mesogenic cycloplatinated monomer (monotropic SmA mesophase) based on a 2,5-di(4-alkenyloxyphenyl)pyridine ligand with 1,1,3,3,5,5- tetramethyltrisiloxane, the phosphorescent liquid-crystalline polymer **109** has been obtained. This polymer displays a SmA mesophase from 64 to 150°C, and shows polarized emission.[158]

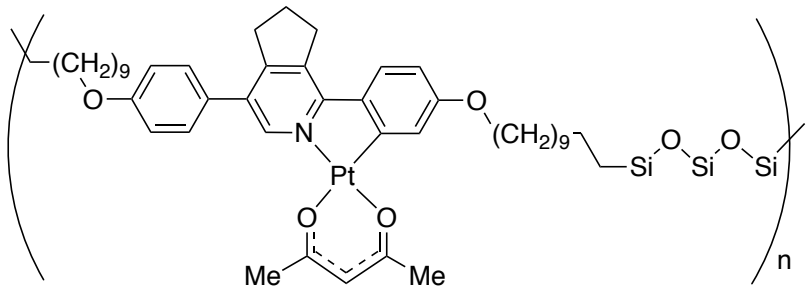

109

Dinuclear platinum complexes containing a 6,12-dihydro-indeno[1,2-b]fluorene bridging unit have also been described (**110**).[159]

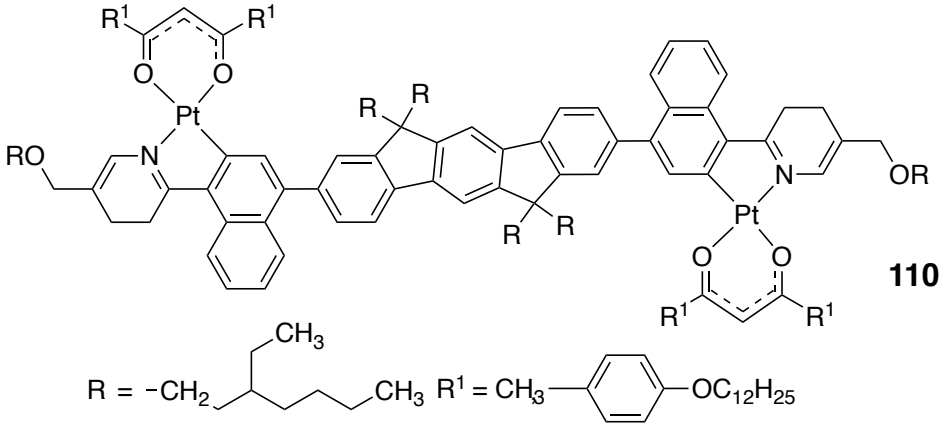

110

These complexes display a smectic mesophase in the temperature range 188–220 °C for $R^1 = CH_3$, and 75–193 °C for the dodecyloxyphenyl derivative. In addition, both complexes display fluorescence (532, 574 nm, $^1\pi,\pi^*$) and phosphorescence (640 nm, $^3\pi,\pi^*$) dual emissions in solution. With the aim of extending these studies to molecules prone to give columnar mesophases, the same research group has developed a new series of platinum complexes bearing triphenylene and carbazole units (**111**).[160]

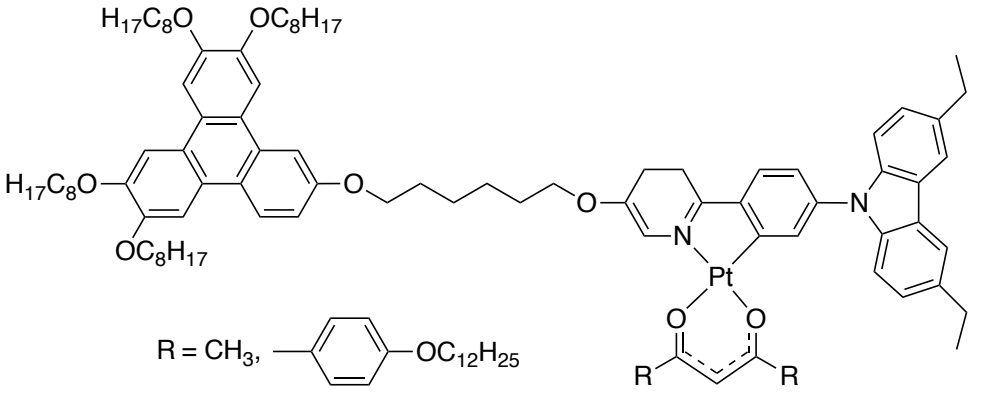

111

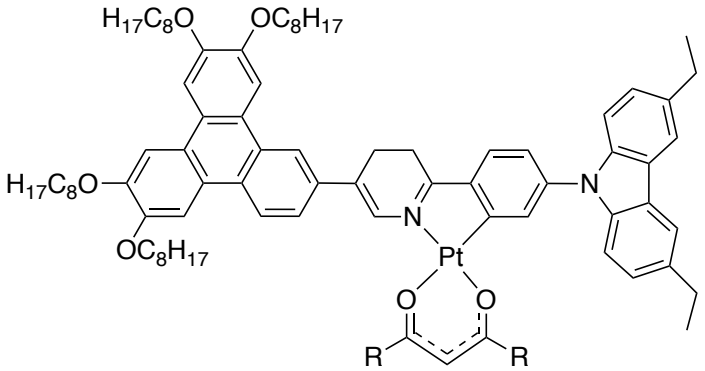

These carbazol derivatives display monomolecular emission both in solution and in neat film, as well as hole mobilities (annealed films) in the range of 10^{-5}–10^{-6} cm^2 V^{-1} s^{-1}. However, only the complex with the triphenylene group directly bonded to the pyridine ring and R = -C_6H_4-O-$C_{12}H_{25}$ is liquid crystal, showing a columnar mesophase from 66 °C to 143 °C.

Cationic ortho-platinated 2-phenylpyridyne complexes containing pyridyl triazole ligands **112** have been found to exhibit columnar hexagonal mesophases over a wide range of temperatures, including room temperature. In addition, they display mechanochromism in the crystal phase.[161] These compounds exhibit environmentally sensitive Pt··· Pt intermolecular interactions, which help the formation of columnar liquid crystalline phases, as well as the mechanochromic behavior.

Tetrazole ligands have also been used as auxiliary ligand to prepare cycloplatinated 2-phenylpyridine complexes with different degrees of substitution.[162] Only the complexes **113** bearing three flexible alkoxy chains are liquid crystals, displaying a complex lamellar mesophase (from 17–32 °C to 205–230 °C) supported by Pt···Pt and $\pi-\pi$ interactions. Aligned films of these complexes show highly polarized phosphorescence with a maximum peak at 653 nm, and a polarization ratio in the range 4.1–7.1. Moreover, they display ambipolar carrier mobility.

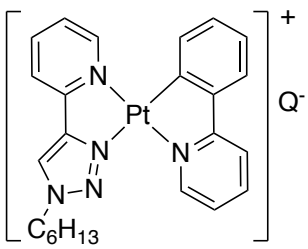

112

Q = SbF_6^-, PF_6^-, BF4, OTf^-

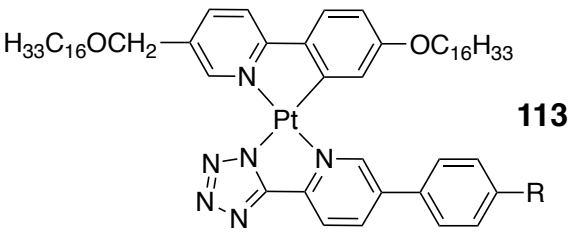

113

R = $OC_{12}H_{25}$, $OC_{16}H_{33}$

Phosphorescent cationic ortho-platinated 2-phenylpyridine complexes **114**, without long peripheral chains, constitute non-conventional examples of columnar mesophases.[163] They show hexagonal columnar mesophase over a wide range of temperatures (96–284 °C for R = H and 101–266 °C for R = OMe). The phenyl and methoxyphenyl groups appear to act as the characteristic "soft" regions of traditional discotic liquid crystal structures. It is worth noting that with longer alkoxy substituent (OC_nH_{2n+1}, n = 2, 4, 6), the mesomorphic behavior is completely lost. This reflects a subtle relationship of the molecular interactions that control the formation of liquid crystals.
Another analogous example of mesomorphic systems without long peripheral chains, although not organometallic in nature, is constituted by cyclopalladated 3,5-disubstituted-2-(2'-pyridyl)pyrroles, **115**.[164] In this case, the mesophase formation is driven by the self-segregation of the trifluoromethyl groups from the rigid organometallic cores, in such a way that the mesophase structure consists of a columnar stacking of the metallic fragments surrounded by the fluoridated region. When these compounds are heated, the fluoridated zones melt at first to form a soft part, which preserves the self-assembly of the central cores so that a columnar mesomorphism is induced.

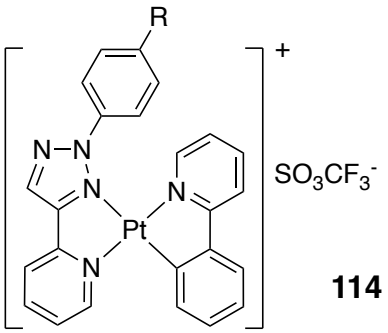

114

R = H, OCH_3,

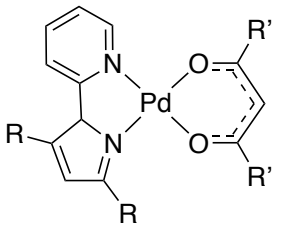

115

R = CH_3, CF_3; R' = CF_3

8.5.4 Other *ortho*-Metalated complexes, and related systems

Using a simple strategy of combining in the same molecule a luminophore group with moieties able to induce liquid crystal behavior, a red emitting columnar mesophase (35–173 °C) containing the cyclopalladated Nile red chromophore has been synthesized (**116**).[165]

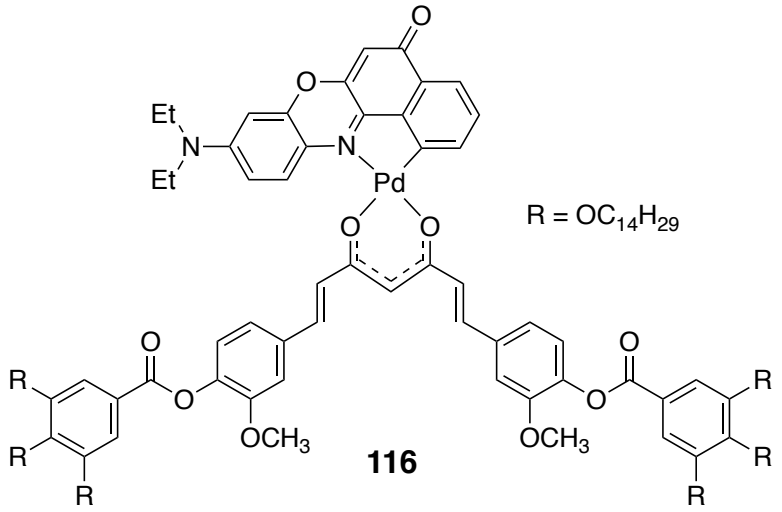

116

Related complexes with a polyalkylated Schiff base as an ancillary ligand are also mesomorphic, showing photoconducting columnar rectangular mesophases from UV–Vis to near IR wavelength. The columnar organization is induced by the formation of dimeric pairs through hydrogen-bonded interactions between Nile red fragments (**117**).[166]

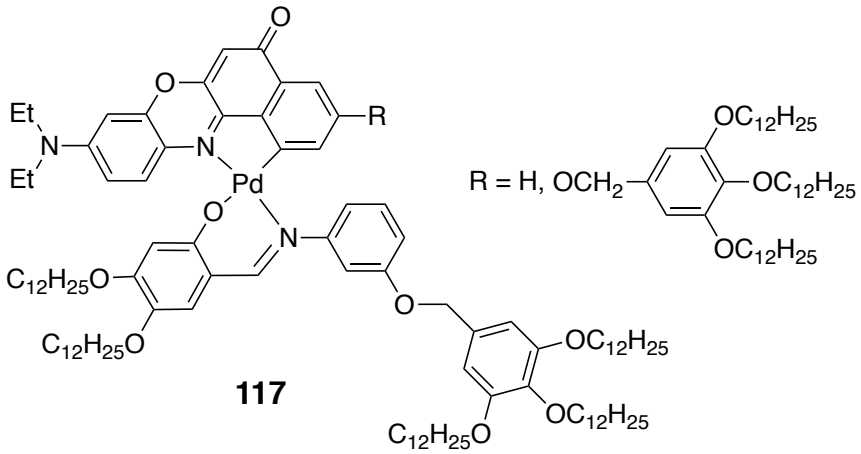

117

The same group has also reported the cationic Nile red cyclopalladated metallomesogen **118**, which displays a Col_r mesophase. However, in contrast to the related neutral derivatives, the emission is quenched due to the presence of the bipyridine ancillary ligand.[167]

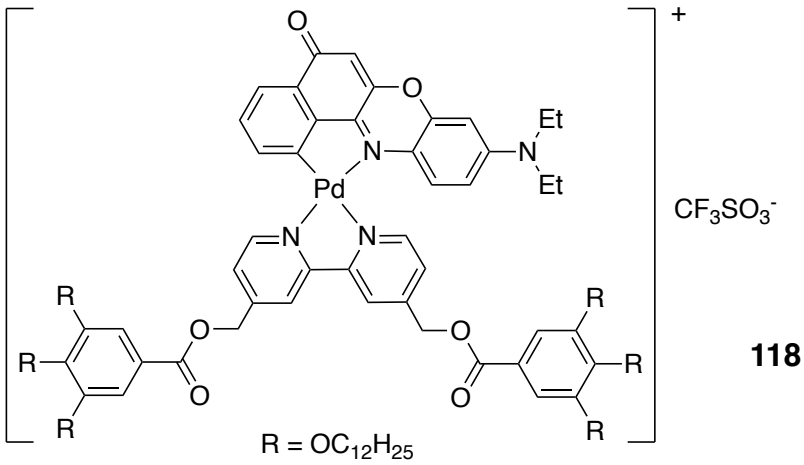

118

C,N,N'-cycloplatinated complexes of 1,3-bis(2-pyridyl)benzene ligands containing a 3,4,5-trialkoxyphenyl group constitute an interesting family of luminescent metallomesogens (**119**).[168] Complexes **119a** show rectangular columnar mesophases for n > 6 (from 92–149 °C to 151–187 °C), whereas compounds **119b** display hexagonal columnar phases (n =10, 12) over a wider range of temperatures (33–220 °C). These Pt(II) complexes show an interesting thermochromic behavior, which depend on the thermal history of the sample. Indeed, when the isotropic liquid is slowly cooled into the mesophase, an orange emission from a monomer is observed. In contrast, a fast cooling leads to a glassy state displaying a red excimer-like emission.

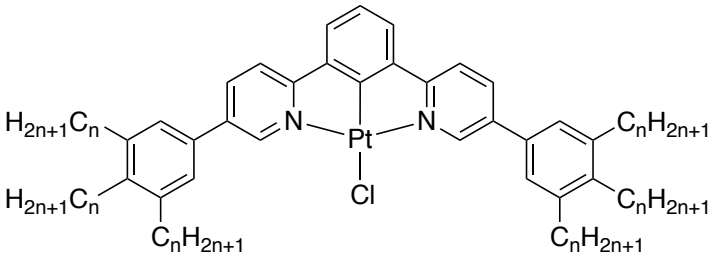

119a

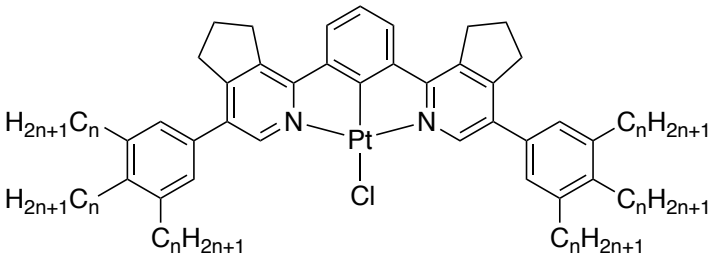

119b

The introduction of fluorine atoms into the central phenyl group changes both the mesophase and photophysical properties of the system.[169,170] Compounds **120** display a mesophase with a monoclinic space group, as well as a P6/mm lattice at higher temperatures. For compound **121** a rhombohedral R3m phase has been indexed. These fluorinated compounds display intense fluorescence in solution and in the solid state, but none exhibit temperature-dependent emission.

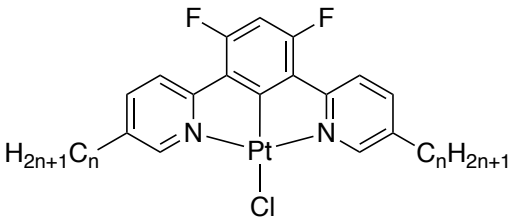

120

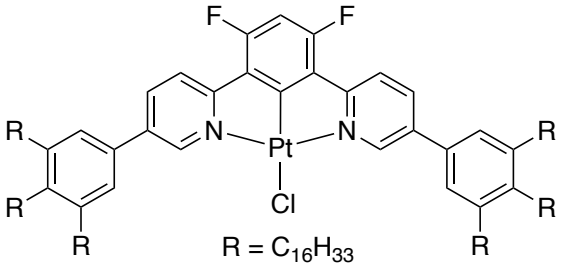

121

Recently, a series of tetradentate platinum(II) complexes **122** displaying red phosphorescence in dichloromethane solution (λ_{max} ≈ 640 nm, $\phi = 4.3\% - 6.7\%$) have been synthesized.[171] However, only the complex with n =12 is liquid crystal, showing a columnar mesophase from 22.0 °C to 78 °C. The mesophase exhibits ambipolar carrier transport (measured by the space charge limited current SCLC method) with hole and electron mobility values of 4.72 x 10^{-4} $cm^2V^{-1}s^{-1}$ and 3.08 x 10^{-4} $cm^2V^{-1}s^{-1}$ respectively. It is remarkable that the carrier mobility in the mesophase is two orders of magnitudes greater than that in the amorphous state.

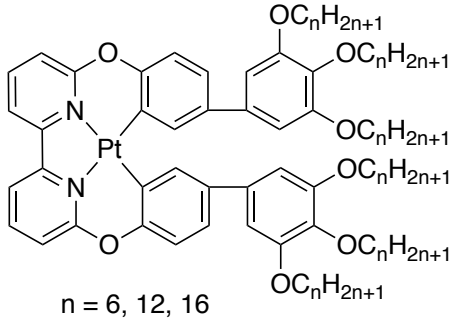

122

Organometallic liquid crystals based on platinum(IV) systems are rare, and for a long time, the only reported examples had been a few cyclometalated azobenzene complexes, showing mainly nematic phases.[172,173] Recently, new mesomorphic ortho-metalated 2-phenylpyridine platinum(IV) complexes **123**, have been obtained.[174] They display a lamellar mesophase (78–265 °C), in which a short-range Pt···Pt correlation is observed. In addition, these complexes are luminescent in deoxygenated dichloromethane solution (λ_{max} = 532 nm, τ = 230 ms, ϕ = 10 %).

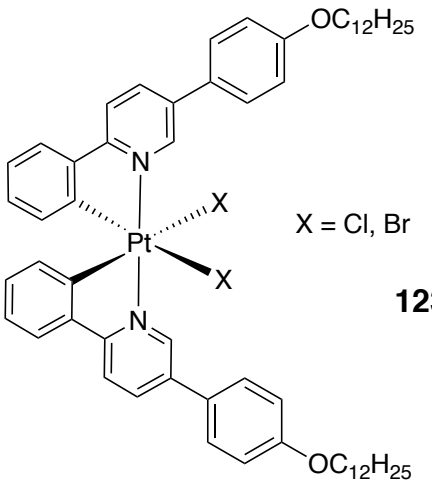

123

9 Organometallic Liquid Crystals of the Group 11 Elements

The majority of the organometallic liquid crystals of the group 11 elements contain an isonitrile (isocyanide) ligand and gold as metal. Gold(I) tends to give linear 2-coordinated compounds, which favors calamitic liquid crystals; even non-mesomorphic ligands often become mesomorphic after coordinating with a gold center. Some other ligands have been used as carbenes. Some silver and copper mesogens are also known, scarcer than for gold. There have been a number of previous specific reviews on gold[175–178] and silver mesogens.[179]

9.1 Isocyanide Complexes

Isocyanide or isonitrile ligands are strongly attached to metal centers, particularly to gold(I) which leads to high thermal stability and liquid crystal behavior. Some isocyanide ligands have been designed in order to add specific functional groups.

9.1.1 Mixed isocyanide acetylide complexes

Alkyl isocyanide combined with alkoxyphenyl acetylide yielded very simple rod-like gold(I) compounds **124a**, with gold–gold distances around 3.6 A in the crystalline state and liquid crystal behavior (R = C_nH_{2n+1}, n = 5–8).[180] They exhibit nematic or smectic A monotropic mesophases at less than 100 °C, although with short mesophase ranges (up to 25 °C). Most interesting are the photophysical properties: a blue phosphorescent emission with quantum yields in the range 8%–50% in the solid state at room temperature, and a lifetime about 50 µs. The same emission was observed with a low the quantum yield for the mesophase and the isotropic liquid, but no emission was found in dilute solutions. Changing phenyl acetylene by biphenyl or naphthyl acetylene led to compounds **124b** (R = C_nH_{2n+1}, n = 5–8) with a wider mesophase range (on heating, from 4 up to 19 °C for the analog hexyloxy derivatives) and to green emission. Now, there are not gold–gold interactions and the two-ring cores slightly expanded the LC temperature range and moved the emission color.[181,182]

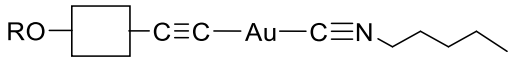

124

9.1.2 Mixed isocyanide halides complexes

Chloro combined with alkoxyphenyl isocyanide led to very simple rod-like gold(I) compounds **125a** (n = 1, R = C_nH_{2n+1}, n = 5–7), which arrange into dimers or chains (always in an *anti* configuration) in the solid state through short gold–gold distances (around 3.3 A).[183] They exhibit smectic enantiotropic mesophases in the range 121 to 172°C with moderate mesophase ranges between 24 and 48 °C. Replacement of alkoxyphenyl by an alkoxybiphenyl isocyanide **125b** (n = 2, R = C_nH_{2n+1}, n = 3–8) kept the solid state arrangement with short gold–gold distances (in acetylide analogues was lost), rises the transition temperatures (melting points from 130 to 218 °C) and mesomorphic ranges, although they decompose without clearing around 300 °C.[184] Most interesting are the photophysical

properties: as observed in the analog acetylide isocyanide compounds, they exhibit an intense blue (phenyl) or green (biphenyl) phosphorescent emission in the solid or liquid crystal states. Quantum yields are in the range 6%–66% depending on the core (better biphenyl) and the length chain. In dilute solutions they are non-emissive or weakly emissive. Compounds **125a** display a reversible "on–off" switching of the luminescence induced by the phase transition between mesophase and isotropic liquid. Moreover, hexyloxy complex **125a** showed thermochromic photoluminescence by the phase transition between crystalline and SmC phases.

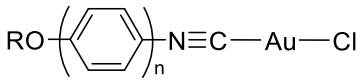

125a (n = 1), **125b** (n = 2)

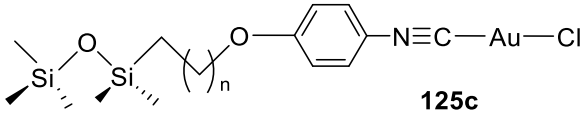

125c

The effect of bonding siloxane groups at the end of an alkoxy chain in a isocyanide was studied.[185] Compounds **125c** (n = 4, 5) showed small changes in the solid state structure, the liquid-crystalline or the emission properties compared to the parent compounds. Again, a reversible "on–off" switching of the luminescence induced by the phase transition was observed. Therefore, these gold mesogens show potential application as materials for light-emitting devices. The emission intensities of the compounds are enhanced in the solid and liquid crystal phases, meaning that they exhibit aggregation–induced emission and can be useful as phosphorescent AIEgens.

As part of a report commented before for iron in Section 6.1, palladium and platinum in Section 8.1, a hydrofluorocarbon alkoxy isocyanide mesomorphic ligand was used to prepare Ag(I) **126a** (X = BF_4, NO_3), Au(I) and Cu(I) **126b** (M = Au, Cu) and dimer Cu(I) **126c** complexes.[68] **126a** and **126b** compounds showed SmA calamitic mesophases stable over a remarkable wide temperature range (148, 83 and 81 °C, respectively for Ag, Au and Cu) and high transition temperatures (up to 274 °C for Au) compared to the similar hydrocarbon compounds. On the contrary, Cu(I) **126c** complexes were non mesomorphic.

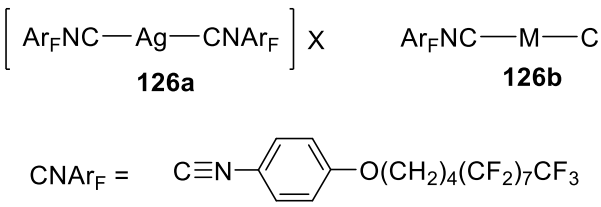

126a

126b

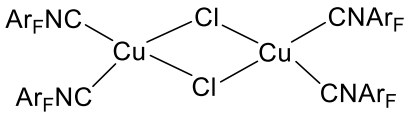

126c

9.1.3 Mixed isocyanide haloaryl complexes

The combination of two equal mesogenic alkoxytetrafluoroaryl ligands and several substituted biphenyl diisocyanides led to nematic dinuclear gold(I) complexes **127** (R = C_nH_{2n+1}, n = 4, 6, 8, 10, R' = H, Cl, Me).[186] Transition temperatures decrease in the order 4,4'-biphenylene > 2,2'-dichloro-4,4'-biphenylene > 2,2'dimethyl-4,4'-biphenylene, which was related to the twist angle (Me > Cl >> H) of the biphenyl and therefore, the planarity of the molecule: more planar means stronger interactions and therefore higher transition temperatures. Complexes show emission maxima in the range 480–532 nm at room temperature in the solid state and also in solution, from 452 to 524 nm.

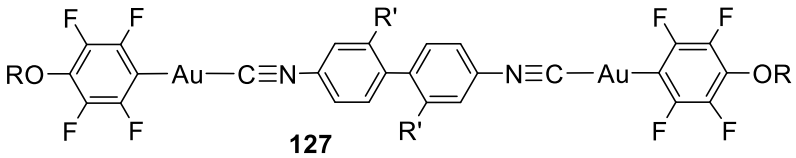

127

Mononuclear gold(I) compounds **128** (Y = H, Z = OC_4H_9, OC_8H_{17}, $OC_{10}H_{21}$, $OC_{12}H_{25}$; Y = Z = OC_4H_9, OC_8H_{17}, $OC_{12}H_{25}$) containing a perfluoroaryl mesogenic unit and a crown ether isocyanide have been prepared.[187] Complexes with one alkoxy chain display a smectic C mesophase at temperatures close to room temperature. The trialkoxy-chain complexes show smectic C or unidentified mesophases, more clearly observed on cooling. The increase of the alkoxy chain length diminishes the melting temperature in these complexes. The bulky and flexible crown ether fragment leads to less intermolecular attractions, lower melting points, less ordered mesophases, and shorter mesophase ranges. These mesogens are emissive not only in the solid, and in solution, but also in the mesophase, and even in the isotropic liquid at mild temperatures. The complexes in the solid state display emission maxima from 457 to 511 nm at room temperature and in the range 450–492 nm at 77 K. They also emit in solution at room temperature in the range 426–445 nm, and at 77 K from 425 to 497 nm.

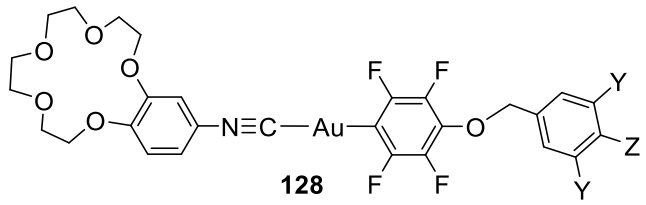

128

The 15-crown ether moiety is able to coordinate sodium cation from $NaClO_4$, solubilizing it in chlorinated solvents, leading to the corresponding bimetallic complexes **129** (Y = H, Z = OC_8H_{17}; Y = Z = OC_8H_{17}), although the liquid crystal behavior is lost.

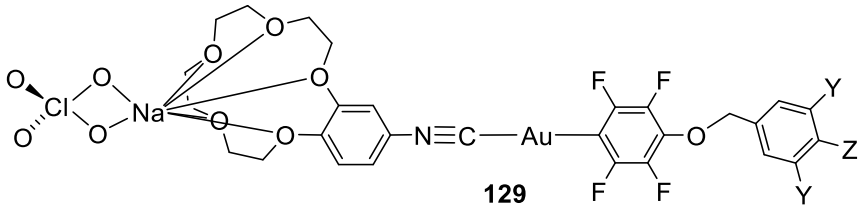

129

9.1.4 Isocyanide Dendrimers

The synthesis and design of liquid crystal metallodendrimers has attracted much interest during the last years.[188] We will describe here the results obtained for organometallic complexes of group 11 metals, and in particular for isocyanide.

Two generations of isocyanide dendrimers have been reported, and, also, the corresponding organometallic complexes **130a** [MCl(CN-G^n)] (M: Au, Cu) and **130b** [{CuCl(CN-G^n)$_2$}$_2$].[123] The free ligands and the first-generation complexes are not mesomorphic, but the second-generation complexes exhibit a thermotropic micellar cubic mesophase, over a large temperature range. In particular the coordination to Au–Cl fragment leads to a mesophase in a wide temperature range of

94–260 °C, 110 to 290 °C for Cu–Cl and from room temperature to 268 °C for the Cu dimer. The palladium and platinum complexes were described in Section 8.1, along with a schematic representation of their structure.

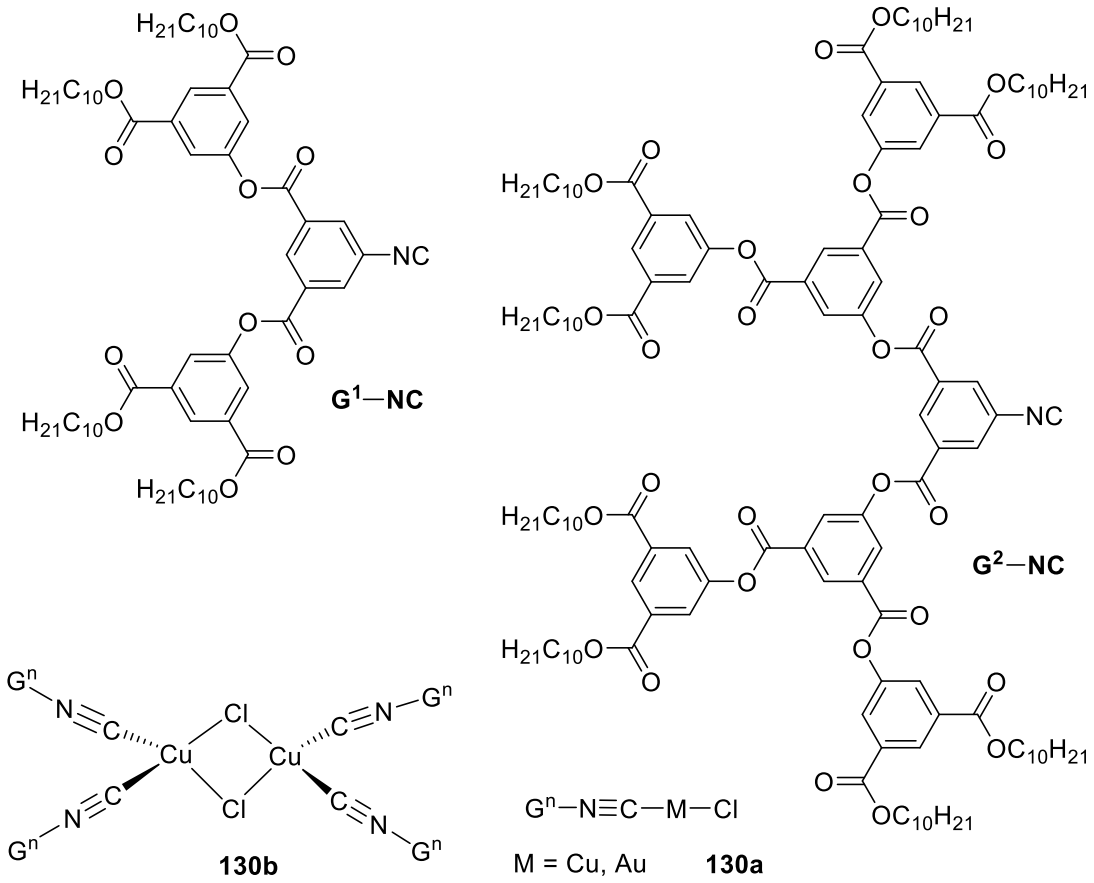

More recently, non-mesomorphic oily dendrimers containing isocyanide as terminal functional groups were designed and prepared.[189] Dendritic polyisocyanides are polytopic ligands able to generate a great diversity of metallodendrimers because of their ability to bind to various transition metals. Moreover, they can be used to build liquid-crystalline organometallic dendrimers. Generation zero, one, and two, with 3, 6, or 12 nitro terminal groups were synthesized, and then transformed into the corresponding polyisocyanides. Three types of gold(I) fragments were connected at the periphery of the dendrimers to give metallodendrimers **131**.

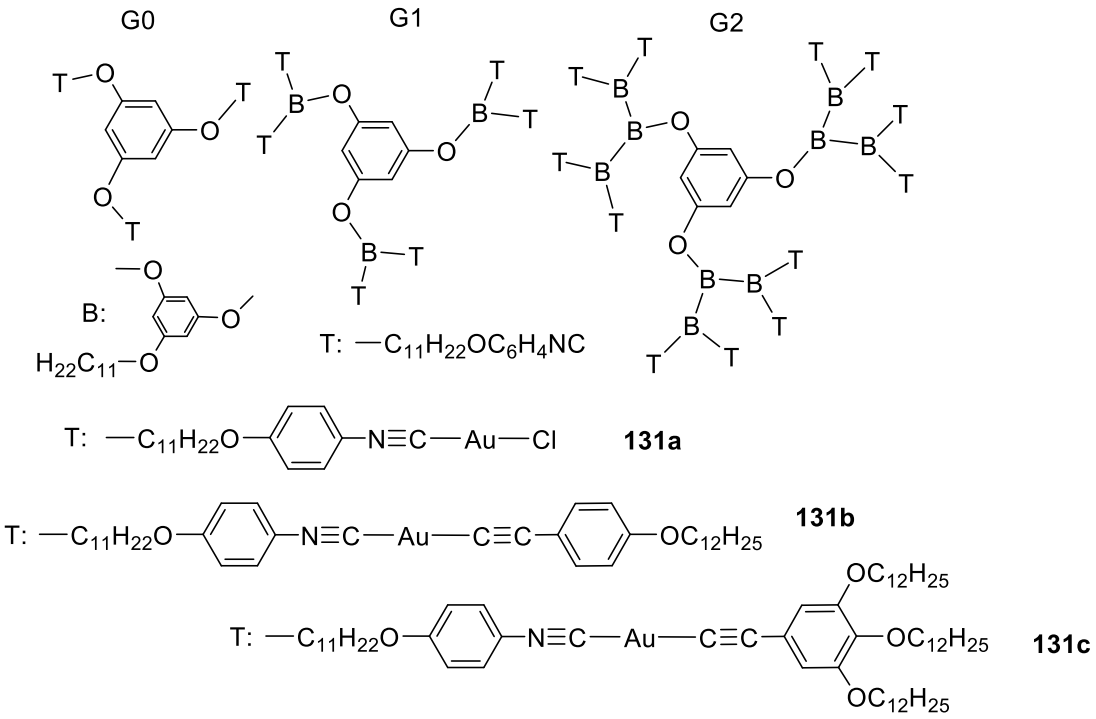

Their liquid crystal properties are largely influenced by the nature of the peripheral gold fragments, while increasing the dendritic generation contributes to a strong stabilization of the mesophases. Smectic C mesophases are observed for **131a** and **131b**, with mesophase temperature ranges 68–173 (G0) and 105–172 °C (G1) for Au–Cl, but only 112–128 (G0) and 110–121 °C (G1) for Au–acetylide. A room temperature columnar hexagonal mesophase is displayed by the three generations of dendritic gold complexes bearing hemipolycatenars **131c**. The clearing temperatures decrease with the generation from 116 (G0) to 73 (G1) and 36 °C (G2). Based on X-ray diffraction studies the columnar phase results from supramolecular aggregation of molecular dendrimers into one-dimensional cylindrical assemblies, which are further organized to give a hexagonal network. On the other hand, the smectic phases form by the lateral two-dimensional registry of the dendrimers in antiparallel head-to-head prolate conformation.

9.1.5 Hydrogen-bonded isocyanide derivatives

4-isocyanobenzoic acid gold(I) complexes [AuX(CNC_6H_4COOH)] (X = Cl, fluoroaryl; metallo-organic acids) have been prepared. These complexes act as proton donors face to decyloxystilbazole, to yield supramolecular metal complexes **132** (R = Cl, C_6F_5, $C_6F_4OC_6H_{13}$, $C_6F_4C_6F_4Br$) showing liquid crystalline behavior.[118,119] **132** with the Au–Cl fragment shows a calamitic SmA mesophase in the short range 170–187 °C, while the Au–fluoroaryl fragments show rod-like SmC mesophases with melting points in the range 127–190 °C, and clearing points from 170 to 190 °C. The fluoroaryl gold(I)–stilbazole aggregates exhibit luminescence in the solid state at room temperature with emission maxima in the range 468–485 nm. This emission has been assigned as an overlapping of the emissions coming from the free stilbazole and the gold(I) moiety. The corresponding H-bond palladium and platinum supramolecular complexes were described in Section 8.1.

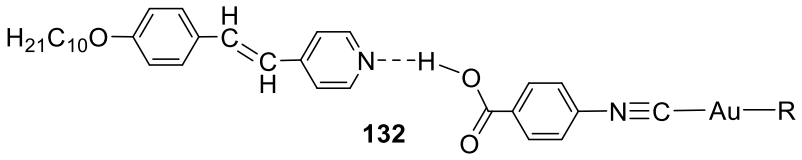

132

In order to reduce the transition temperatures, supramolecular metal complexes **133** (R = C_6F_5, $C_6F_4OC_{10}H_{21}$) formed through H-bonds between tris(3,4,5-decyloxy)stilbazole and several gold(I) acids [AuR(CNC_6H_4COOH)] were prepared.[120] Unexpectedly, the compounds are not mesomorphic, although the corresponding palladium and platinum *trans* complexes show hexagonal columnar mesophases (Section 8.1). Remarkably, the H-bond in the gold aggregate [Au($C_6F_4OC_{10}H_{21}$)(CNC_6H_4COOH)] survives on the water surface giving rise to Langmuir films where the molecules are parallel to the water surface. Both gold adducts emit intensely at room temperature in the solid state, with emission maxima at 497 and 528 nm, respectively. The emission was related to the luminescent stilbazole modified by the gold fragment.

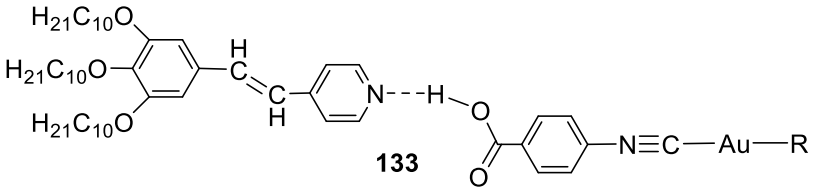

133

This strategy can lead not only to calamitic mesogens but also to discotic liquid crystals. As commented in Sections 4 and 6.1, supramolecular aggregates were reported by reaction of carboxylic acid, namely *para*-isocyanobenzoic metal complex (carbonyl compounds of Fe, Cr, Mo and), with 2,4,6-triarylamino-1,3,5-triazine.[61] They behave as discotic liquid crystals at room temperature. By using this strategy, mono- and dinuclear thiolatobenzoic gold(I) [Au(PR_3)(x-SC_6H_4COOH)] and [μ-(BINAP){Au(x-SC_6H_4COOH)$_2$}] (x = 2 or 4; BINAP: 2,2'-Bis(diphenylphosphino)-1,1'-binaphthalene) metalloacids were combined with the same triazine to yield the corresponding adducts **134a** (*ortho*, *para* substitution; R = $C_{10}H_{21}$) and **134b** (P–P = *R*-BINAP, *S*-BINAP; *ortho*, *para* substitution; R = $C_{10}H_{21}$) by means of H-bonds.[190] They show Col_{hex} mesophases at room temperature, with clearing temperatures in the short range 43–57 °C, close or lower than for the free triazine (57 °C), while for the previous metallo-acids (Fe, Cr, Mo, and W) is higher. The diffractograms in the mesophase display a new broad peak, which may be related to gold–gold distances from closest neighbors. Remarkably, hexagonal columnar mesophases found in the free triazine were preserved in the metal-containing supramolecular aggregates. The nine alkoxy chain triazine structure is able to swallow metal-organic fragments, even containing bulky ligands as phosphines.

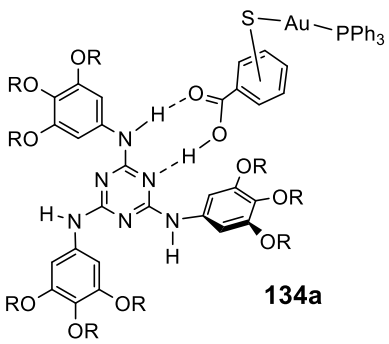

134a

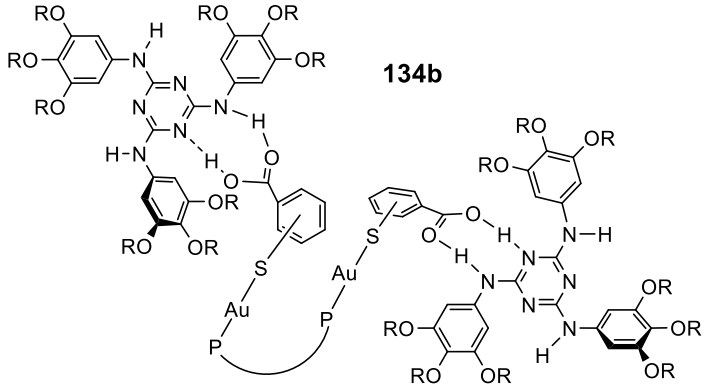

134b

As commented in Section 4 for chromium(0) $[Cr(CO)_5(z\text{-}PPh_2C_6H_4COOH)]$ (z = 2 or 4), an extension of this work was carried out by synthesizing neutral gold(I) and gold(III) $[AuX_n(z\text{-}PPh_2C_6H_4COOH)]$ (n = 1, X = Cl, z = 2 or 4; n= 3, X = C_6F_5, z = 2 or 4) and cationic gold(I) $[Au(z\text{-}PPh_2C_6H_4COOH)_2](CF_3SO_3)$ (z = 2 or 4), *ortho* and *para* phosphino metallo-acids.[62] X-Ray diffraction show dimeric structures with the expected double carboxylic H-bonds in $[AuCl(4\text{-}PPh_2C_6H_4COOH)]$ and $[Au(C_6F_5)_3(4\text{-}PPh_2C_6H_4COOH)]$, whereas $[Au(C_6F_5)_3(2\text{-}PPh_2C_6H_4COOH)]$ display monomeric species with the carboxylic acid H bonded to cocrystallized solvent molecules. Gold compounds are emissive at 77 K with emission maxima from 404 to 520 nm, and some of them also at room temperature with emission maxima in the range 441−485 nm. Reactions with the 2,4,6-triarylamino-1,3,5-triazine mesogen leads to hydrogen-bonded gold(I) supramolecular adducts, while the related gold(III) complexes do not form adducts likely by steric reasons. Only the 4-diphenylphosphinobenzoic adducts **135a** and **135b** show a columnar hexagonal mesophase at room temperature, with clearing temperatures in the range 36−60 °C for gold(I). The aggregates are luminescent at 77 K, with emission maxima in the range 419−455 nm. Again is confirmed the triazine bearing nine lateral alkoxy chains is able to accommodate large metal−organic fragments to produce adducts without losing the mesomorphic behavior, although the weakness of the connection of the two components limits the thermal stability. However, the *ortho*-phosphine metalloacids are clearly detrimental for the formation of these adducts and the liquid crystal behavior.

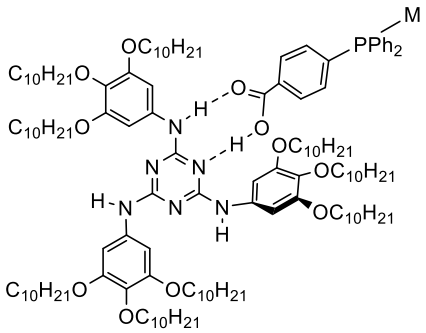

M = nothing, AuCl

135a

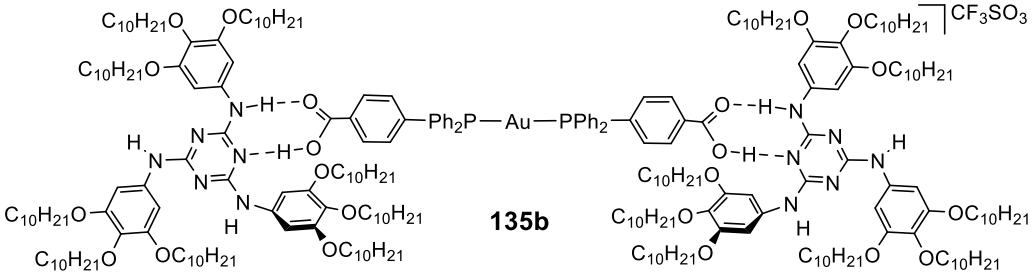

135b

By this approach 4-isocyanoanilides have been used to prepare Ag(I) neutral complexes **136a** [Ag(X)(CN−C_6H_4−NHCOR)] (R = Me, X = NO_3^-, $CF_3SO_3^-$; R = C_9H_{19}, X = NO_3^-) and cationic complexes **136b** [Ag(CN−C_6H_4−NHCOR)$_2$]X (R = Me, X = NO_3^-, $CF_3SO_3^-$, BF_4^-; R = C_9H_{19}, X = NO_3^-, $H_{25}C_{12}OSO_3^-$, $CF_3SO_3^-$, BF_4^-).[191] Single crystal X-ray diffraction studies of methyl derivatives show layered supramolecular structures supported by Ag−O interactions and hydrogen bonds, induced by the amide group and the anionic ligand. Substitution of the methyl group by a nonyl chain in the amide leads to mesomorphic complexes, which display SmA mesophases as expected by the methyl structures, and supported by the presence of H-bonds in the FTIR spectra. Melting temperatures go from 91 to 144 °C, while clearing temperatures are in the range 138–200 °C, with a maximum liquid crystal range of 109 °C for compound **136b** (R = C_9H_{19}, X = NO_3^-).

[AgXL] **136a** [AgL_2]X **136b**

L = 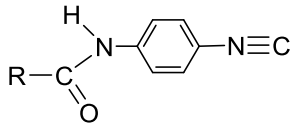

9.1.6 Isocyanide for discotic mesogens

We have described that organometallic discotic mesogens have been synthesized by means of H–bonds around a 2,4,6–triarylamino–1,3,5–triazine core. These bonds are labile and the corresponding liquid crystals are stable over a short temperature range. A better strategy for preparing organometallic discotic mesogens is the use of suitable covalent bonds around an appropriate core.

Hexaalkoxy triphenylene derivatives have been thoroughly used to prepare purely organic columnar discotic liquid crystals. The right functionalization allows coordinating metal fragments, which in many cases are mesogens. By this approach, the new ligand 1–isocyano–2,3,6,7,10,11–hexadodecyloxytriphenylene (CN–TriPh) have been synthesized in order to prepare organometallic mononuclear gold(I) **137a** (X = Cl, C_6F_5, C_6F_4O–$C_{10}H_{21}$, C_6F_4O–(R)–2–octyl), dinuclear gold(I) **137b**, copper(I) **137c** and silver(I) **137d**.[192] The free isocyanide ligand and the gold(I) **137a–b** compounds exhibit typical hexagonal columnar mesophases over a wide range of temperatures, from 5 to 220 °C. Melting points are 37 °C for the ligand and from 5 to 7 °C for **137a**; clearing points are 130 °C for the ligand and in the range 204–220 °C for **137a**. Gold compound **137b** displays a rectangular columnar mesophase between 102 and 122 °C, and a nematic mesophase till 172 °C. On the contrary copper and silver complexes **137c–d** are not mesomorphic. This may be explained for complex **137d** due to the presence of two *trans* coordinated isocyanide ligands, which cannot be coplanar due to the too short linker, while the longer linker in **137b** compound allows planarity. All the compounds show a fluorescent emission in solution centered on the triphenylene core in the range 421−467 nm; the emission is lost in concentrated solutions or in aggregate states. The nature of the metallic fragment is dramatically affecting the liquid crystal behavior, which can be mainly related to the fact than the isocyanide is directly bonded to the triphenylene core.

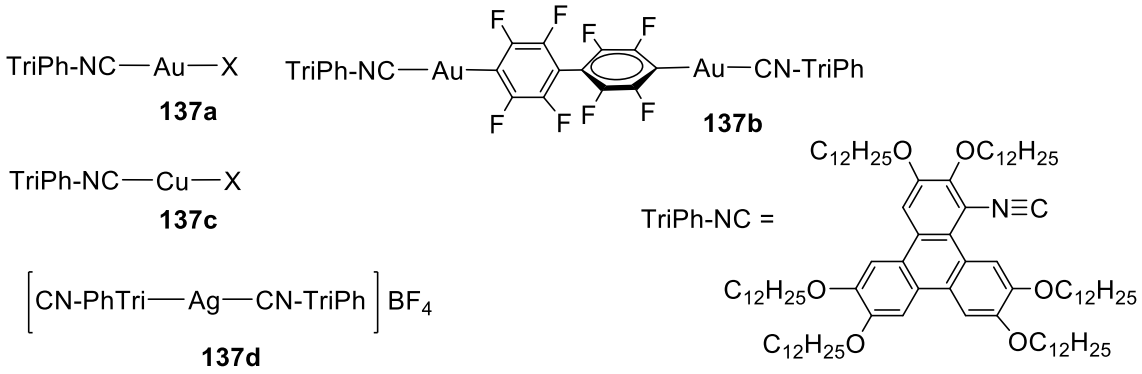

As commented above in the Section 8.1 (palladium and platinum), and following the same approach, a new isocyano ligand namely 2-(6-(4-isocyanophenoxy)hexyloxy)-3,6,7,10,11-pentakisdodecyloxytriphenylene have been prepared and used to synthesize organometallic gold(I) and copper(I) **138a** (M = Au, X = Cl, C_6F_5, C_6F_4O-$C_{10}H_{21}$, CN; M = Cu, X = Cl), dinuclear gold(I) **138b**, and dinuclear copper(I) **138c** complexes.[121] Compounds **138a** (only [Au(CN)(CNR)] and [CuCl(CNR)]) and **138c** display a rectangular columnar mesophase in a short range: 61–98 °C, 46–79 °C and 72–79 °C, respectively. **138b** shows a lamellar rectangular columnar mesophase in a wider range: 22–98 °C. Both types of mesophase show at the same time, π–stacking of the triphenylene cores and aggregation of the metallic fragments into segregated columnar zones. Therefore, heterocolumnar arrangements are obtained as a consequence of the nanosegregation induced by the different nature of the molecular components. All these complexes show again fluorescence in solution related to the isocyanide triphenylene ligand. Pd and Pt complexes exhibit semiconducting mesophases as commented above. The previous isocyanide triphenylene was equipped with six equal alkoxy chains and the isocyanide was directly bound to the triphenylene core, therefore the metallic moiety was dramatically affecting the thermal properties. However, in this case the triphenylene was equipped with five equal alkoxy chains and the isocyanide is at the end of the sixth alkoxy chain: the effect is much less intense, but the metals can form their own column inducing a heterocolumnar rearrangement.

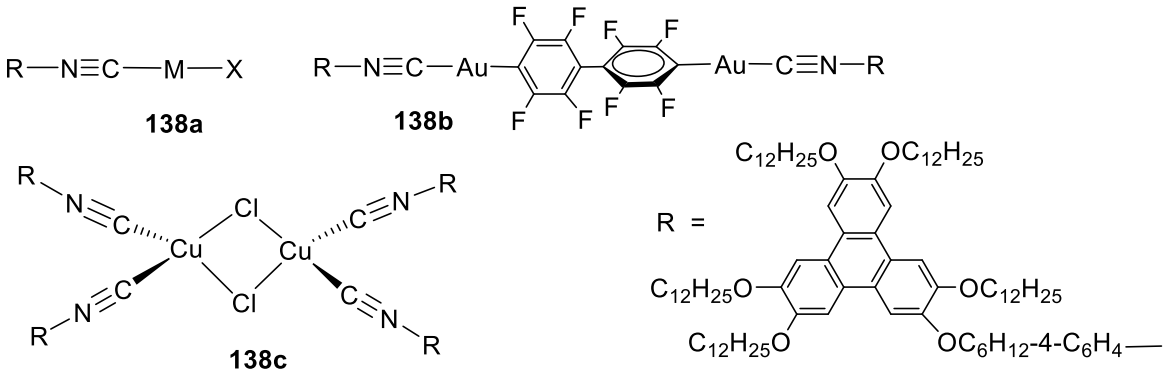

In addition to triphenylene, cyclotriphosphazene has been used as core to support columnar discotic liquid crystals. Aminocyclotriphosphazenes have been reacted with the isocyanide silver(I) complex [Ag(OTf)(CNR)] (OTf =OSO_2CF_3) in molar ratio 1:3, to give room temperature columnar metallomesogens **139** (R = R' = Me; R = H, R' = Cy).[193] The same complexes in molar ratios 1:1 or 1:2 are not mesomorphic. Each silver fragment "AgCNR" is bonded to one nitrogen in the phosphazene

core. The starting silver complex [Ag(OTf)L] and the trinuclear complexes equipped with nine alkoxy chains display a columnar hexagonal mesophase with isotropization temperatures of 145, 61 and 72 ^{o}C, respectively, for [Ag(OTf)(CNR)] and the two trinuclear silver phosphazenes. A model consisting of two complementary molecules leads to an overall disk shape, which promotes the supramolecular columnar rearrangement driven by efficient space–filling and nanosegregation of chemically different zones.

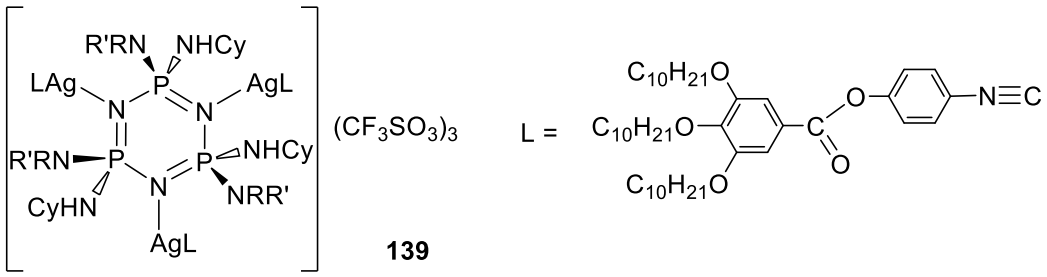

139

9.1.7 Isocyanide as a colorant

The introduction of dyes into mesomorphic systems is a useful strategy for the preparation of new functional materials. 4,4'–Disubstituted azobenzene compounds with adequate substituents have been used to prepare *ortho*-metalated mesogens, mainly with group 9–10 metals. Azo derivatives are well known dyes and the color is usually transferred to the new compounds. The coordinated azo fragment is blocked in its *trans* conformation, and therefore the photosensitivity is lost. New azo isocyanide mesogens were designed, with an azo, an isocyanide, and an alkoxy chain as functional groups. These ligands exhibit nematic and SmA mesophases for n > 4, and they are able to coordinate metals through the isocyanide. The new complexes are intensely orange and the most interesting feature is that possess a free photosensitive azo functional group. Their gold(I) compounds **140** (X = Cl, C_6F_5; n = 4, 8, 12), also display nematic and SmA mesophases, but with higher transition temperatures and wider mesophase ranges.[194] The complexes are photoresponsive in solution due to fast *trans* to *cis* isomerization of the azo group under UV light (365 nm lamp), which goes back photochemically or thermally to the *trans* isomer. Most relevant, the process can be carried out in the mesophase by irradiation with a very intense He–Cd laser, which produces rapid isomerization, and consequent destabilization to an isotropic liquid. The initial mesophase is recovered as soon as illumination stops (Figure 9). As expected, linear gold complexes exhibit high birefringence values (Δn from 0.51 to 0.59) than the free azo ligand (Δn are 0.32), because of gold increases the molecular anisotropy. In summary, these colored azo gold–containing mesogens are photosensitive, not only in solution but also in the mesophase, remarkably the photoisomerization has been demonstrated in a mesophase showed by a pure metallomesogen.

<Figure 9 near here>

Figure 9. Changes in azo isocyanide gold mesogens **140** after irradiation with a laser.

Following the same approach, azulene, a classical azure–blue chromophore was functionalized with an isocyanide group and coordinated to gold(I) synthons to prepare mononuclear **141a** (X = Cl, C_6F_5), **141b** (x = 1, R = C_8H_{17}, $C_{10}H_{21}$; x = 2, R = $C_{10}H_{21}$),), **141c** (R = Me, $C_{10}H_{21}$), and dinuclear **141d**

complexes.[195] Gold compounds **141b** (x = 1, 2; R = $C_{10}H_{21}$) and **141c** (R = $C_{10}H_{21}$) display SmA mesophases being the widest range for the alkynyl ligand from 106 to 150 °C. The free isocyanoazulene derivative shows a weak fluorescent emission centered on the azulene group at 380 nm, which diminishes upon coordination to the gold moieties. All the compounds are intensely blue colored. Theoretical studies confirmed that the UV–vis absorption (color) and emission are centered on the azulene core.

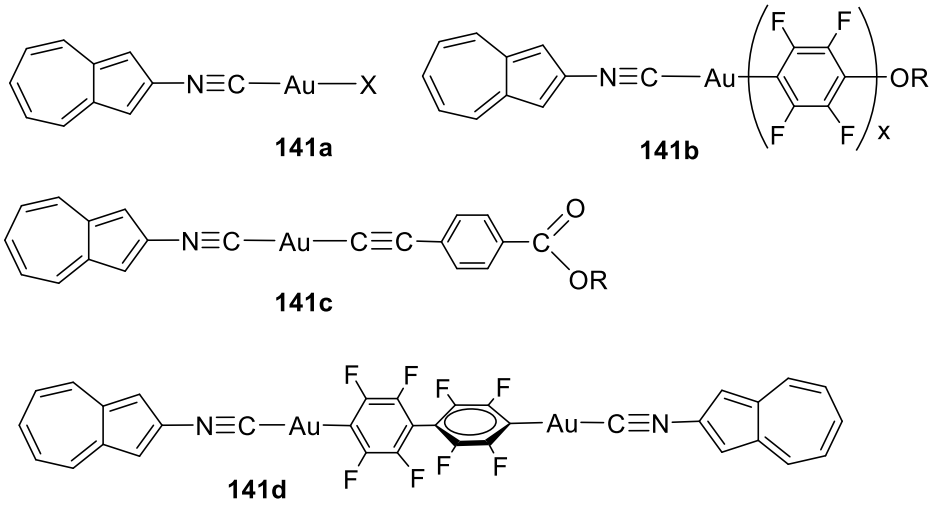

9.2 Carbene Complexes

N–heterocyclic carbenes may be easily modified to modulate their electronic and steric properties, a strategy commonly used to improve catalyst but can be also useful for the design of liquid crystals. A series of *N*–heterocyclic carbene (NHC) imidazole gold(I) complexes **142** (*n* = 12, 18, *m* = 1, 6, 12, 18; *n* = 16, *m* = 10, 12, 14, 16, 18) have been prepared.[196] They exhibit a SmA mesophase, typical for ionic liquid crystals. The melting and clearing temperatures can be tuned mainly by the imidazole alkyl chain length: longer chain, higher clearing and melting points. The widest intervals are obtained for the C_{18} carbene: the melting points are from 57.3 to 101.5 °C, and the clearing points from 96.9 to 124.1 °C. These complexes were used to obtain gold nanoparticles in organic phase by chemical reduction. The related complexes [AuCl(NHC)] and $[Au(NHC)_2][NO_3]$ are not mesomorphic although they possess two or four alkyl chains.

Self–assembly of N–heterocyclic carbenes containing two different chains (one amide able to form H–bonds and one aliphatic) yields gold(I) and silver(I) complexes **143** (R = C_nH_{2n+1}; n = 12, 14, 16, 18. R' = $CH_2C(O)NH_2$. M = Au and X = Br, NO_3, BF_4. M = Ag and X = NO_3, BF_4), which behave as enantiotropic liquid crystals.[197] They display SmA mesophases with melting points around 150 °C for gold, 170 °C for silver–BF_4 and 110 °C for silver–NO_3, and clearing points up to 226 °C for gold (being the best with *n* = 16 and bromide as anion) and 200 °C for silver with decomposition. Gold(I) compounds form xerogels in DMSO and show oriental lantern–shaped bundles of belts and helical fibers when observed by transmission electron and scanning electron microscopies. These gels display smaller chain motion than in the mesophase, closer to found in the solid state, as studied by infrared spectroscopy.

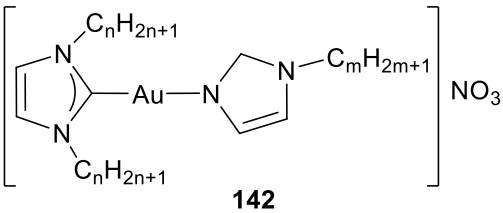

142

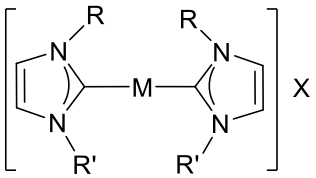

143

Imidazolium salts are well known as ionic liquids and also as ionic liquid crystals. Moreover, they can be used as N–heterocyclic carbene (NHC) precursors. A series of bis(imidazolium) salts with appropriate mesogenic groups (cyanobiphenyl or cholesteryl) linked through a flexible alkyl spacer have been designed and prepared in order to get their silver carbene complexes **144**.[198] The silver complexes and the bis(imidazolium) salts display SmA mesophases with close melting point but wider temperature ranges for silver. The silver complex with cholesteryl group shows higher transition temperatures (51 to 180 °C) than the complexes containing cyanobiphenyl mesogenic groups (36 to 54 °C, 39 to 76 °C). The silver complexes show a blue emission centered around 450 nm in solid state, as 10% PMMA (Polymethylmethacrylate) films, in isotropic and LC phase, and in dichloromethane solution (centered in this case at 360 nm), which it is related to the bis(imidazolium) salts.

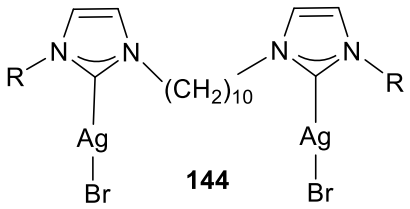

144

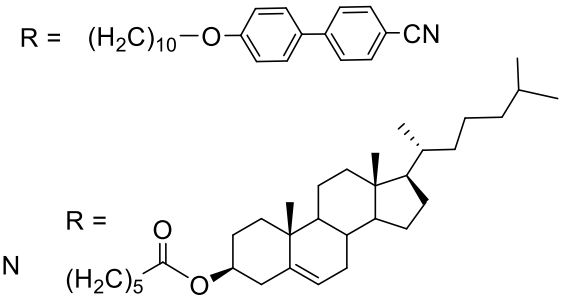

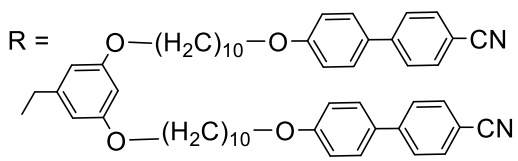

By the same approach, propylene bridged bis(imidazolium) salts bearing benzyl group functionalized with one or two long alkyl chains have been synthesized. The corresponding N–heterocyclic carbene dinuclear gold(I) complexes **145** (R = CH_2–3,4–C_6H_3–$(OC_{12}H_{25})_2$; X = Br, PF_6, BF_4) have been also prepared but only complexes with eight aliphatic chains show lamellar mesophases in a short range.[199]

Imidazol core can be substituted by benzimidazol, and equipped with an eighteen alkyl chain on one N atom and an alkyl or substituted benzyl moiety on the other N. The corresponding mononuclear silver(I) N–heterocyclic dicarbene complexes **146** (R = C_nH_{2n+1}; n = 10, 12, 14, 16. R = 4–CH_2–C_6H_4–R'; R'= H, CH_3, CN) have been prepared.[200] Only two silver complexes containing two long alkyl chains display monotropic SmA in a short range (the best 21 °C) at temperatures under 100 °C. The related silver carbene compounds with R = Me, and alkyl chains C_nH_{2n+1} (n = 12, 14, 16, 18) instead of eighteen in **146** are not mesomorphic.[201] As seen in other reports, the use of bulky hexafluorophosphate is detrimental for liquid crystal behavior and it is the only anion in this work.

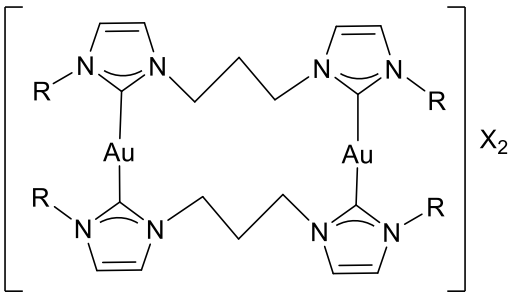

145

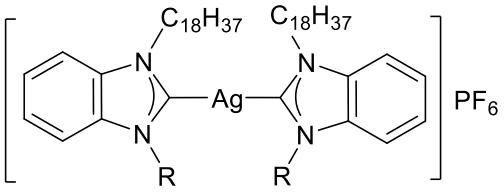

146

N–heterocyclic carbene silver(I) complex $[\{Ag(NHC)_2\}_2][Ag_2Cl_4]$ **147a** (R = CH_2–CH(OH)–$C_{14}H_{29}$; R' = $C_{16}H_{33}$) behaves as liquid crystal while the related gold(I) complexes **147b** and **147c** (X = BF_4, PF_6) are soft materials.[202] This carbene combines an alkyl chain with an hydroxy alkyl chain in order to facilitate not only hydrophobic interactions but also hydrogen bonding. A typical SmA mesophase is observed in a narrow 5 °C temperature range of 92.6 to 97.6 °C, expanding to 50 °C upon cooling. Complexes **147a** and **147b** exhibit yellow (569 nm) and orange (607 nm) emissions.

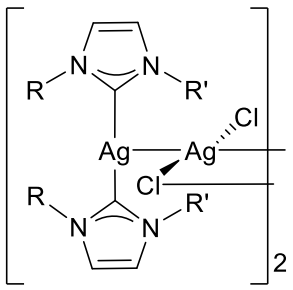

147a

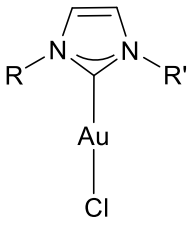

147b

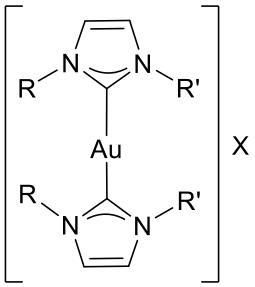

147c

Gold(I) complexes **148** combining alkoxy acetylide and a carbene derived from benzimidazolium equipped with two alkoxy chains in the phenyl ring have been reported. Only the trialkoxy compound behaves as monotropic liquid crystal and displays a SmA mesophase in a short range (190–203 °C). This complex exhibit an intense blue phosphorescence at room temperature in the solid state (quantum yield 0.33; lifetime 36 µs).[203]

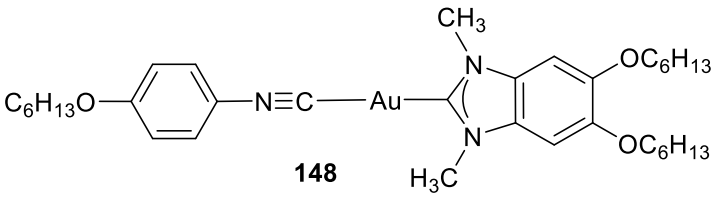

148

A series of N–heterocyclic carbene complexes **149a** [MX(NHC)] (R= R'= Tph; M = Cu, X = Br; M = Au, X = Cl, CCPh), and silver **149b** (R = Me, R' = Tph; R = R'= Tph), with the carbene bearing one or two triphenylene fragments have been reported.[125] Copper(I) **149a** and silver(I) **149b** complexes align into columnar liquid crystals (rectangular or hexagonal symmetries), driven by peripheral hexaalkoxy triphenylene moieties. Melting points go from 30 to 55 °C and clearing points are in the range 57−98 °C. Models point to multicolumnar systems obtained by nanosegregation of triphenylene columns and metal carbene moieties, separated by alkoxy chains. The complexes show a blue emission

related to the triphenylene core in solution, in the mesophase, in the isotropic liquid, and in the solid state.

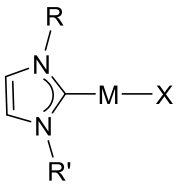

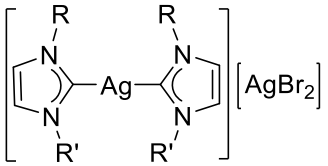

149b

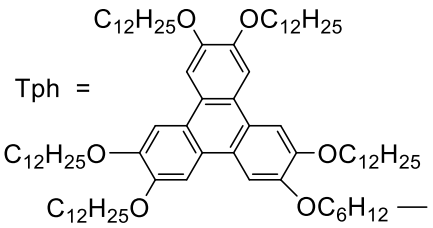

Finally, a series of phosphorescent gold(I) N–heterocyclic allenylidene complexes **150** (X = Cl, CF_3SO_3, PF_6) have been reported.[204] These organometallic complexes exhibit a strong blue emission (centered 414–450 nm) in acetonitrile solutions with life time in the range 1.4–5.6 micros and quantum yield from 7 to 14%. Complex with imidazole substituents and chloride formed lyotropic chromonic mesophases (N phase) in aqueous solutions.

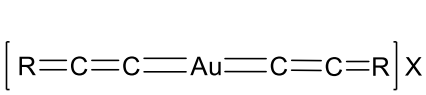

150

R =

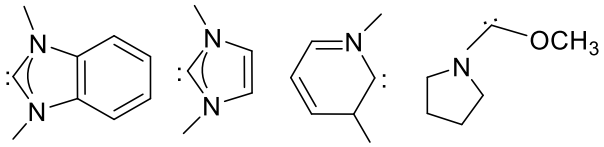

10 Concluding Comments

The literature on organometallic mesogens is more limited than that on mesomorphic coordination compounds and is dominated by *ortho*–metalated complexes (mainly Pd(II) and Pt(II)), and ferrocene derivatives. In general, the M–C bond is not very thermally stable and tends to be labile and easily reacts with moisture and oxygen. That is why M–CO and especially M–CNR with the metal in low oxidation state, which are quite stable, are also typical fragments in many metallomesogens. However, ligand design has made it possible to decorate chelates (to metalate), cyclopentadienyls (in ferrocene) and isocyanides with a huge number of chemical motifs to add or enhance the optical, electrical, and magnetic properties of liquid crystal materials.

Acknowledgement

We gratefully acknowledge the Ministerio de Economía y Competitividad (Project CTQ2017–89217–P) and the Junta de Castilla y León (Project VA224P20) for financial support.

References

1 Donnio, B.; Guillon, D.; Bruce, D.W.; Deschenaux, R. Metallomesogens. In *Comprehensive Organometallic Chemistry III: From Fundamentals to Applications*; Crabtree, R.H.; Mingos, D.M.P. Eds.; Elsevier: Oxford, UK, 2006; Volume 12, Chapter 12.05, pp. 195–293.

2 Jonas, U.; Petri, C.; Kunzler, C.; Spiess, H.W. *Polymeric Discotic Liquid Crystals, Reference Module in Materials Science and Materials Engineering*, Elsevier, 2017.

3 Zhu, L.; Li, C. Y. (Eds.), *Liquid Crystalline Polymers*, Springer, 2020.

4 Prakash, J.; Khan, S.; Chauhan, S.; Biradar, A. M. *J. Mol. Liq.* **2020**, *297*, 112052.
5 Ermakov, S. F.; Myshkin, N. K., *Liquid-Crystal Nanomaterials: Tribology and Applications*, Springer, 2018.
6 Choudhary, A.; Singh, G.; Biradar, A. M. *Nanoscale* **2014**, *6*, 7743–7756.
7 Serrano, J.L. *Metallomesogens: Synthesis, Properties and Applications*; WILEY-VCH: Weinheim, Germany, 1996.
8 Donnio, B.; Guillon, D.; Deschenaux, R.; Bruce, D. W. Metallomesogens. In *Comprehensive Coordination Chemistry II*; McCleverty, J. A., Meyer, T. J., Eds.; Elsevier: Oxford, UK, 2003, Vol. 7, Chapter 7.9, pp 357–627.
9 Torroba, J.; Bruce, D.W. Metallomesogens. In *Comprehensive Inorganic Chemistry II (Second Edition): From Elements to Applications,* Reedijk, J.; Poeppelmeier, K. Eds.; Elsevier, 2013, Vol. 8, chapter 8.21, pp. 837–917.
10 Pucci, D.; Donnio, B. Metal-containing liquid crystals. In *Handbook of Liquid Crystals; Non-Conventional, Supramolecular, Chromonic and Amphiphilic Liquid Crystals*; Goodby, J.W., Collings, P.J., Kato, T., Tschierske, C., Gleeson, H., Raynes, P., Eds.; Wiley-VCH: Weinheim, Germany, 2014; Vol. 5, chapter 4, pp 1–67.
11 Barón, M. *Pure Appl. Chem.* **2001**, *73*, 845–895.
12 Leadbetter, A. J.; *Thermotropic Liquid Crystals*; Gray, G. W., Ed.; Wiley: Chichester, 1987; Chapter 1, pp 1–27.
13 Gray, G. W.; Goodby, J. W. *Smectic Liquid Crystals; Textures and Structures*; Leonard Hill: Glasgow, 1984. c) Dierking, I. *Textures of Liquid Crystals*, Wiley-VCH, Weinheim, 2003.
14 Malthete, J.; Nguyen, H.-T.; Destrade, C. *Liq. Cryst.* **1993**, 13, 171–187.
15 Nguyen, H. L.; Destrade, C.; Malthête, J. *Adv. Mater.* **1997**, *9*, 375–388.
16 Ros, M. B.; Serrano, J. L.; de la Fuente, M. R.; Folcia. C. L. *J. Mater. Chem.*, **2005**, *15*, 5093–5098.
17 Collings, P. J.; Goodby, J. W. *Introduction to Liquid Crystals: Chemistry and Physics* (second edition), CRC Press, Taylor & Francis Group, 2019.
18 Collings, P. J.; Hird, M. *Introduction to Liquid Crystals: Chemistry and Physics*, CRC Press, Taylor & Francis Group, 1997.
19 Collings, P.J. *Liquid Crystals*, Princeton University Press: New Jersey, NJ, USA, 1990.
20 Reinitzer, F. *Monatsch. Chem.* **1888**, *9*, 421–441.
21 Heintz, W. *J. Prakt. Chem.* **1855**, *66*, 1–51.
22 Vorländer, D. *Z. Phys. Chem.* **1923**, *105*, 211–254.
23 Giroud-Godquin, A.-M.; Maitlis, P. M. *Angew. Chem., Int. Ed. Engl.* **1991**, *30*, 375–402.
24 Acree, W. E.; Chickos, J. S. *J. Phys. Chem. Ref. Data*, **2006**, *35*, 1051–1330.
25 Gray, G. W.; Harrison, K. J.; Nash, J. A. *Electron. Lett.* **1973**, *9*, 130–131.
26 Yang, D.-K.; Wu, S.-T. *Fundamentals of Liquid Crystal Devices*, John Wiley & Sons, 2014
27 Tschierske, C. (Guest Editor), *Theme issue: liquid crystals beyond display applications*, *J. Mater. Chem.* **2008**, *18*, 2857–3060.
28 Bisoyia, H. K.; Kumar, S. *Chem. Soc. Rev.* **2010**, *39*, 264–285.
29 Kaafarani, B. R. *Chem. Mater.* **2011**, *23*, 378–396.
30 Goossens, K.; Lava, K.; Bielawski, C. W. ; Binnemans, K. *Chem. Rev.* **2016**, *116*, 4643−4807.
31 Kim, D.-Y.; Jeong, K.-U. *Liq. Cryst. Today* **2019**, *28*, 34–45.
32 Yun, C.-J.; Song, J.-K. *J. Inf. Disp.* **2017**, *18*, 119–129.
33 Wei, D. *Liq. Cryst. Today* **2015**, *24*, 35–36.
34 Kasch, N. *Liq. Cryst. Today* **2013**, *22*, 70–71.

35 Bushby, R. J.; Kelly, S. M.; O'Neill M. (Eds.) *Liquid Crystalline Semiconductors: Materials, properties and applications*, Springer, 2012.
36 Zhao, J.; Gulan, U. ; Horie, T.; Ohmura, N. ; Han, J. ; Yang, C. ; Kong, J. ; Wang, S. ; Xu, B. B. *Small* **2019**, *15*, 1900019.
37 Binnemans, K. *J. Mater. Chem.* **2009**, *19*, 448–453.
38 Gasparb, A. B.; Seredyuka, M.; Gütlich P. *Coord. Chem. Rev.* **2009**, *253*, 2399–2413.
39 Binnemans K. Physical properties of metallomesogens. In *Molecular materials. Inorganic materials series. 4.* Bruce D.W., O'Hare D., Walton R.I., editors. Chichester: Wiley; 2010. p. 61–141.
40 Wang, Y.; Shi, J.; Chen, J.; Zhu, W.; Baranoff, E. *J. Mater. Chem. C* **2015**, *3*, 7993–8005.
41 Wöhrle, T.; Wurzbach, I.; Kirres, J.; Kostidou, A.; Kapernaum, N.; Litterscheidt, J.; Haenle, J. C.; Staffeld, P.; Baro, A.; Giesselmann, F.; Laschat, S. *Chem. Rev.* **2016**, *116*, 1139−1241.
42 Wu, X.; Zhu, M.; Bruce, D. W.; Zhu, W.; Wang, Y. *J. Mater. Chem. C* **2018**, *6*, 9848–9860.
43 Guy, K.; Ehni, P.; Paofai, S.; Roiland, C.; Amela-Cortes, M.; Cordier, S.; Laschat, S.; Molard Y. *Angew. Chem. Int. Ed.* **2018**, *57*, 11692–11696.
44 Binnemans, K. Lanthanidomesogens. In *Handbook on the Physics and Chemistry of Rare Earths*, Bünzli, J. C. G.; Pecharsky, V. K. Eds.; 2013, vol. 43, chapter 254, pp 1–158.
45 Guerra, S.: Dutronc, T.; Terazzi, E.; Buchwalder, K.–L.; Guénée, L.; Deschenaux, R.; Eliseeva, S.V.; Petoud, S.; Piguet, C. *Coord. Chem. Rev.* **2017**, *340*, 79–97.
46 Rajendiran, K.; Yoganandham, S. T.; Arumugam, S.; Arumugam, D.; Thananjeyan, K. *J. Mol. Liq.* **2021**, *321*, 114793.
47 Ringstrand, B.; Jankowiak, A.; Johnson, L.E.; Kaszynski, P.; Pociecha, D.; Górecka, E. *J. Mater. Chem.* **2012**, *22*, 4874–4880.
48 Pecyna, J.; Sivaramamoorthy, A.; Jankowiak, A.; Kaszynski, P. *Liq. Cryst.* **2012**, *39*, 965–971.
49 Tatum, L. A.; Johnson, C. J.; Fernando, A. A. P.; Ruch, B. C.; Barakoti, K. K.; Alpuche-Aviles, M. A.; King, B. T. *Chem. Sci.* **2012**, *3*, 3261–3264.
50 Wöhrle, T.; Baro A.; Laschat, S. *Materials* **2014**, *7*, 4045–4056.
51 Wöhrle, T.; Gündemir, R.; Frey, W.; Knecht, F.; Köhn, A.; Laschat, S. *Chem. Eur. J.* **2017**, *23*,4149 – 4159.
52 Takahashi, K.; Shimoi, M.; Watanabe, T.; Maeda, K.; Geib, S. J.; Curran, D. P.; Taniguchi, T. *Org. Lett.* **2020**, *22*, 2054−2059.
53 Cui, L.; Zhu, L. *Langmuir* **2006**, *22*, 5982–5985.
54 Karahaliou, P. K.; Kouwer, P. H. J.; Meyer, T.; Mehl, G. H.; Photino, D. J. *Soft Matter*, **2007**, *3*, 857–865.
55 Wang, X.; Cho, C. M.; Say, W. Y.; Tan, A. Y. X.; He, C.; On Chan, H. S. O.; Xu, J. *J. Mater. Chem.*, **2011**, *21*, 5248–5257.
56 Shao, Y.; Xu, X.; Yin, G.-Z.; Han, S.-Y.; Han, D.; Fu, Q.; Yang, S.; Zhang, W.-B. *Macromolecules* **2019**, *52*, 2361−2370.
57 Miao, J.; Zhu, L. *J. Phys. Chem. B* **2010**, *114*, 1879–1887.
58 Cui, L.; Collet, J. P.; Xu, G.; Zhu, L. *Chem. Mater.* **2006**, *18*, 3503–3512.
59 Thurmes, W. N.; More, K. M.; Meadows, M. R.; O'Neill, M. B.; Vohra, R. T.; Wand, M. D. *Liq. Cryst.* **2009**, 36, 461–477.
60 Parera, E.; Comelles, F.; Barnadas, R.; Suades, J. *Chem. Commun.* **2011**, *47*, 4460–4462.
61 Coco, S.; Cordovilla, C.; Domínguez, C.; Donnio, B.; Espinet, P.; Guillon, D. *Chem. Mater.* **2009**, *21*, 3282–3289.

62 Miguel−Coello, A. B.; Bardají, M.; Coco, S.; Donnio, B.; Heinrich, B.; Espinet, P. *Inorg. Chem.* **2014**, *53*, 10893−10902.
63 Allenbaugh, R. J.; Aoyama, Y.; Hyatt, M. G.; Reynolds, T. H.; Morgan, M. L.; Adler, A. M.; Schauer, C. K. *Liq. Cryst.* **2013**, *40*, 783–786.
64 Cardinaels, T.; Ramaekers, J.; Nockemann, P.; Driesen, K.; Van Hecke, K.; Van Meervelt, L.; Lei, S.; De Feyter, S.; Guillon, D.; Donnio, B.; Binnemans, K. *Chem. Mater.* **2008,** *20,* 1278–1291.
65 Cardinaels, T.; Ramaekers, J.; Nockemann, P.; Driesen, K.; Van Hecke, K.; Van Meervelt, L.; Wang, G.; De Feyter, S.; Iglesias, E.F.; Guillon, D.; Donnio, B.; Binnemans, K.; Bruce, D. W. *Soft Matter.* **2008**, *4*, 2172–2185.
66 Cardinaels, T.; Ramaekers, J.; Driesen, K.; Nockemann, P.; Van Hecke, K.; Van Meervelt, L.; Goderis, B.; Binnemans, K. *Inorg. Chem.* **2009**, *48*, 2490–2499.
67 Januszko, A.; Kaszynski, P.; Grüner,B. *Inorg. Chem.* **2007**, *46*, 6078–6082.
68 Dembinski, R.; Espinet, P.; Lentijo, S.; Markowicz, M.W.; Martín-Alvarez, J.M.; Rheingold, A.L.; Schmidt, D.J.; Sniady, A. *Eur. J. Inorg. Chem.* **2008**, 1565–1572
69 Frein, S.; Auzias, M.; Sondenecker, A.; Vieille-Petit, L.; Guintchin, B.; Maringa, N.; Süss-Fink, G.; Barberá, J.; Deschenaux, R. *Chem. Mater.* **2008**, *20*, 1340−1343.
70 Pitto-Barry, A.; Barry, N. P. E; Russo, V.; Heinrich, B.; Donnio, B.; Therrien, B.; Deschenaux, R. *J. Am. Chem. Soc.* **2014**, *136*, 17616−17625.
71 Alvariño, C.; Heinrich, B.; Donnio, B.; Deschenaux, R.; Therrien, B. *Inorg. Chem.* **2019**, *58*, 9505−9512.
72 Astruc D. *Eur. J. Inorg. Chem.* **2017**, 6–29.
73 Kadkin, O. N.; Yu, G. G. *Russ. Chem. Rev.* **2012**, *81*, 675–699.
74 Deschenaux, R. Ferrocene–containing thermotropic liquid crystals, in *Ferrocenes: Ligands, Materials and Biomolecules*, Stepnicka, P. (Ed.); John Wiley & Sons, 2008, pp. 446–463.
75 Long, N. J.; Kowalski, K. Ferrocene–containing polymers and dendrimers, in *Ferrocenes: Ligands, Materials and Biomolecules*, Stepnicka, P. (Ed.); John Wiley & Sons, 2008, pp. 393–446.
76 Hussein, M. A.; Asiri, A. M. *Des. Monomers Polym.* **2012**, *15*, 207–251.
77 Zhai, X.; Yu, H.; Wang, L.; Deng, Z.; Zain-Ul-Abdin; Tong, R.; Yang, X.; Chen, Y.; Saleem, M. *Appl. Organomet. Chem.* **2016**, *30*, 62–72.
78 Liu, X.; Zhao, L.; Liu, F.; Astruc, D.; Gu, H. *Coord. Chem. Rev.* **2020**, *419*, 213406.
79 Wu, J.; Wang, L.; Yu, H.; Zain-Ul-Abdin; Khan, R.U.; Haroon M. *J. Organomet. Chem.* **2017**, *828*, 38–51.
80 Carlescu, I.; Scutaru, A. M.; Apreutesei, D.; Alupei, V.; Scutaru, D. *Appl. Organomet. Chem.* **2007**, *21*, 661–669.
81 Carlescu, I.; Scutaru, A. M.; Apreutesei, D.; Alupei, V.; Scutaru, D. *Liq. Cryst.* **2007**, *34*, 775–785.
82 Nakamura, N.; Ishimizu, M.; Nishikawa, M.; Dogen, N. *Mol. Cryst. Liq. Cryst.* **2010**, *516*, 114–121.
83 Kadkin, O. N.; Han, H.; Galyametdinov, Y. G. *J. Organomet. Chem.* **2007**, *692*, 5571–5582.
84 Nakamura, N.; Hiro, K.; Nishikawa, M.; Okabe, T.; Uno, K. *Mol. Cryst. Liq. Cryst.* **2010**, *516*, 122–131.
85 Nakamura, N.; Mizoguchi, R.; Ueda, M.; Hanasaki, T. Mol. Cryst. Liq. Cryst., 1998, 312, 127–136.
86 Majumdar, K. C.; Chakravorty, S.; Pal, N.; Sinha, R. K. *Tetrahedron* **2009**, *65*, 7998–8006.
87 Majumdar K. C.; Shyam P. K. *Mol. Cryst. Liq. Cryst.* **2010**, *528*, 3–9.
88 Majumdar K. C.; Shyam P. K.; Rao, D. S. S.; Prasad, K. *Liq. Cryst.* **2012**, *39*, 1117–1123.
89 Majumdar, K. C.; Ghosh, T.; Shyam, P. K. *Liq. Cryst.* **2011**, *38*, 567–573.

90 Cheng, H.; Ma, M.; Chen, Y.; Ni, H.-L., Feng, C.; Wang, B.-Q.; Zhao, K.-Q.; Yu, W.-H.; Hu, P. *Liq. Cryst.* **2017**, *44*, 1450–1461.
91 Zhao, H. Y.; Guo, L.; Chen, S. F.; Bian, Z. X. *J. Mol. Struct.* **2013**, *1054–1055*, 164–169.
92 Kim, S. Y.; Kadkin, O. N.; Kim, E. H.; Choi, M. G. *J. Organomet. Chem.* **2011**, *696*, 2429–2437.
93 Navale, D. N.; Zote S. W.; Ramana M. M. V. *Liq. Cryst.* **2013**, *40*, 1333–1338.
94 Cheng, Z.; Chang, X.; Qiu, Y.; Tan, G.; Cheng, F.; Fan, H.; Ren, B. *J. Organomet. Chem.* **2018**, *869*, 81−87.
95 Tokunaga, S.; Itoh,Y.; Tanaka, H.; Araoka, F.; Aida, T. *J. Am. Chem. Soc.* **2018**, *140*, 10946−10949.
96 Kadkin, O. N.; Kim, E. H.; Kim, S. Y.; Rha, Y. J.; Tae, J.; Choi, M.-G. *Chem. Eur. J.* **2009**, *15*, 10343–10347.
97 Kim, E. H.; Kadkin, O. N.; Kim, S. Y.; Choi, M.-G. *Eur. J. Inorg. Chem.* **2011**, 2933–2941.
98 Okabe, T.; Nakazaki, K.; Igaue, T.; Nakamura, N.; Donnio, B.; Guillon, D.; Gallani, J. L. *J. Appl. Cryst.* **2009**, *42*, 63–68.
99 Nakamura, N.; Kagawa, S. *Mol. Cryst. Liq. Cryst.* **2011**, *549*, 150–159.
100 Bitter, S.; Kunkel, M.; Burkart, L.; Mang, A.; Winter,R. F.; Polarz, S. *ACS Omega* **2018**, *3*, 8854−8864.
101 Kadkin, O. N.; An, J.; Han, H.; Galyametdinov Y. G., *Eur. J. Inorg. Chem.* **2008**, 1682–1688.
102 Chae, H.W.; Kadkin, O.N.; Choi, M.-G. *Liq. Cryst.* **2009**, *36*, 53–60.
103 Kadkin, O. N.; Kim, E. H.; Kim, S. Y.; Choi, M. G. *Polyhedron* **2009**, *28*, 1301–1307.
104 Li, Z.; Liu, J.; Zhao, H.; Li, B.; Bian, Z. *Res. Chem. Intermed.* **2015**, *41*, 8545–8556.
105 Guillon, D.; Donnio, B.; Deschenaux, R. [60]Fullerene–Containing Thermotropic Liquid Crystals. In *Supramolecular Chemistry of Fullerenes and Carbon Nanotubes*; Martín, N., Nierengarten, J.-F., Eds.; Wiley-VCH, Weinheim 2012; chapter 9, pp 203−235.
106 Campidelli, S.; Severac, M.; Scanu, D.; Deschenaux, R.; Vazquez, E.; Milic, D.; Prato, M.; Carano, M.; Marcaccio, M.; Paolucci, F.; Aminur Rahman, G. M.; Guldi, D. M. *J. Mater. Chem.* **2008**, *18*, 1504–1509.
107 Dvinskikh, S.V., Yamamoto, K., Scanu, D., Deschenaux, R., Ramamoorthy, A. *J. Phys. Chem. B*, **2008**, *112*, 12347–12353.
108 Li,C.-Z.; Matsuo, Y.; Nakamura, N. *J. Am. Chem. Soc.* **2010**, *132*, 15514–15515.
109 Giménez, R.; Elduque, A.; López, J. A.; Barberá, J.; Cavero,E.; Lantero, I.; Oro, L. A.; Serrano, J. L. *Inorg. Chem.* **2006**, *45,* 10363–10370.
110 Rota Martir, D.; Zysman-Colman, E. *Coord. Chem. Rev.* **2018**, *364*, 86–117.
111 Szerb, E. I.; Talarico, A. M.; Aiello, I.; Crispini, A.; Godbert, N.; Pucci, D.; Pugliese, T.; Ghedini, M. *Eur. J. Inorg. Chem*. **2010**, 3270–3277.
112 Talarico, A. M.; Ghedini, M.; Cesare Oliverio Rossi, C. O.; Szerb, E. I. *Soft Matter*. **2012**, *8*, 11661–11669.
113 Wu,X.; Xie, G.; Cabry, C. P.; Xu, X.; Cowling, S. J.; Bruce, D. W.; Zhu, W.; Baranoff, E.; Wang, E. Y. *J. Mater. Chem.* C **2018**, 6, 3298–3309.
114 Santoro, A.; Prokhorov, A.M.; Kozhevnikov, V.N.; Whitwood, A.C.; Donnio, B.; Williams, J. A. G.; Bruce, D.W. *J. Am. Chem. Soc*. 2011, *133*, 5248–5251.
115 Wang, Y.; Cabry, C.P.; Xiao, M.; Male, L.; Cowling, S. J.; Bruce, D.W.; Shi, J.; Zhu, W.; Baranoff, E. *Chem. Eur. J.* **2016**, *22*, 1618–1621.
116 Prokhorov, A.M.; Santoro, A.; Williams, J.A.G.; Bruce, D.W. *Angew. Chem. Int. Ed.* **2012**, *51*, 95–98.

117 Zou, G.; Zhao, L.; Zeng, L.; Luo, K.; Ni, H.; Wang, H.; Li, Q.; Yu, W.; Li, X. *Inorg. Chem.* **2019,** *58*, 861–869.
118 Coco, S.; Espinet, E.; Espinet, P.; Palape, I. *Dalton Trans.*, **2007**, 3267–3272.
119 Coco, S.; Cordovilla, C.; Domínguez, C.; Espinet, P. *Dalton Trans.*, **2008**, 6894–6900.
120 Domínguez, C.; Donnio, B; Coco, S.; Espinet, P. *Dalton Trans.*, **2013**, *42*, 15774−157984.
121 Chico, R.; de Domingo, E.; Domínguez, C.; Donnio, B.; Heinrich, B.; Termine, R.; Golemme, A.; Coco, S.; Espinet, P. *Chem. Mater*. **2017**, *29*, 7587−7595.
122 Tritto, E.; Chico, R.; Ortega, J.; Folcia, C. L.; Etxebarria, J.; Coco, S.; Espinet, P. *J. Mater. Chem. C* **2015**, *3*, 9385−9392.
123 Coco, S.; Cordovilla, C.; Donnio, B.; Espinet, P.; García-Casas, M. J.; Guillon, D. *Chem. Eur. J.,* **2008**, *14*, 3544–3552.
124 Wang, X.; Sobota, M.; Kohler, F. T. U.; Morain, B.; Melcher, B. U.; Laurin, M.; Wasserscheid, P.; Libuda, J.; Meyer, K. *J. Mater. Chem.*, **2012**, *22*, 1893–1898.
125 Miguel−Coello, A. B.; Bardají, M.; Coco, S.; Donnio, B.; Heinrich, B.; Espinet, P. *Inorg. Chem.* **2018**, *57*, 4359−4369.
125a Camerel, F.; Ziessel, R.; Donnio, B.; Bourgogne, C.; Guillon, D.; Schmutz, M.; Iacovita, C.; Bucher, J.-P. *Angew. Chem. Int. Ed*. **2007**, *46*, 2659–2662.
126 Mayoral, M. J.; Cornago, P.; Claramunt, R. M.; Cano, M. *New J. Chem.*, **2011**, *35*, 1020–1030.
127 Mayoral, M. J.; Ovejero, P.; Campo, J. A.; Heras, J. V.; Oliveira, E.; Pedras, B.; Lodeiro, C.; Cano, M. *J. Mater. Chem.*, **2011**, *21*, 1255–1263.
128 Moreno-Mañas, M.; Reichardt, Ch.; Sebastián, R. M.; Barberá, J.; Serrano, J. L.; Sierra, T. *J. Mater. Chem.*, **2005**, *15*, 2210–2219.
129 Donnio B., Bruce D. W . Liquid crystalline orthopalladated complexes. In *Palladacycles*. Dupont J, Pfeffer M, editors. Weinheim: Wiley-VCH; 2008. pp 239–283.
130 Ghedini; M. Pucci, D.; Viñuales, A. *Mol. Cryst. Liq. Cryst*. **2007**, *465*, 59–70.
131 Godbert, N.; Dattilo, D.; Termine, R.; Aiello, I.; Bellusci, A.; Crispini, A.; Golemme, A.; Ghedini, M. *Chem. Asian J.* **2009**, *4*, 1141–1146.
132 Choudhury, T. D.; Shen, Y.; Rao, N. V. S;. Clark, N. A. *J. Organomet. Chem.* **2012**, *712*, 20–28.
133 Arias, J.; Bardají, M.; Espinet, P. *J. Organomet. Chem.* **2006**, *691*, 4990–4999.
134 Coco, S.; Cordovilla, C.; Espinet, P.; Gallani, J.-L.; Guillon, D.; Donnio, B. *Eur. J. Inorg. Chem*. **2008**, 1210–1218.
135 Bilgin-Eran, B.; Ocak , H.; Tschierske, C.; Baumeister, U. *Liq. Cryst.* **2012**, *39*, 467–476.
136 Bilgin-Eran, B.; Tschierske, C.; Dielec, S.; Baumeister; U *J. Mater. Chem*., **2006**, *16*, 1136–1144.
137 Bilgin-Eran, B.; Tschierske, C.; Dielec, S.; Baumeister; U. *J. Mater. Chem.*, **2006**, *16*, 1145–1153.
138 Mocanu, A. S.; Ilis, M.; Dumitrascu, F.; Ilie, M.; Cîrcu, V. *Inorg. Chim. Acta* **2010**, *363*, 729–736.
139 Ilis, M.; Micutz, M.; Dumitrasçu, F.; Pasuk, I.; Molard, Y.; Roisnel, T.; Cîrcu, V. *Polyhedron*, **2014**, *69*, 31–39.
140 Ilis, M.; Batalu, D.; Pasuk, I.; Cîrcu, V. *J. Mol. Liq*. **2017**, 233, 45–51.
141 Ilis¸ M.; Micutz, M.; Cîrcu, V. *J. Organomet. Chem.* **2017**, *836–837*, 81–89.
142 Micutz, M.; IPasuk, I.; Iliş, M. *J. Mol. Liq.*, **2017,** *243***,** 151–156.
143 Baena, M. J.; Espinet, P.; Folcia, C. L.; Ortega, J.; Etxebarría, J. *Inorg. Chem.* **2010**, *49*, 8904–8913.
144 Cîrcu, V.; Simonescu, C. M. *Cryst. Res. Technol*. **2010**, *45*, 512–516.
145 Cîrcu, V.; Dumitrascu, F. *Mol. Cryst. Liq. Cryst.*, **2011**, *534*, 41–49.
146 Tritto, E.; Chico, R.; Sanz-Enguita, G.; Folcia, C. L.; Ortega, J.; Coco, S.; Espinet, P. *Inorg. Chem.* **2014**, *53*, 3449−3455.

147 Pucci, D.; Barberio, G.; Bellusci, A.; Crispini, A.; Ghedini. M. *J. Organomet. Chem.* **2006**, *691*, 1138–1142.
148 Hegmann, T.; Kain, J.; Diele, S.; Schubert, B.; Bögel, H.; C. Tschierske, C. *J. Mater. Chem.*, **2003**, *13*, 991–1003.
149 Damm, C.; Israel, G.; Hegmann, T.; Tschierske, C. *J. Mater. Chem.*, **2006**, *16*, 1808–1816.
150 Venkatesan, K.; Kouwer, P. H. J.; Yagi, S.; Müller, P.; Swager, T. M. *J. Mater. Chem.*, **2008**, *18*, 400–407.
151 Wang, Y.; Liu, Y.; Luo, J.; Qi, H.; Li, X.; Nin, M.; Liu, M.; Shi, D.; Zhu, W.; Cao, Y. *Dalton Trans.*, **2011**, *40*, 5046–5051.
152 Yang, X.; Wu, X.; Zhou, D.; Yu, J.; Xie, G., Bruce, D. W.; Wang, Y. *Dalton Trans*. **2018**, *47*, 13368–13377.
153 Zou, G.; Luo, K.; Zhao, L.; Ni, H.; Wang, H.; Li, Q. *Liq. Cryst.* **2018**, 45, 593–606.
154 Yang, B.; Ni, H.; Wang, H.; Hu, Y.; Luo, K.; Yu, W. *J. Phys. Chem. C* **2020**, *124*, 23879−23887.
155 Qian, G.; Yang, X.; Wang, X.; Herod, J. D.; Bruce, D. W.; Wang, S.; Zhu, W.; Duan, P.; Wang, Y. *Adv. Optical Mater.* **2020**, 2000775.
156 Santoro, A.; Whitwood, A. C.; Williams, J. A. G.; Kozhevnikov, V. N.; Bruce, D. W. *Chem. Mater.* **2009**, *21*, 3871–3882.
157 Spencer, M.; Santoro, A.; Freeman, G. R.; Díez, A.; Murray, P. R.; Torroba, J.; Whitwood, A. C.; Yellowlees, J. Y.; Williams, J. A. G.; Bruce, D. W. *Dalton Trans*., **2012**, *41*, 14244–14256.
158 Díez, A.; Cowling, S. J.; Bruce, D. W. *Chem. Commun.*, **2012**, *48*, 10298–10300.
159 Wang, Y.; Fan, J.; Li, T.; Wang, O.; Shi, J.; Qu, Z.; Tan, H.; Liu, Y.; Zhu, W. RSC Adv. **2016**, *6*, 45864–45872.
160 Wang, Y.; JFan, J.; Shi, J.; Qi, H.; Baranoff, E.; Xie, G.; Li, Q.; Tan, H.; Liu, Y.; Zhu, W. *Dyes Pigm.*, **2016**, *133*, 238–247.
161 Krikorian, M.; Liu, S.; Swager, T. M. *J. Am. Chem. Soc*. **2014**, *136*, 2952−2955.
162 Geng, H.; Luo, K.; Zou, G.; Zhao, L.; Wang, H.; Li, Q.; Ni, H. *Dyes Pigm,* **2018***, 149*, 82–91.
163 Geng, H.; Luo, K.; Cheng, H.; Zhang, S.; Ni, H.; Wang, H.; Yu, W.; Li, Q. *RSC Adv*., **2017**, *7*, 11389–11393.
164 Pucci, D.; Aiello, I.; Aprea, A.; Bellusci, A.; Crispini, A.; Ghedini, M. *Chem. Commun.*, **2009**, 1550–1552.
165 Ghedini, M.; Pucci, D.; Crispini, A.; Bellusci, A.; La Deda, M.; Aiello, I.; Pugliese, T. *Inorg. Chem. Commun*. **2007**, *10*, 243–246.
166 Ionescu, A.; Godbert, N.; Crispini, A.; Termine, R.; Golemme, A.; Ghedini, M. *J. Mater. Chem.* **2012**, *22*, 23617–23626.
167 Ionescu, A.; Godbert, N.; Aiello, I.; Crispini, A.; Ghedini, M. *Mol. Cryst. Liq. Cryst.* **2012**, *558*, 84–92.
168 Kozhevnikov, V. N.; Donnio, B.; Bruce, D. W. *Angew. Chem. Int. Ed*. **2008**, *47*, 6286–6289.
169 Kozhevnikov, V. N.; Donnio, B.; Heinrich, B.; Bruce, D. W. *Chem. Commun.*, **2014**, *50*, 14191–14193.
170 Kozhevnikov, V. N.; B. Donnio, B.; Heinrich, B.; Williams, J. A. G.; Bruce, D. W. *J. Mater. Chem. C*, **2015**, *3*, 10177–10187.
171 Zhao, L.; Yang, B.; Zeng, L.; Luo, K.; Wang, H.; Ni, H.; Yang, C.; Li, Q. *Dyes Pigm.* **2019**, *164*, 398–406.
172 Ghedini, M.; Pucci, D.; Barberio, G. *Organometallics* **1999**, *18*, 2116–2124.
173 Ghedini, M.; Pucci, D.; Barberio, G. *Liq. Cryst*. **2000**, *27*, 1277–1283.

174 Parker, R. R.; Sarju, J. S.; Whitwood, A. C.; Williams, J. A. G.; Lynam, J. M.; Bruce, D. W. *Chem. Eur. J.* **2018**, *24*, 19010–19023.
175 Espinet, P. *Gold Bull.* **1999**, *32*, 127–134.
176 Bardají, M. Liquid crystals. In *Modern Supramolecular Gold Chemistry: Gold–Metal Interactions and Applications*; Laguna, A., Ed.; Wiley-VCH: Weinheim, Germany, 2008; Chapter 7, pp. 403–428.
177 Coco, S.; Espinet, P. Liquid crystals based on gold compounds. In *Gold Chemistry*; Mohr, F., Ed.; Wiley-VCH Verlag GmbH & Co. KGaA: Weinheim, Germany, 2009; Chapter 8, pp. 357–396.
178 Bardají, M. *Inorganics* **2014**, *2*, 433–454.
179 Pucci, D. *Liq. Cryst.* **2011**, *38*, 1451–1465.
180 Fujisawa K.; Kawakami N.; Onishi Y.; Izumi Y.; Tamai S.; Sugimoto N.; Tsutsumi O.. *J. Mater. Chem. C* **2013**, *1*, 5359–5366.
181 Sugimoto N.; Tamai S.; Fujisawa K.; Tsutsumi O. Mol. Cryst. Liq. Cryst. 2014, 601, 97– 106.
182 Younis O.; Rokusha Y.; Sugimoto N.; Fujisawa K.; Yamada S.; Tsutsumi O. Mol. Cryst. Liq. Cryst. 2015, 617, 21–31.
183 Fujisawa K.; Okuda Y.; Izumi Y.; Nagamatsu A.; Rokusha Y.; Sadaike Y.; Tsutsumi O. *J. Mater. Chem. C* **2014**, *2*, 3549–3555.
184 Yamada S., Rokusha Y., Kawano R., Fujisawa K., Tsutsumi O. *Faraday Discuss.* **2017**, *196*, 269–283.
185 Fujisawa, K.; Mitsuhashi F.; Anukul, P.; Taneki, K.; Younis, O.; Tsutsumi O. *Polym. J.* **2018**, *50*, 761–769.
186 Coco, S.; Cordovilla, C.; Espinet, P.; Martín-Alvarez, J.M.; Muñoz, P. *Inorg. Chem.* **2006**, *45*, 10180–10187.
187 Arias, J.; Bardají, M.; Espinet, P. *Inorg. Chem.* **2008**, *47*, 3559–3567.
188 Donnio, B. Liquid-crystalline metallodendrimers. *Inorg. Chim. Acta* **2014**, *409*, 53–67.
189 Cordovilla, C.; Coco, S.; Espinet, P.; Donnio, B. *J. Am. Chem. Soc.* **2010**, *132*, 1424–1431.
190 Domínguez, C.; Heinrich, B.; Donnio, B.; Coco, S.; Espinet, P. *Chem. Eur. J.* **2013**, *19*, 5988–5995.
191 Baena, M. J.; Coco, S.; Espinet, P. *Cryst. Growth Des.* **2015**, *15*, 1611−1618.
192 Chico, R.; Domínguez, C.; Donnio, B.; Heinrich, B.; Coco, S.; Espinet, P. *Cryst. Growth Des.* **2016**, *16*, 6984−6991.
193 Jiménez, J.; Sanz, J. A.; Serrano, J. L.; Barberá, J.; Oriol, L. *Inorg. Chem.* **2020**, *59*, 4842−4857.
194 Arias, J.; Bardají, M.; Espinet, P.; Folcia, C.L.; Ortega, J.; Etxebarría, J.P. *Inorg. Chem.* **2009**, *48*, 6205–6210.
195 de Domingo, E.; Barcenilla, M.; Martín–Alvarez, J. M.; Miguel, J. A.; Coco, S. *Dyes Pigm.* **2020**, *176*, 108195–108204.
196 Huang, R.T.W.; Wang, W.C.; Yang, R.Y.; Lu, J.T.; Lin, I.J.B. *Dalton Trans.* **2009**, 7121–7131.
197 Hsu, T.H.T.; Naidu, J.J.; Yang, B.–J.; Jang, M.–Y.; Lin, I.J.B. *Inorg. Chem.* **2012**, *51*, 98–108.
198 Pana, A.; Ilis, M.; Micutz, M.; Dumitrascu, F.; Pasuk I.; Circu, V. *RSC Adv.* **2014**, *4*, 59491–59497.
199 Baron, M.; Bellemin–Laponnaz, S.; Tubaro, C.; Heinrich, B.; Basato, M.; Accorsi, G. *J. Organomet. Chem.* **2016**, *801*, 60–67.
200 Yeap, C. W.; Haque, R. A.; Yam, W. S.; Razali, M. R. *J. Mol. Liq.* **2019**, *277*, 341–348.
201 Yeap, C. W.; Haque, R. A.; Yam, W. S.; Razali, M. R. *Liq. Cryst.* **2018**, *45*, 1210–1222.
202 Syu,H. J. H.; Chiou, J. Y. Z.; Wang J.–C.; Lin I. J. B. *RSC Adv.* **2017**, *7*, 14611–14617.
203 Kuroda, Y.; Nakamura, S.; Srinivas, K.; Sathyanarayana, A.; Prabusankar, G.; Hisano, K.; Tsutsumi, O. *Crystals* **2019**, *9*, 227–239.

204 Xiao, X.–S.; Zou, C.; Guan, X.; Yang, C.; Lu, W.; Che, C.–M. *Chem. Commun.* **2016**, *52*, 4983—4986.